Analysis of the post-transcriptional regulatory role of aconitase from *Streptomyces viridochromogenes* Tü494

Dissertation

der Mathematisch-Naturwissenschaftlichen Fakultät

der Eberhard Karls Universität Tübingen

zur Erlangung des Grades eines

Doktors der Naturwissenschaften

(Dr. rer. nat.)

vorgelegt von

Ewelina Atasayar

(geb. Michta)

aus Kościerzyna, Polen

Tübingen

2014

Tag der mündlichen Qualifikation:	14.04.2014
Dekan:	Prof. Dr. Wolfgang Rosenstiel
1. Berichterstatter:	Prof. Dr. Wolfgang Wohlleben
2. Berichterstatter:	Prof. Dr. Klaus Hantke

Erklärung

Hiermit erkläre ich, dass ich diese Schrift selbständig und nur mit den angegebenen Hilfsmitteln verfasst habe. Ferner sind alle Stellen, die im Wortlaut oder dem Sinn nach den Werken anderer Autoren entnommen sind, durch Angabe der Quellen kenntlich gemacht. Eine detaillierte Abgrenzung meiner eigenen Leistungen von den Beiträgen meiner Kooperationspartner habe ich im Anhang vorgenommen.

…….

Tübingen, den 07.03.2014

Table of Contents

1. Zusammenfassung 6

2. Summary 7

3. Introduction 8

3.1.The genus *Streptomyces* 8

3.2. Peptide antibiotics 9

3.3. *S. viridochromogenes* Tü494 11

3.4. PTT biosynthesis 12

3.5. The characteristics of aconitases from *S. viridochromogenes* Tü494 14

3.6. Oxidative stress and the role of iron regulatory proteins (IREs) 16

3.5. Regulatory activity of aconitases in Gram-negative and Gram-positive bacteria 17

4. Objectives 20

5. Results 21

5.1. The influence of the *acnA* mutation on the physiology of *S. viridochromogenes* Tü494 21

5.1.1 The influence of accumulated organic acids on MacnA growth and differentiation 21

5.1.2. The influence of oxidative stress and increasing temperature on the growth of MacnA 22

5.2. Analysis of the regulatory role of AcnA 24

5.2.1. Heterologous expression of AcnA derivatives in *S. lividans* T7 24

5.2.2. *In vitro* analysis of the AcnA binding to IRE-like structures 25

5.2.3. Transcriptional analysis to study the role of AcnA in the regulation of *recA* expression under oxidative stress conditions 29

5.2.4. The use of artificial IRE motifs for the AcnA-mediated transcript stabilization 30

5.3. Comparative proteomic analysis of *S. viridochromogenes* MacnA in response to oxidative stress 32

6. Discussion 36
6.1. Aconitase from *S. viridochromogenes* Tü494 is an RNA-binding protein and exhibits a regulatory function on post-transcriptional level 36
6.2. The lack of the regulatory function of AcnA and accumulation of citrate contribute to the morphological defect of MacnA 41
6.3. The regulatory function of aconitase is involved in oxidative stress defense, cellular differentiation and presumably other pathways 43
7. References 47
8. List of publications 57
8.1. Publication 1 (Michta *et al.*, 2012) 58
6.2. Publication2 (Michta *et al.*, 2014) 78
9. Contribution 89

1. Zusammenfassung

Aconitasen gehören zu den wichtigsten Enzymen der zentralen Stoffwechselwege in Citrat- und Glyoxylat-Zyklus und katalysieren hier die Isomerisierung von Citrat zu Isocitrat über cis-Aconitat. Zusätzlich zu ihrer katalytischen Funktion besitzen Aconitasen in einigen Fällen auch eine regulatorische Funktion. Unter Eisenmangelbedingungen oder oxidativem Stress verliert das [4Fe-4S]- Cluster ein Fe^{2+}-Ion und Aconitase somit auch ihre katalytische Funktion. In diesem Zustand ist die Aconitase regulatorisch aktiv und kann als Iron Regulatory Protein (IRP) an sogenannte Iron Responsive Elements (IREs), die auf mRNAs lokalisiert sind, binden und deren Expression posttranskriptional regulieren.

In dieser Arbeit wurde die Aconitase aus *S. viridochromogenes* Tü494 (AcnA) untersucht, weil man davon ausging, dass es eine Verknüpfung zwischen primären- und sekundären Metabolismus herstellen kann. Die *S. viridochromogenes* Aconitase-Mutante (MacnA) hat einen Differenzierungsdefekt, der durch das Ausbleiben von Sporulation, Luftmycelbildung und fehlende Antibiotikaproduktion gekennzeichnet ist. Diese Mutante ist außerdem empfindlich gegenüber oxidativem Stress und Hitzestress.

Mit Hilfe von *in silico* Analysen konnten konservierte IRE-Motive in *S. viridochromogenes*-Genom identifiziert und deren Funktionalität in RNA-Gelshift-Experimenten mit aufgereinigter Aconitase verifiziert werden. Außerdem wurde erstmalig durch Immunoblot-Experimente gezeigt, dass AcnA die Menge des RecA Proteins, die erforderlich ist um DNA-Schäden unter oxidativem Stress zu reparieren, regulatorisch beeinflusst. Diese Ergebnisse wurden zusätzlich durch RT-PCR-Experimente bestätigt. Vergleichende Proteom-Analysen lieferten neuartige *in vivo* Beweise für eine regulatorische Funktion der Aconitase in *S. viridochromogenes* unter oxidativem Stress.

2. Summary

Aconitases are one of the major enzymes in tricarboxylic acid and glyoxylate cycles but in some cases also can act as regulators on post-transcriptional level. As enzymes they catalyze the interconversion of citrate to isocitrate via *cis*-aconitate. However, under conditions of iron starvation or oxidative stress the [4Fe-4S] cluster is disassembled and aconitases function as post-transcriptional regulators that bind specific mRNA secondary structures known as iron responsive elements (IREs). In this study the aconitase from *S. viridochromogenes* Tü494 (AcnA) was analyzed, since it was assumed that this protein may constitute a linkage between primary and secondary metabolism. The *S. viridochromogenes* aconitase mutant (MacnA) is unable to develop aerial mycelium, to sporulate or to produce antibiotic. This mutant is also highly sensitive to oxidative stress and higher temperatures.

In silico analysis of the *S. viridochromogenes* genome revealed the presence of several conserved IRE-like structures. In this study, their functionality was validated in electrophoretic mobility shift experiments. It could be shown that AcnA from *S. viridochromogenes* is an RNA binding protein and exhibits regulatory function on post-transcriptional level. Furthermore, the previously suggested AcnA-mediated regulation of the synthesis of recombinase A (RecA), which is required to repair DNA damage under oxidative stress, was confirmed. It was shown that the *recA* transcript is more stabile under oxidative stress in the WT than in MacnA. The proteomic approach provided new *in vivo* evidence for AcnA-mediated regulation under oxidative stress conditions and allowed to identify proteins, of which the expression may be associated with the impaired defense of MacnA against free radicals.

3. Introduction

3.1. The genus *Streptomyces*

The genus *Streptomyces* belongs to the order of Actinomycetales, which are Gram-positive, obligatory aerobic, filamentous bacteria. *Streptomyces* evolved about 450 million years ago as organisms adapted to the decomposing of organic elements (Chater, 2006). In this way they are the most abundant organisms among soil bacteria and they play an important role in soil biodegradation by secreting exoenzymes which catabolize polymers in dead plant, animal and fungal material (Hodgson, 2000; McCarthy and Williams 1992). This makes *Streptomyces* the key organisms in carbon recycling. Characteristic for these microorganisms is a high G+C content (apx.70%) of the relatively large genome (8 – 10 Mb) and a complex life cycle.

The lifestyle of *Streptomyces* is very similar to that of filamentous fungi. The morphological differentiation starts with an arthrospore. These spores are resistant to drought but are much less resistant to chemicals and heat than the spores from *Bacillus* species (Ensign, 1978). Under favorable conditions and nutrient availability the spores start to germinate. The germ tubes grow by tip extension to form substrate (vegetative) mycelium. The vegetative hyphae are divided by cross walls, thus *Streptomyces* are a rare example of multi-cellular prokaryotes. In response to nutrient depletion or other stress conditions the aerial mycelium is formed and the onset of secondary metabolism takes place (Flärdh and Buttner, 2009). Most of the cells in substrate mycelium die during aerial mycelium formation. This allows the aerial mycelium to reuse biomass from the degraded substrate mycelium (Méndez *et al*., 1985). The aerial mycelium further differentiates into chains of hydrophobic spores. In liquid culture most of the *Streptomyces* grow only as vegetative mycelium and do not sporulate. One of the seldom exceptions is *Streptomyces griseus* that sporulates also in liquid culture (Glazebrook *et a*l., 1990).

Streptomyces undergoe also physiological differentiation what enables them to produce a variety of secondary metabolites including antibiotics. *Streptomyces* are known to be the most efficient producers of natural antibiotics (Watve *et al*.,

2001). The genes encoding enzymes involved in antibiotic production are generally clustered (usually 20-30 genes) and are associated with regulatory and resistance genes (van Wezel and McDowall, 2011; Nett *et al*., 2009). The antibiotic production is growth phase-dependent and under not yet fully understood control. The specific control of antibiotic production and aerial hyphae formation includes regulatory proteins and extracellular factors such as γ-butyrolactone signaling molecules. The formation of antibiotics is also controlled by the availability of nitrogen, phosphorous or carbon (Sánchez *et al*., 2010).

Industrially important secondary metabolites derived from *Streptomyces* include e.g. therapeutics used in medical treatment (ertythromycin, streptomycin, tetracycline) (Watve *et al*., 2001), antitumor drugs (anthracyclines (Minotti *et al*., 2004), bleomycin (Umezawa *et al*., 1966)), enzyme inhibitors with potential utilization in medicine and agriculture (chymostatin) (Umezawa *et al*., 1970), immunosuppressants (rapamycin) (Vézina *et al*., 1975), antiparasitics (avermectins) (Burg *et al*., 1979) or herbicides (phosphinothricin tripeptide=PTT) (Bayer *et al*., 1972).

3.2. Peptide antibiotics

Antibiotics are a biologically and chemically diverse group of compounds. They can be classified according to different criteria, such as origin, biological effects, mode of action or chemical structure. Classifications according to the chemical structure divide antibiotics in e.g. β-lactam antibiotics, aminoglycoside antibiotics, polyketide antibiotics, peptide antibiotics, etc. (Bérdy, 2005; Gräfe, 1992).

Peptide antibiotics may consist of proteinogenic amino acids but also of non-proteinogenic amino acids, D-amino acids, hydroxy acids or other unusual building blocks. In addition they may be modified by N or C methylation, cyclization, etc. (Kleinkauf and von Döhren, 1990). According to the mechanism of biosynthesis they can be divided into two groups: the one that are synthesized by ribosomes (lantibiotics) or these that are synthesized by multifunctional enzyme complexes called nonribosomal peptide synthethases (NRPS) (nonribosomally synthesized peptide antibiotics). Antibiotics build with

more than 20 amino acids are usually synthesized by ribosomes and use mRNA as a template to guide the synthesis. Peptide antibiotics composed of oligopeptides (less than 20 amino acids) are formed primarily by NRPSs.

NRPSs consist of molecular modules, of which each is responsible for the incorporation of one defined monomer into the peptide chain (Fig.1). A single module is composed out of catalytic domains, such as: adenylation (A) domain-responsible for the selection and activation of the amino acid; thiolation or peptidyl carrier protein domain (PCP)-responsible for the propagation of the peptide chain; condensation (C) domain-responsible for the condensation of the amino acid by formation of the peptide bound; and a thioesterase (TE) domain associated with the product release. The TE domain is located in the termination module and releases the peptide by hydrolysis or macrocyclization (Strieker *et al.*, 2010; Kopp and Marahiel, 2007).

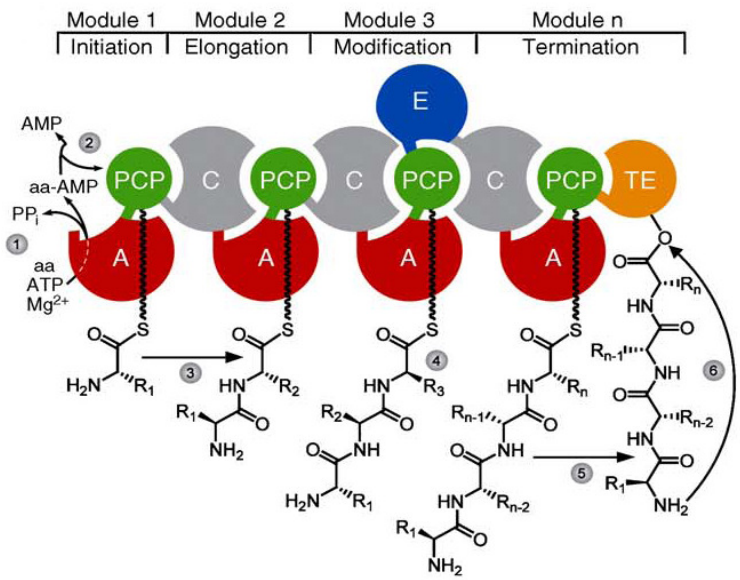

Fig. 1 Mechanism of nonribosomal peptide (NRP) synthesis.

(1) Activation of amino acid as aminoacyl-AMP. (2) Transfer of the amino acid onto the PCP domain. (3) Condensation of PCP-bound amino acids. (4) Possibility of amino acid modifications. (5) Transesterification of the peptide chain from the terminal PCP onto the TE domain. (6) TE-catalyzed product release (Strieker *et al.*, 2010).

The initiation of the NRP biosynthesis starts with the activation of the first amino acid as aminoacyl-AMP by the adenylation domain (A). This domain has a high substrate specificity. Each A domain comprises a large N-terminal core domain and a small C-terminal subdomain (A_{sub}). The cycle starts with the open conformation of the A domain where A_{sub} is far from the active site. Such open structure is able to bind the amino acid and ATP. Upon docking of the amino acid and ATP, an adenylating intermediate is formed and the conformation of A domain is closed. The activated amino acid is converted into a thioester and

attached to the PCP domain. This transfer leads to the rotation of A_{sub} back to an open conformation. Important is that each peptidyl carrier protein (PCP) must be modified by a phosphopantetheinyl group that is covalently bound to a specific, highly conserved serine residue (GGXS). This process is called priming. The phosphopantetheinyl arm is used for attachment of the amino acid residue. During PCP phospantetheinylation some mispriming events can occur, which may interrupt the NRP assembly. These misprimed PCP species are repaired by type II thioesterases (TEII) (Koglin *et al*., 2008). The elongation of the polypeptide chain is performed by the mutual interactions of condensation (C), adenylation (A) and PCP domain. The activated carboxyl group of the last amino acid is transferred to the amino group of the next amino acid what results in an N-to-C condensation. It is not fully elucidated how the condensation domain is involved in the formation of the peptide bond but a conserved double histidine motive seems to be essential (Stachelhaus *et al*., 1998). Once, the polypeptide chain reaches its final length, a specialized C-terminal thioester domain I (TEI) catalysis the product release by hydrolysis or cyclization. A number of modifications of polypeptide chain may occur. This can be done by the activity of cyclases, methyltransferases, dehydratases or epimerases that are localized on the additional domains (Keating and Walsh, 1999).

3.3 *S. viridochromogenes* Tü494

S. viridochromogenes Tü494 is the producer of the nonribosomally assembled peptide antibiotic phosphinothricin-tripeptide (PTT). A structurally identical tripeptide, called bialapos, is produced by *Streptomyces hygroscopicus* ATCC21767 (Kondo *et al*., 1973). These two species are taxonomically distinct and were isolated from different parts of the world but they use very similar enzymes for PTT production (Hara *et al*., 1991). The entire PTT gene cluster (appx. 33 kb, 24 genes) was identified and sequenced (Alijah *et al*., 1991; Blodgett *et al*., 2005; Schwartz *et al*., 2004). PTT (bialaphos) consists of two molecules of L-alanine linked to the nonproteinogenic amino acid phosphinothricin (PT). Interestingly, PT possesses a C-P-C bond that is rare in natural compounds. The bioactive compound PT is a structural analogue of glutamic acid and thus competitively inhibits bacterial and plant glutamine

synthetases. However, the glutamic acid uptake systems in bacteria are very specific and they do not accept phosphinothricin as a substrate. Bacterial cells are able to incorporate this antibiotic in the form with di-alanine residue. The transport of the tripeptide antibiotic into the bacterial cells occurs via oligopeptide transport systems. Inside the cell, PTT is hydrolyzed by peptidases and the PT moiety is released (Diddens *et al*., 1976). The accumulation of PT leads to the fatal accumulation of ammonium which inhibits photosynthesis in plants. Due to this phenomenon, this antibiotic can be used as herbicide. The ammonium salt of L/D phosphinothricin is industrially produced as Basta® and the PTT tripeptide is available as Herbiace®. Also PT-resistant transgenic plants have been generated by use of the resistance gene *pat* from the PTT biosynthetic gene cluster of *S. viridochromogenes* or *bar* from *S. hygroscopicus*. These resistance genes encode demethylphosphinothricin acetyltransferase (DPAT), which confers the antibiotic resistance by acetylation of phosphinothricin. Interestingly the same enzyme is also an integral part of the PTT biosynthetic pathway (Wohlleben *et al*., 1988; Thompson *et al*., 1987; Kumada *et al*., 1988).

3.4. PTT biosynthesis

The PTT biosynthetic pathway was proposed after investigation of accumulated and converted intermediates in a set of *S. hygroscopicus* PTT-non producing mutant. The alanine residues are delivered from primary metabolism while the nonproteinogenic amino acid PT is synthesized via the demethylphosphinothricin (DMPT) intermediate in secondary metabolite biosynthesis (Schwartz *et al*., 2004) (Fig.2).

24 genes involved in PTT biosynthesis were identified within the cluster (Blodgett *et al*., 2005; Schwartz *et al*., 2004). PTT is assembled nonribosomally by peptide synthetases. The inactivation of peptide synthetases in *S. viridochromogenes* (*phsA*, *phsB*, *phsC*) resulted in non-PTT-producing mutants (Schwartz *et al*., 2004; Schwartz *et al*., 1996). The role of PhsA is the activation of PT precursor *N*-acetyl-demethylphosphinothricin *N*-Ac-DMPT (or alternatively the methylated PT precursor *N*-acethyl-phosphinothricin *N*-Ac-PT). The PhsB and PhsC function as the elongation modules and activate alanine residues.

What is unusual about nonribosomal synthesis of PTT is that all three peptide synthetase genes encode only one peptide synthetase module, while normally NRPSs are multimodulare enzymes. These three genes are not clustered but are located at different positions in the PTT gene cluster. Furthermore, the thioesterase function domains, which usually are located on the C-terminus of PhsB or PhsC, in this case are located on separate proteins (encoded by two external thioesterase genes: *theA*, *theB*). Surprisingly, in the N-terminus of PhsA highly conserved thioesterase motif GXSXG was identified but the region surrounding the motif does not show homology to other thioesterases domains. However, the deletion of this motif in PhsA causes lack of PTT production. This might suggest that the TE motif is required for PTT production. Probably it releases PTT from NRPS complex (Eys *et al.*, 2008). This unique organization of NRPSs components, involved in PTT biosynthesis, represents perhaps an archetype of the well known multimodular peptide synthesis. Possibly such evolutionary step allowed for more effective antibiotic production (Schinko *et al.*, 2009).

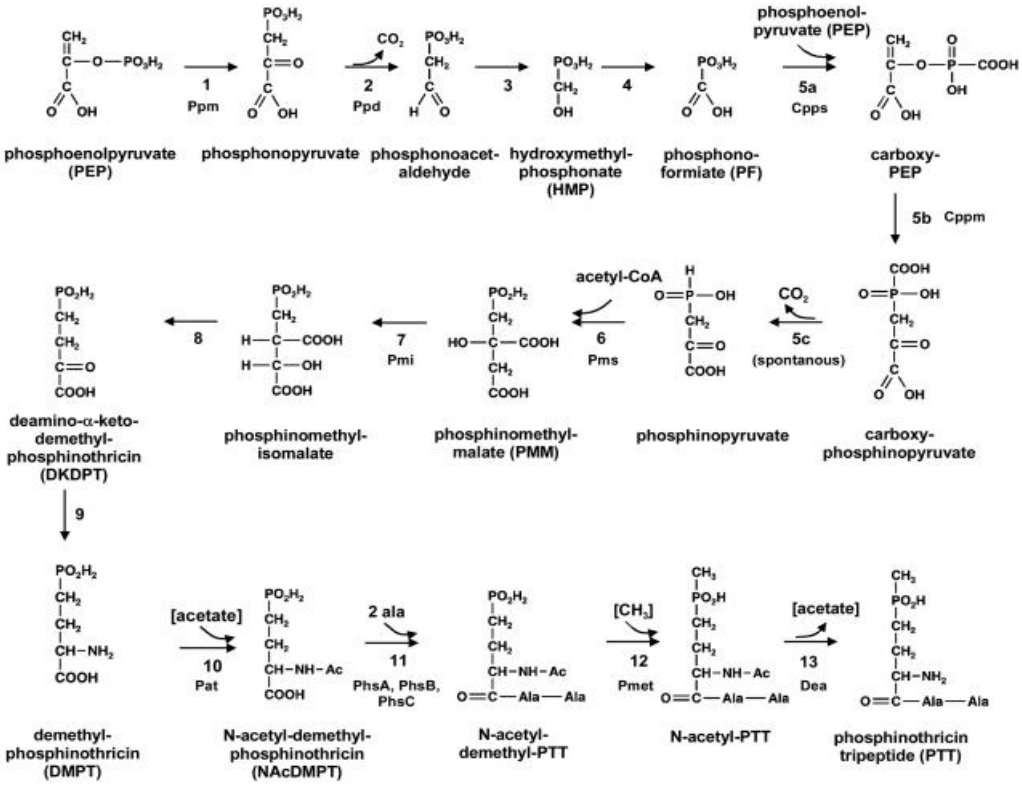

Fig.2 Postulated PTT biosynthetic pathway (Schwartz *et al.*, 2004).

3.5. The characteristics of aconitases from *S. viridochromogenes* Tü494

Aconitase (citrate (isocitrate) hydro-lyase, EC 4.2.1.3) is one of the key enzymes in tricarboxylic acid cycle (TCA). The TCA cycle plays a significant role in *Streptomyces* growth and development. This cycle provides reducing equivalents important for oxidative stress defense, energy generation and biosynthetic reactions, along with precursors for lipid and amino acid synthesis. Aconitase is an enzyme that catalyzes one of the initial steps in TCA: the stereo-specific isomerization of citrate to isocitrate via *cis*-aconitate. First, citrate is recognized by aconitase and dehydrated to stabile *cis*-aconitate. Then the product is released, turns by 180˚ and binds to aconitase again. The aconitate is rehydrated and finally forms isocitrate (Lloyd *et al*., 1999).

Aconitase from *S. viridochromogenes*, similarly as all other aconitases, possess the [4Fe-4S] cluster, which is present in the active site of the enzyme. Aconitases are composed out of four domains. Three domains, forming a base triangle, are located around the catalytic center and the fourth domain is localized on the top of the active site (Dupuy *et al*., 2006). Aconitases can be classified in three groups depending on the position of the peptide linker, which binds the three base domains with the domain on the top (Fig. 3) (Gruer *et al*., 1997). Group A includes the aconitase type A from prokaryotes, mitochondrial (mAcn) and cytosolic (cAcn) aconitases from eukaryotes, as well as iron regulatory proteins (IRPs) (Lauble *et al*., 1994). Aconitase type B, that possesses an additional fifth domain, is found in Gram-negative bacteria, such as *E. coli* or *Helicobacter pylori* (Williams *et al*., 2002). The C group, which lacks any linker at all, contains isopropylmalate aconitase (IPMI), homoaconitases and Aconitase X from Archaea (Yasutake *et al*., 2004).

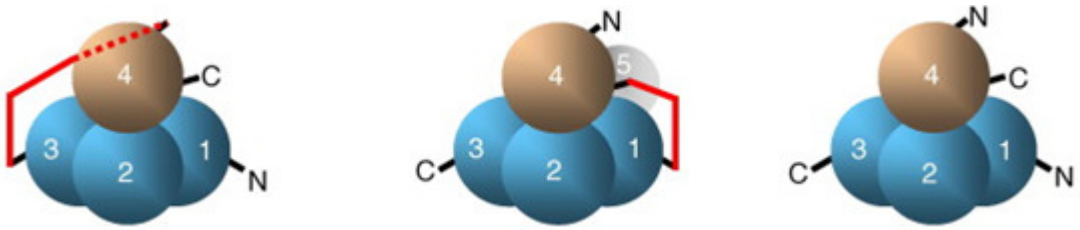

Fig.3 Domain organization of the members of the aconitase family (Schinko *et al*., 2009).

In the substrate free aconitase the [4Fe-4S] cluster is ligated to cysteine residues via three out of four Fe atoms. The fourth Fe atom contains a hydroxyl group, which is the site of substrate interaction. Binding of substrate leads to the protonation of this hydroxyl group, which increases the coordination number of Fe from four to six. It is known that at least 23 amino acid residues from all four domains of aconitase contribute to the function of the active site. All the residues involved in [4Fe-4S] cluster formation, substrate recognition and catalysis have been identified (Lloyd *et al*., 1999; Lauble *et al*., 1992; Lauble *et al*., 1994).

In addition to the aconitase from primary metabolism, *S. viridochromogenes* possesses an additional aconitase-like enzyme called Pmi (phosphimomethylmalate isomerase). This enzyme drives the isomerization of phosphinomethylmalate to isophosphinomethylmalate during the biosynthesis of PTT. AcnA and Pmi show 55% similarity on protein sequence level. Also the two corresponding reactions catalyzed by these enzymes are highly similar. However, AcnA and Pmi probably cannot substitute for each other. (Heinzelmann *et al*., 2001; Schinko *et al*., 2009). Beside that, the two enzymes are presumably differently regulated, since their promoter regions show no similarities. The transcription of *pmi* is influenced by the pathway specific activator PrpA, whereas the promoter region of *acnA* includes binding sites for global regulators, such as Fur or MarR that are known to be involved in iron stress response (Heinzelmann *et al*., 2001; Schinko *et al*., 2009). Probably AcnA and Pmi evolved from some ancient aconitase gene by gene duplication and thus represent an example of evolution of secondary metabolism specific enzyme from primary metabolism enzyme (Heinzelmann *et al*., 2001). The occurrence of secondary metabolism genes with counterparts in primary metabolism was also identified e.g. in *S. coelicolor* for the acyl carrier protein *acpP* gene in actinorhodin biosynthesis or for the p-aminobenzoate synthase gene *pab*AB in folic acid and chloramphenicol biosynthesis in *S. venezuelae* (Revill *et al*., 1996; Brown *et al*., 1996).

3.6. Oxidative stress and the role of iron regulatory proteins (IRPs)

Iron is necessary for all living organisms but exhibits also a potential toxicity. Therefore, uptake and storage of iron is a very important cellular function. During oxidative stress but also as a side product of aerobic growth, reactive oxygen species are formed. The cellular iron level and oxidative stress are often regulated together in Fenton reaction. This reaction is catalyzed by iron ions and these use hydrogen peroxide and superoxide anions ($\cdot O^{2-}$) as substrates. As a consequence reactive radicals are produced that damage DNA and organic compounds in the cell. In bacteria the stress response is controlled primarily by transcriptional regulators, such as Fur (regulator of iron metabolism), SoxRS (regulator of superoxide dismutase), OxyR (regulator of antioxidant genes), FNR (regulator of genes involved in adaptation to growth under oxygen limiting conditions) or MerR (multiple regulator) (Pohl *et al*., 2003; Demple, 1991; Kiley and Beinert, 1998; Brown *et al*., 2002). However, one of the mechanisms helping to overcome the problem of oxidative stress and iron storage involves the action of iron recognition proteins (IRPs).

In mammals IRP1 (the cytoplasmic aconitase) is such a protein. All bacterial aconitases are related to IRPs from mammals. IRPs have a catalytic activity but also show regulatory function. Under iron sufficiency conditions IRPs act as enzymatically active aconitase but when the iron concentration decreases, the [4Fe-4S] cluster of aconitase is disassembled and the enzyme loses its catalytic activity. As a consequence of this structural change, the protein becomes opened and accessible for the binding to specific sequences: iron responsive elements (IREs) (Dupuy *et al*., 2006). IREs are stem-loop structures of ribonucleotides that are located on the untranslated regions (URTs) of mRNAs encoding genes involved in iron metabolism, oxidative stress response or morphological differentiation. For IRP1 it has been shown that its binding to the 5' end of UTRs inhibits translation, while binding to the 3' end stabilizes the transcript by protecting it from ribonucleases and thus promotes translation (Muckenthaler *et al*., 2008). The IRE sequences of all eukaryotes are conserved. They consist of five bases forming a CAGUG loop, five unspecific bases forming the stem and a cytosine (C) at the bulge position. IRPs bind to IREs through the loop region and through the C that forms the bulge on the IRE

stem (Henderson *et al*., 1994). In prokaryotic cells, the IRE loop sequence can differ from the consensus sequence of eukaryotes (Tang and Guest, 1999; Alen and Sonenshein, 1999; Banerjee *et al*., 2007). Additionally, instead of the typical C at the bulge position also an 'A bulge' can form a functional IRE sequence (Henderson *et al*., 1994) (Fig.4). For several bacterial organisms including *Escherichia coli*, *Bacillus subtilis* or *Mycobacterium tuberculosis* it has been shown that their aconitases also possess a regulatory function (Tang and Guest, 1999; Alen and Sonenshein, 1999; Banerjee *et al*., 2007). In *S. viridochromogenes* both, AcnA and Pmi harbor a conserved motif (DLVIDHSIQVD) on the N-terminus of the respective proteins that is involved in IRE interaction (Schinko *et al*., 2009). However, only AcnA exhibits a clear regulatory activity (Schinko *et al*., 2009).

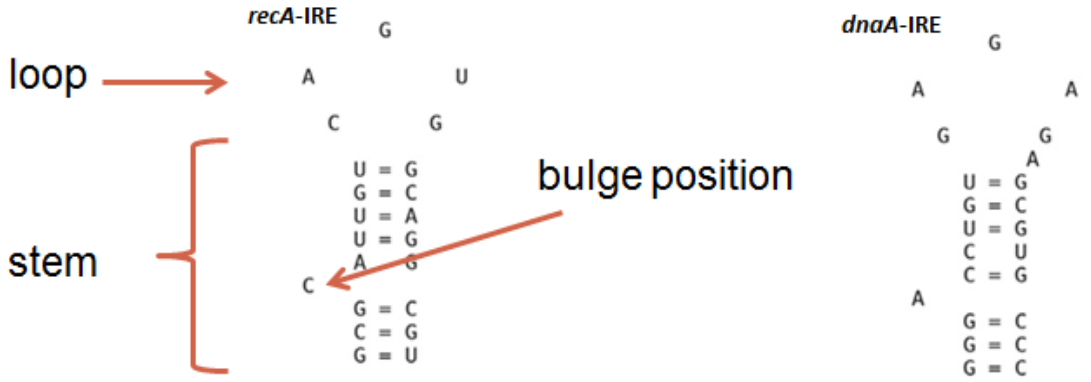

Fig. 4 The examples of the secondary IRE structures, from *S. viridochromogenes* genome, with different loop sequences and bulge positions.

3.7. Regulatory activity of aconitases in Gram-negative and Gram-positive bacteria

Two phylogenetically distinct aconitases were isolated from *E. coli*: AcnA and AcnB. AcnA is expressed during stationary phase and is specifically induced by iron and oxidative stress. AcnB is synthesized during exponential growth, shows higher catalytic activity but is less stable than AcnA. Due to the higher activity, AcnB is considered to be the major TCA cycle aconitase. Both of them, regardless to their catalytic activity, exhibit also regulatory functions (Tang and Guest, 1999). AcnB shows a different organization of the protein domains because it contains a fifth HEAT-like domain. Nevertheless, AcnB is still highly

conserved at the active site. In other proteins the HEAT domain is involved in protein-protein communications, thus it is possible that in AcnB this domain provides a surface for such interactions (Williams *et al*., 2002). Moreover, AcnB form homodimers. The formation of these homodimers requires iron, while the binding to mRNA is inhibited by iron. Thus, it was proposed that the monomer-dimer formation mediated by the concentration of iron is involved in switching between the catalytic and regulatory form of this protein. Interestingly, in this case the iron availability is not sensed by the [4S-4Fe] cluster but by a regulatory side located in domain 4. It was suggested that the dimer acts catalytically and the monomer as a post-transcription regulator (Tang *et al*., 2005). What is more, for *E. coli* it has been shown that the synthesis of AcnA and AcnB is positively autoregulated at post-transcriptional level. AcnA and AcnB interact with 3' UTRs of the *acnA* and *acnB* mRNA under oxidative stress conditions. Apo-AcnB shows a higher affinity to acn 3' UTRs than apo-AcnA. Thus, AcnB plays the major role in response to oxidative stress by enhancing the synthesis of the more stable AcnA for survival purposes (Tang and Guest, 1999). Moreover, AcnA and B have an opposite effect on the synthesis of superoxide dismutase (SodA). The stability of the *sodA* transcript is reduced by AcnB but enhanced by AcnA. By modulating the translation of *sodA* expression, aconitases in *E. coli* protect the cells against the basal level of oxidative stress (Tang *et al*., 2002).

It has been shown that also aconitases from Gram-positive bacteria, such as that of *B. subtilis* exhibit bifunctional activity. In *B. subtilis* the aconitase is encoded by a single gene *citB*. The product of this gene can specifically bind to IRE-like sequences located on the mRNA of some iron related genes, such as *goxD*, coding for an iron containing protein cytochrome aa_3 oxidase, and *feuAB*, coding for receptors of iron (Alén and Sonenshein, 1999). It is known that the catalytic activity of the aconitase is required for the initiation of sporulation (Craig *et al*., 1997). A null mutation of *citB* causes accumulation of citrate and a block of genes expression which are dependent on Spo0A-the major transcription factor for early sporulation-specific genes. It has been suggested that citrate sequesters divalent cations that are needed for phosphorelay system involved in the activation of Spo0A (Craig *et al*., 1997). This dysfunction

is related to the lack of the catalytic activity of aconitase. However, late sporulation requires a second function of aconitase. When the site-directed mutagenesis was used to create a *B. subtilis* aconitase mutant that retained catalytic activity but lost RNA binding activity, the resulting strain had a defect at the late stage of sporulation. Furthermore, *in vitro* experiments have shown that *B. subtilis* aconitase can bind to 3' UTR of *greE* mRNA and stabilize the transcript. GreE is a transcription regulator of many genes required for the late sporulation. In this case the lack of regulatory activity of aconitase is responsible for the improper spore formation (Serio *et al*., 2006).

In *M. tuberculosis* the aconitase is encoded by a single copy of the *acn* gene. Acn is a monomeric, bifunctional protein. In gel retardation assays it has been shown that *M. tuberculosis* can bind to known mammalian IRE-like sequence, as well as to 3' UTR of thioredoxin (*trxC*) and 5' UTR of the iron-dependent repressor and activator IdeR (*ideR*), present in the *M. tuberculosis* genome (Banerjee *et al*., 2007).

In some pathogenic bacteria, such as *Staphylococcus aureus*, *Xanthomonas campestris* pv. *campestris*, or *Pseudomonas aeruginosa*, aconitases are involved in the regulation of the production of pathogenicity factors (Somerville *et al*., 1999; Wilson *et al*., 1998). It has been shown for *S. aureus* that the aconitase mutant enters earlier into stationary phase and produces lower amount of virulence factors (Somerville *et al*., 2002). Furthermore, in the mouse tissue infection model, the *S. aureus* aconitase mutant caused the decreased production of bactericidal oxidants, such as nitric oxide ($NO^{\cdot}$). Therefore, it has been speculated that aconitase disruption may alert the host's response to the bacteria (Massilamany *et al*., 2011). In *Salmonella enterica* serovar Typhimurium AcnB regulates the flagellum protein (FliC) synthesis on post-transcriptional level. Consequently, the *acnB* mutant possesses less flagellum, is less motile and exhibits impaired binding to the surface of macrophage-like cells (Tang *et al*., 2004).

Objectives

The goal of this study is to analyze the regulatory function of aconitase from *S. viridochromogenes* Tü494. Gel shift assays aim to validate the functionality of *in silico* identified iron regulatory motifs (IREs) and to show that AcnA from *S. viridochromogenes* is an RNA-binding protein. It is also in focus to analyze if the interaction between aconitase and IREs is sequence specific and requires secondary structure of RNA.

Another objective of this work is to provide *in vivo* evidence for the AcnA-mediated post-transcriptional regulation of the recombinase A (RecA) synthesis, which is required to repair DNA damage under oxidative stress. The RT-PCR analysis of the *recA* transcript stability in the WT and MacnA under oxidative stress aims to prove that AcnA stabilizes *recA*-mRNA.

A proteomic approach was taken to compare the proteome of the WT and MacnA under oxidative stress in order to provide more insight into the regulatory function of AcnA and to identify enzymes that are involved in *S. viridochromogenes* oxidative stress adaptation.

4. Results

4.1. The influence of *acnA* mutation on the physiology of *S. viridochromogenes* Tü494

The *S. viridochromogenes* MacnA mutant shows strong morphological and physiological defects. This strain does not form any aerial mycelium, is unable to sporulate and to produce PTT (Schwartz *et al*., 1999). Here, the aim was to reveal the reasons for the severe growth defect of MacnA and to determine if the lack of AcnA-mediated regulation contributes to the impaired physiology of the mutant strain (Publication 1, Michta *et al*., 2012).

4.1.1. The influence of accumulated organic acids on MacnA growth and differentiation

For *S. coelicolor* it has been shown that the *acnA* mutation resulted in the accumulation of citrate (Viollier *et al*., 2001a). To analyze if the intracellular accumulation of citrate contributes to the growth defect of MacnA in *S. viridochromogenes*, the WT strain was plated on agar plates with increasing concentrations of trisodium citrate, which presumably is transported into the cells via citrate transporters. In *S. viridochromogenes* at least two citrate transporters have been identified (SSQG_01282, SSQG_01602). For comparison, the WT was also grown in the presence of other organic acids that also might be accumulated as a consequence of *acnA* lesion, what has been shown for *S. coelicolor* (Viollier *et al*., 2001b). On plates with 2 mM trisodium citrate the WT showed normal growth, whereas on plates with 10 mM trisodium citrate only the substrate and aerial mycelium were formed but no spore production was observed. The agar plate supplementation with 20 mM trisodium citrate additionally led to the lack of aerial hyphae formation. This morphology reflects the phenotype of the MacnA mutant. Interestingly, when the same concentrations of other organic acids, such as sodium acetate or succinic acid were added to the medium, *S. viridochromogenes* WT growth was normal and only spore production was impaired at 20 mM of sodium acetate or succinic acid (Fig. 5). Obviously, the high concentration of citrate influences the normal

growth behavior of the WT. Thus, accumulation of citrate in MacnA may contribute to its defective morphology. This might be because citrate is a strong chelator of divalent cations, which are important for the functioning of enzymes involved in the sporulation process (Craig *et al*., 1997). Moreover, these results show that accumulation of another organic acids as well as medium acidification is not the main reason for the growth defect of the *S. viridochromogenes acnA* mutant.

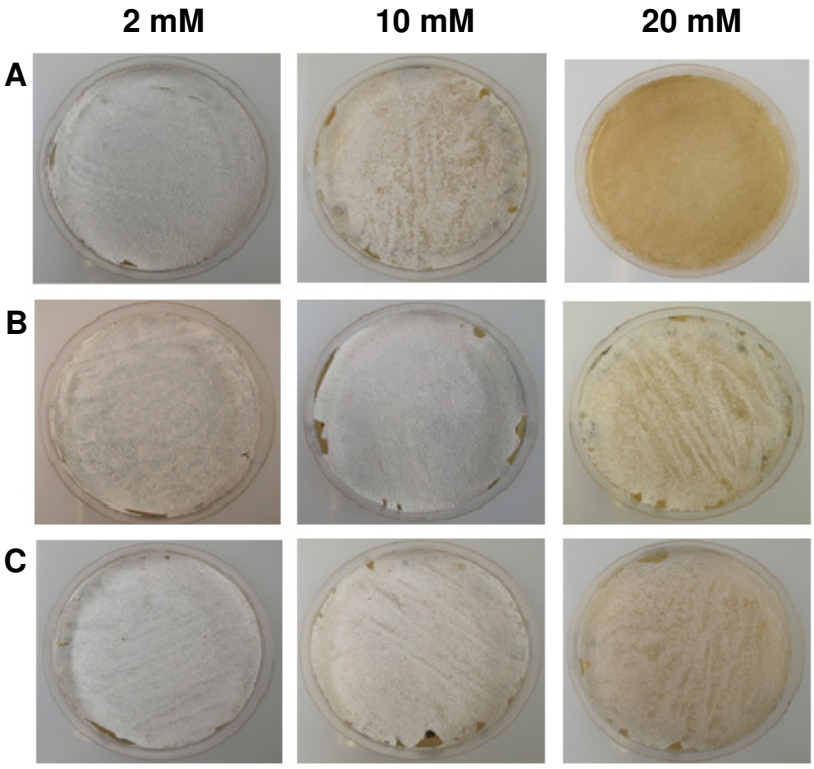

Fig. 5 Morphological comparison of *S. viridochromogenes* WT. The strain was grown on YM agar plates supplemented with different concentrations of organic acids: trisodium citrate (A), sodium acetate (B), succinic acid (C) (Publication 1, Michta *et al*., 2012).

4.1.2. The influence of oxidative stress and increasing temperature on the growth of MacnA

To study the influence of oxidative stress on the growth behavior of MacnA in comparison to the WT, the sensitivity of both strains towards hydrogen peroxide (H_2O_2) was examined (Publication 1, Michta *et al*., 2012). WT and MacnA were grown on HM agar plates in the presence of filter rings soaked with different concentrations of hydrogen peroxide (H_2O_2). Inhibition zones caused by the toxicity of hydrogen peroxide were observed on both plates, however they were significantly larger in MacnA than in the WT strain (Fig. 6).

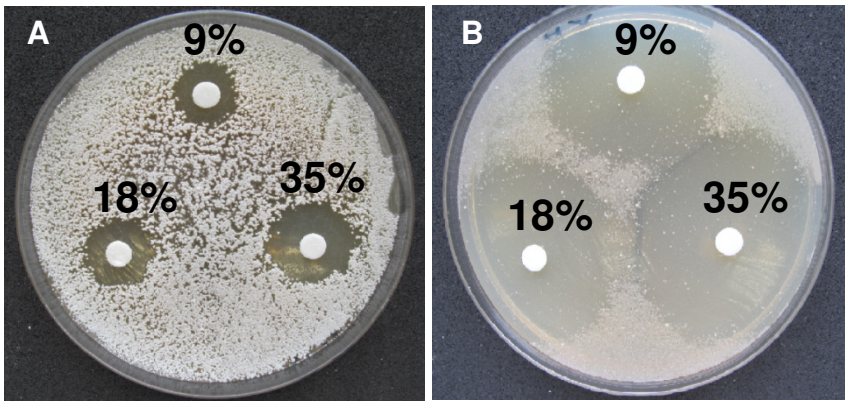

Fig. 6
The susceptibility of WT (A) and MacnA (B) to oxidative stress. Filter rings contain indicated concentrations of H_2O_2 (Publication 1, Michta *et al.*, 2012).

It is known that an increased temperature enhances the production of hydroxyl radicals (Lüders *et al.*, 1999). Thus, also the heat stress resistance of the WT and the MacnA mutant were tested (Publication 1, Michta *et al.*, 2012). Liquid cultures of both strains were incubated at 27°C, 37°C and 39°C respectively (Fig. 7). The WT strain showed no sensitivity towards high temperatures. In contrary, the MacnA was highly sensitive and was unable to grow already at 37°C.

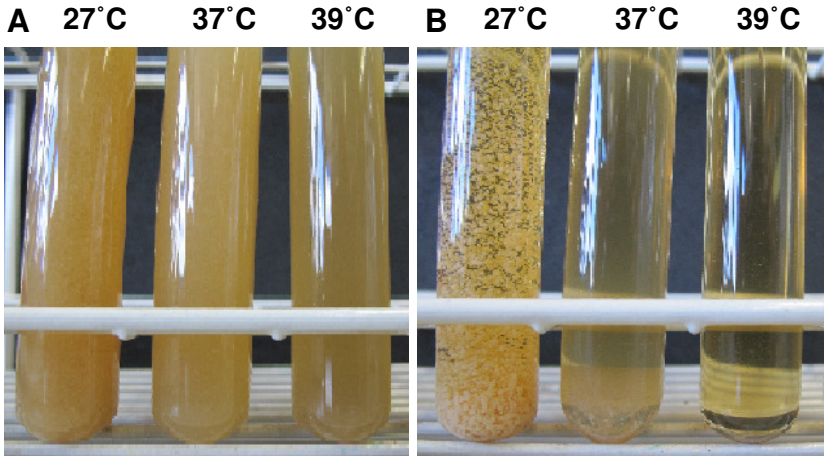

Fig. 7
The susceptibility of *S. viridochromogenes* WT (A) and MacnA (B) to heat stress.

The higher sensitivity of MacnA to oxidative and heat stress may be related with the lack of AcnA-mediated regulation. For *E. coli* it has been shown that the *acnA* mutation confers hypersensitivity to oxidative stress due to the lack of superoxide dismutase A (*sodA*) transcript stabilization by AcnA (Tang *et al.*, 2002). Additionally, the high sensitivity of MacnA to oxidative stress may result from the lack of an alternative protective function of AcnA: the AcnA protein is particularly susceptible for superoxide attack, thus very effectively spare other targets from reactive oxygen species (Messner and Imlay 1999). The absence

of this protective buffer may enhance the sensitivity of the mutant strain to oxidative or heat stress.

4.2. Analysis of the regulatory role of AcnA

4.2.1. Heterologous expression of AcnA derivatives in *S. lividans* T7

To analyze the regulatory role of AcnA from *S. viridochromogenes* different derivatives of the AcnA protein: his-AcnA(Δ125-129), his-AcnA(C538A), his-AcnA(R763E/R767E) have previously been constructed (Schad, 2006). In this work, his-AcnA as well as its mutated derivatives were overexpressed in *S. lividans* T7, purified under native conditions on FPLC and visualized on SDS-PAGE (Fig. 8) (Publication 1, Michta *et al*., 2012).

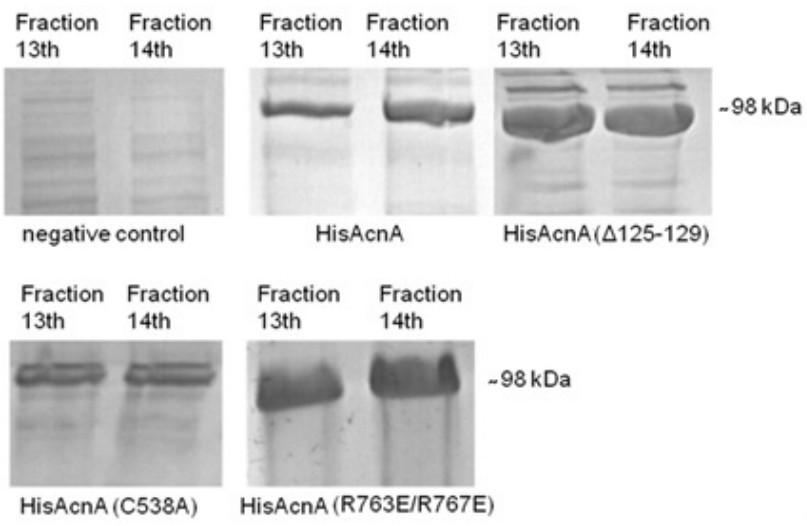

Fig. 8

Determination of the molecular weight of the overexpressed his-AcnA and its mutated his-tagged derivatives: AcnA(Δ125-129), AcnA(C538A), AcnA(R763E/R767E). Purification fractions 13th, 14th were used in band shift assays.

Due to the highly oxidative conditions provided by high imidazol concentration, the [4Fe-4S] cluster was disassembled during the purification process. As a consequence all purified proteins were present in the apo-form and possessed an open [4S-4Fe] cluster accessible for the binding to IREs. Protein purification fractions containing pure, sufficiently concentrated protein were used in band shifts assays with Cy5 labeled RNA that comprises the IRE structures identified *in silico* in *S. viridochromogenes* genome (Fig. 10-14). Shifts with lysate from *S. lividans* T7 with the empty vector served as negative control.

The his-AcnA(Δ125-129) was purified and used in band shift assays to determine if the putative amino acids 125-129 (Fig. 9) are involved in RNA

coordination as it has been reported previously (Basilion *et al*., 1994). The catalytically inactive his-AcnA(C538A) and the regulatory inactive his-AcnA(R763E/R767E) aconitase derivatives were used to examine if the catalytic and the regulatory roles of AcnA are interconnected (Fig. 13A). The his-AcnA(C538A) protein does not show catalytic activity because the cysteine 538 is crucial for [4Fe-4S] cluster coordination. Thus, the replacement of the Cys538 by the alanine residue leads to the catalytic inactivity of AcnA. Arg763 and Gln767 (Fig. 9) were predicted as amino acids involved in the regulatory function of AcnA in *S. viridochromogenes*. This prediction was done by comparison of the AcnA with the human IRP1 which is highly similar, possess regulatory activity and for which crystal structure exists (Dupuy *et al*., 2002).

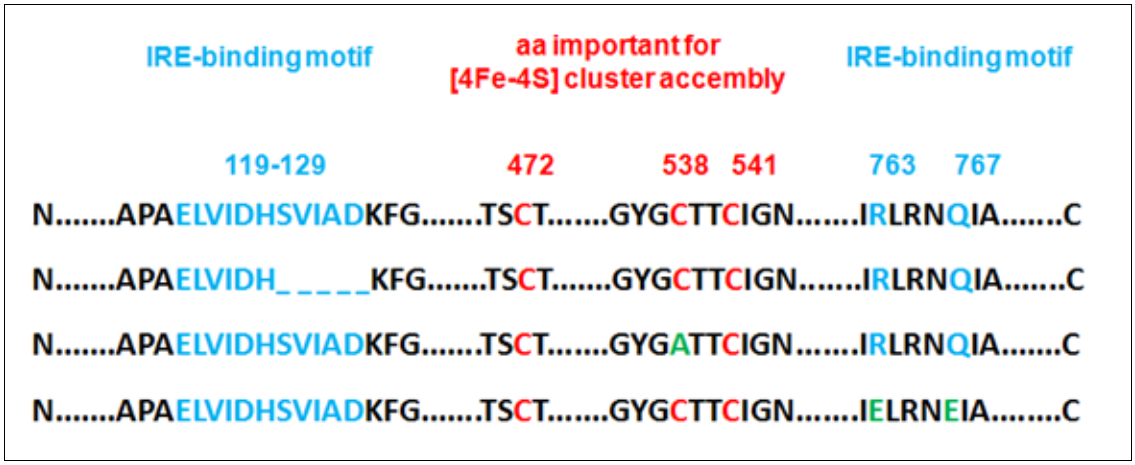

Fig. 9 Composition of amino acid sequences (from the top): his-AcnA, his-AcnA(Δ125-129), his-AcnA(C538A) and his-AcnA(R763E/R767E). Deleted amino acids are marked with dash (_), substituted amino acids are marked with green color.

4.2.2. *In vitro* analysis of AcnA binding to IRE-like structures

To confirm the regulatory role of AcnA from *S. viridochromogenes* and to examine if the identified IREs of the strain with different loop sequences really serve as binding sites for AcnA, band shift assays were performed with his-AcnA and its mutated derivatives (Publication 1, Michta *et al*., 2012). The lysate from *S. lividans* T7 with the empty vector served as negative control. Shifts performed with his-AcnA and his-AcnA(Δ125-129) together with chemically synthesized RNA containing the *recA* and *ftsZ* IRE sequences as targets, confirmed that both structures form complexes with the his-AcnA, as well as

with the mutated his-AcnA(Δ125-129). Shifts did not appear in a control sample (empty vector) and in samples where protein was not added. None of the proteins prefer the GAGAG loop of *ftsZ* or the CAGUG loop of *recA*. Both RNAs were recognized identically (Fig. 10). Interestingly, the his-AcnA(Δ125-129) always led to stronger shifts than the his-AcnA. This indicates that his-AcnA(Δ125-129) has a stronger affinity to IRE motifs than the native protein.

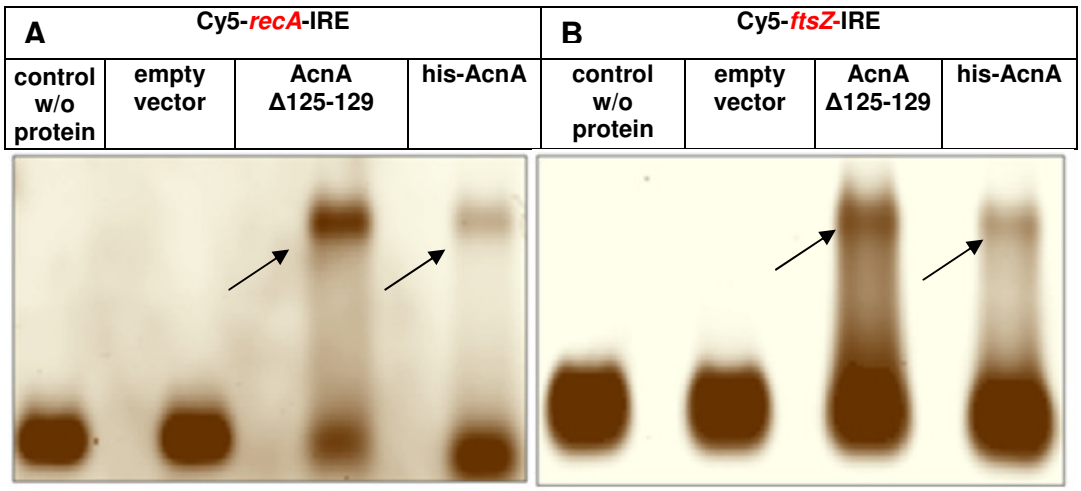

Fig. 10 Analysis of the complex formation between the his-AcnA or his-AcnA(Δ125-129) and *recA*-IRE (A) or *ftsZ*-IRE (B) (Publication 1, Michta *et al.*, 2012).

To verify the specificity of aconitase-IRE binding, increasing concentrations of unlabeled *recA*-IRE were added to the mixture. It led to the decrease of Cy5-*recA*-IRE complex formation. The unlabeled *recA*-IRE gradually displaced the Cy5-*recA*-IRE from the protein (Fig. 11).

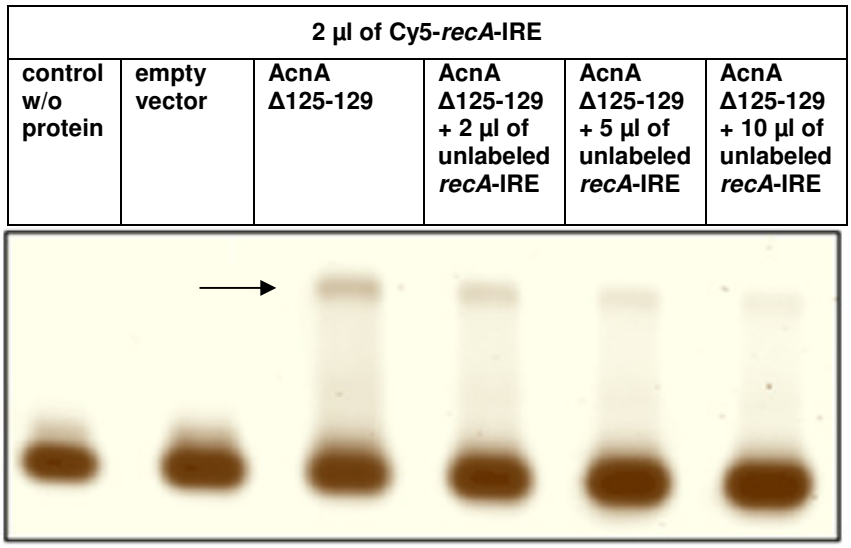

Fig. 11 Analysis of the specificity of aconitase-IRE binding: constant concentration of Cy5-*recA*-IRE with his-AcnA(Δ125-129) and increasing concentrations of unlabeled *recA*-IRE.

To confirm that the protein can bind to RNA only in the form which is devoid of the [4Fe-4S] cluster, the protein was reactivated after purification using reducing conditions in the presence of iron salt. The rebuilt [4Fe-4S] cluster prevented aconitase from complex formation, which proves that the only open, Fe-devoid cluster is accessible for RNA binding (Fig. 12A.). As an additional control, the binding of his-AcnA(Δ125-129) to an internal fragment of *hrd*B-mRNA was examined. This fragment does not possess any IRE-like structure. Even at high concentration of the protein, no complex formation was detected with *hrd*B and his-AcnA(Δ125-129) (Fig. 12B). This demonstrated that binding of aconitase is IRE-sequence specific.

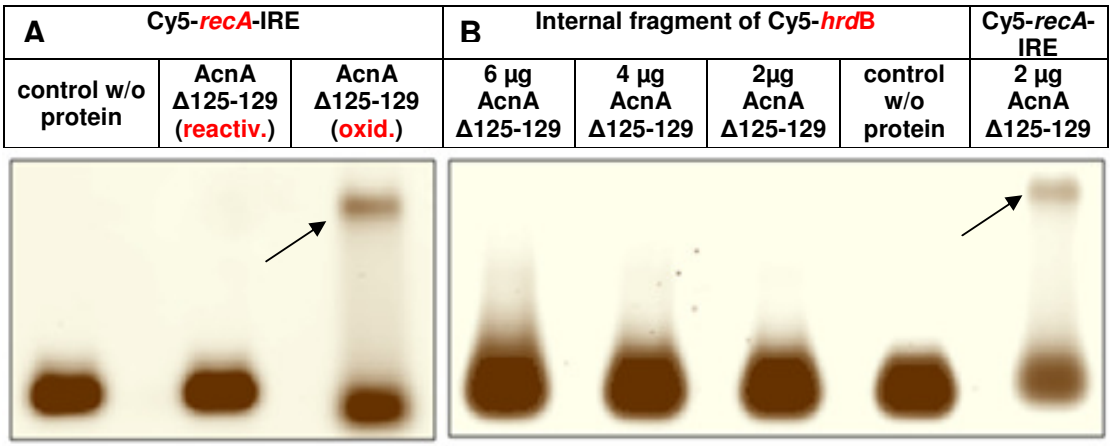

Fig. 12 Analysis of the interaction between *recA*-IRE and oxidized or reactivated his-AcnA(Δ125-129) (A); control analysis: lack of complex formation between his-AcnA(Δ125-129) and internal fragment of *hrdB* (B).

In order to analyze if the regulatory activity of AcnA is interconnected with its catalytic function, the catalytically inactive aconitase his-AcnA(C538A) was assayed for *ftsZ*-IRE binding. In these gel shift assays a shifted band was observed what indicates that the mutation C538A preventing the [4Fe-4S] cluster formation does not disturb the RNA-binding ability. In contrast, his-AcnA(R763E/Q767E) mutated in the amino acids that are responsible for the coordination of the RNA, could not bind to the IRE-like structure of *ftsZ*. Thus, his-AcnA(R763E/Q767E) is regulatory inactive (Fig. 13A.). This result confirmed the involvement of the two predicted amino acids arginine 763 and glutamine 767 in RNA coordination. Interestingly, this protein was also catalytically

inactive in previous enzymatic assay (Schad, 2010). It points out that some of the same amino acids are involved in both functions of AcnA.

To determine if the secondary stem-loop structure formed by IREs is necessary for AcnA recognition and binding, the shift experiments were performed with his-AcnA(Δ125-129) and *recA*-IRE where the stem and the loop were absent as they were exchanged with a sequences that cannot form any secondary structures. Only the native *recA*-IRE sequence was recognized by his-AcnA(Δ125–129). The IREs without stem structure or with changed loop sequence did not shift. These results showed that the presence of both, stem and loop are essential for AcnA binding (Fig. 13B).

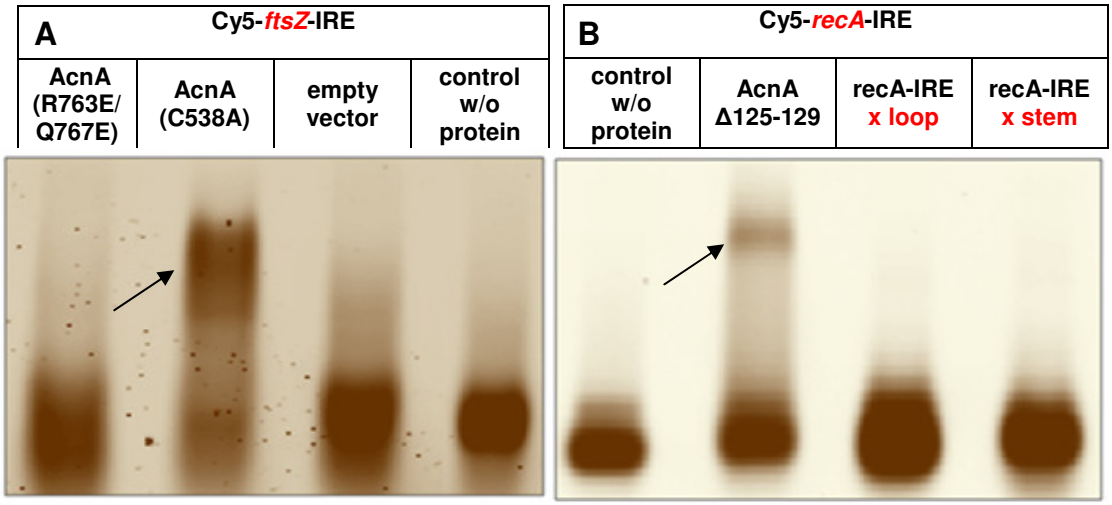

Fig. 13 Analysis of the interaction between *ftsZ*-IRE and his-AcnA(R763E/Q767E) or his-AcnA(C538A) (A); Interaction analysis of his-AcnA(Δ125-129) with recA-IRE without stem or loop (B) (Publication 1, Michta *et al*., 2012).

To further elucidate if *in silico* identified IRE sequences are also targets for aconitase, the RNA fragment containing the *SSQG_00552* IRE sequence with a CUGUG loop, *SSQG_1218* IRE with a CAGUG loop as well as four different RNAs harboring a CAGCG loop were assayed in gel shifts with his-AcnA(Δ125–129). Only the *SSQG_00552* (coding for FAD-binding oxidoreductase) and *SSQG_1218* (coding for uracil-DNA glycosylase) RNA samples were shifted. All the RNAs with the CAGCG loop were not recognized by his-AcnA(Δ125-129). Furthermore, the *SSQG_00552* IRE was bound with the same efficiency as control *recA*-IRE and *SSQG_01218*-IRE. Thus, the CUGUG loop was not

preferred over the CAGUG loop (Fig. 14). These data confirmed that *SSQG_00552* and *SSQG_01218* are functional IREs recognized by AcnA.

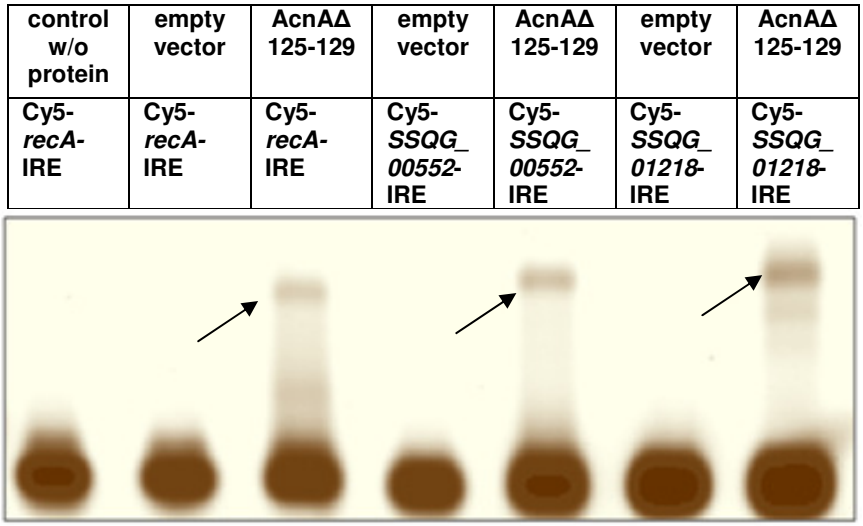

Fig. 14 Analysis of the his-AcnA(Δ125-129) binding to the *recA*-IRE, *SSQG_00552*-IRE and *SSQG_0121*-IRE, respectively (publication 1, Michta *et al*., 2012).

4.2.3. Transcriptional analyses to study the role of AcnA in the regulation of *recA* expression under oxidative stress conditions

Since AcnA binding to *recA*-IRE in shift experiments has been shown, it was the aim to prove *in vivo* that AcnA really regulates the RecA synthesis on post-transcriptional level. Thus, we investigated the *recA* transcript stability under oxidative stress conditions by RT-PCR (Publication 1, Michta *et al*., 2012). We also expected to confirm the previously obtained Western-blot results where the addition of methyl viologen (MV) resulted in a higher amount of RecA protein in the WT strain but not in MacnA (Schad, 2010). For the RT-PCR experiment the WT and MacnA strains were grown to the mid-exponential phase, when rifampicin was added in order to exclude any regulatory effect on transcriptional level. To apply oxidative stress and to convert the majority of the AcnA proteins into the regulatory active form, MV was added to the cultures. The supply of oxidative stress in the presence of rifampicin led to a higher transcript stability of *recA*-mRNA in WT in comparison to MacnA. This suggests that the *recA* transcript is stabilized by AcnA. Together with the previous Western-blot analysis, these results support the post-transcriptional regulatory role of AcnA in the synthesis of RecA under the condition of oxidative stress (Fig. 15).

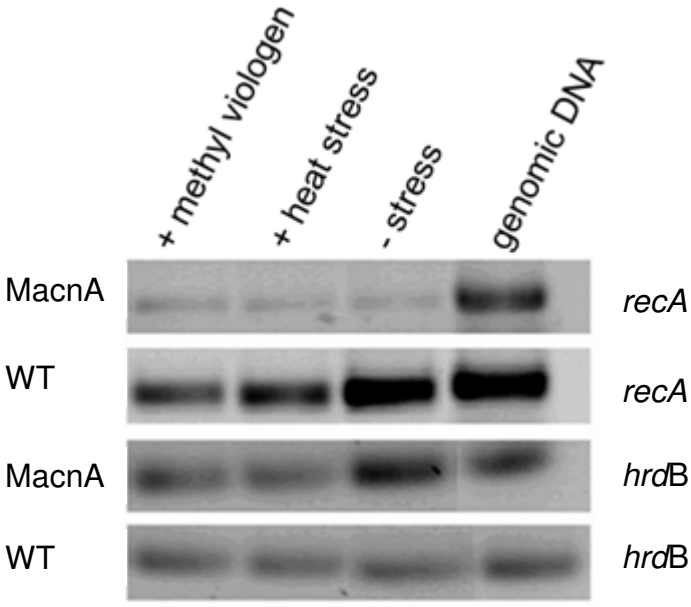

Fig. 15
The RT-PCR analysis of *recA* transcript amount during mid-exponential growth phase in WT in comparison to MacnA. The constitutive transcript of *hrd*B was used as control (Publication 1, Michta *et al.*, 2012)

4.2.4. The use of artificial IRE motifs for the AcnA-mediated transcript stabilization

PrpA is a putative pathway-specific transcription regulator that binds to the promoter regions of several genes of the PTT gene cluster. The inactivation of *prpA* resulted in a PTT-non producing mutant (Muschko, 2005). Since it has been shown that PrpA is an activator of PTT biosynthesis, the aim of this experiment was to examine in bioassays a change in antibiotic production due to the *prpA* transcript stabilization in the presence of artificial IRE motifs. According to what has been shown for eukaryotes (Muckenthaler *et al.*, 2008), it was expected that the presence of an IRE on the 3' end of *prpA* will stabilize the transcript while its presence on the 5' end will prevent translation, due to AcnA-mediated regulation.

First, an artificial IRE sequence was cloned at the 3' end of *prpA* by using genomic DNA as a template and primers ATTCTAGACGGCCCTGACGGCCACGCGGCT and GAATTCGCCCTGGACGGCCAGTGGCCGTTCGCGGCCGGTGCGG. The latter primer (reverse) contained an IRE sequence located 50 bp after the transcriptional stop codon of *prpA*. The 1307 bp large *prpA* fragment containing the 3' IRE was cloned into pDrive, excided with *Xba*I and *Eco*RI and cloned in the vector pTS/kan. The pTS/kan vector contains a kanamycin resistance cassette and integrates into the genome via the attachment site. The *S.*

viridochromogenes ΔprpA mutant, with an apramycin cassette instead of the *prpA* gene, was complemented with pTS/kan carrying *prpA* with the 3' IRE motif under the native *prpA* promoter. The *ΔprpA* mutant complemented with pTS/kan carrying the *prpA* gene without an IRE motif served as a control. The constructed complementation plasmids were sequenced and the complemented *ΔprpA* mutant was checked by PCR for the presence of the *aphII* (969 bp), *apra* (689 bp) and *prpA* (819 bp) genes (Fig. 16).

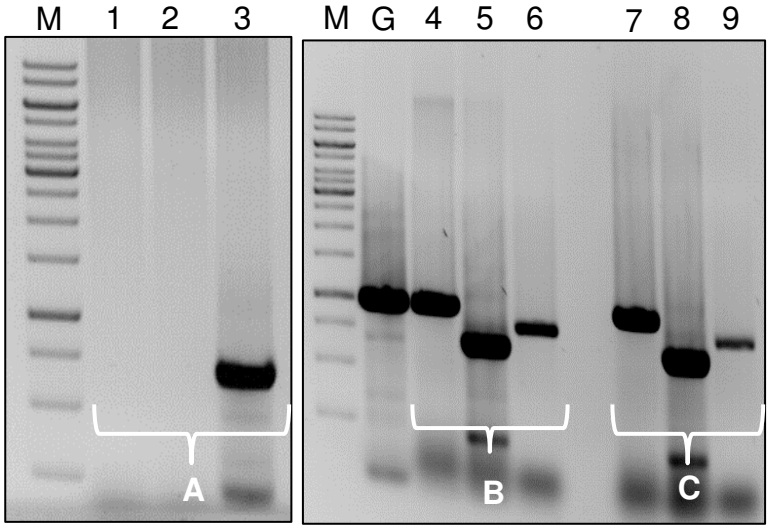

Fig. 16
PCR confirmation of the *ΔprpA* mutant (A) and its complementation with: pTS+3' IRE *prpA* (B) and pTS+*prpA* (control) (C). 1, 4, 7 kanamycin primers; 3, 5, 8 apramycin primers; 2, 6, 9 internal *prpA* primers. M-marker, G-genomic DNA

The *prpA* transcript stability under oxidative stress was compared between the WT strain, the control strain and the *ΔprpA* mutant complemented with 3' IRE *prpA* gene. All three strains were grown in liquid medium for 24 h when rifampicin and MV were added to the cultures. The RNA was isolated and RT-PCR was performed in order to assess the stability of the *prpA* transcript.

It turned out that the *prpA* transcript was more stable in the *ΔprpA* mutant complemented with 3' IRE *prpA* than the *prpA* transcript from WT strain or the one from the control (Fig. 17). At the same time no increase in PTT production was detected in bioassays. However, the overexpression of *prpA* previously also did not lead to increased antibiotic production (Schwartz *et al.*, 2004). Intriguingly, the presence of the *prpA* gene was not detected at all in the WT strain. The reason for that might be the very early time point of the sample collection for RNA isolation. Perhaps the onset of secondary metabolism did not occur yet and thus the *prpA* transcript was not detected.

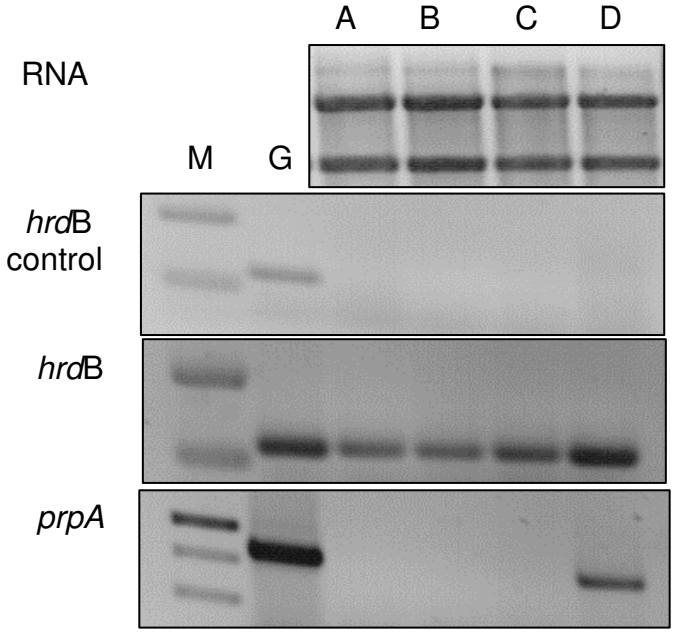

Fig. 17
RT-PCR analysis of *prpA* transcript stability. WT (A), *ΔprpA* (B), *ΔprpA*+pTS *prpA* (control) (C), *ΔprpA*+pTS 3' IRE *prpA* (D). M-marker, G-genomic DNA.

4.3. Comparative proteomic analysis of *S. viridochromogenes* MacnA in response to oxidative stress

A comparative proteomic approach was used to analyze the regulatory role of AcnA in changes of protein expression that may contribute to the weakened defense of MacnA against free radicals, as well as those important for the *S. viridochromogenes* oxidative stress adaptation (Publication 2, Michta *et al.*, 2014).

The shift assays, RT-PCR analysis and previously performed immunoblot experiment indicated that AcnA plays an important role in resisting peroxide stress by influencing the expression of the proteins that are important for oxidative stress defense. It has also been demonstrated that the *acnA* mutation confers sensitivity to H_2O_2 as likewise suggested previously for *E. coli* (Craig *et al.*, 1997).

Cultures of the WT and MacnA were grown to the mid-exponential phase. The bacteria were then treated with MV to disassemble the [4Fe-4S] cluster and to introduce the regulatory active form of AcnA. Samples untreated with MV served as controls. To differentiate the proteins perturbed by *acnA* lesion from those perturbed by stress conditions, the proteins with changed expression were identified separately for WT and MacnA. This was performed by a comparison of the proteome of the MV-treated WT strain with the proteome of the MV-untreated WT strain sample. The same was done for the MacnA

mutant. The protein spots with significant up- or downregulation due to oxidative stress treatment were later identified by mass spectrometry (Publication 2, Michta *et al*., 2014).

The changes identified in the WT strain included 62 protein spots, among which 37 were upregulated and 25 were downregulated. In the MacnA strain, 27 proteins were differentially expressed: 16 among them were upregulated and 11 were downregulated (Table S1 in Publication 2, Michta *et al*., 2014). The occurrence on the gel of a single protein as multiple spots was most likely due to post-translation modifications.

Because the proteomes of WT and MacnA were not matched with each other for visual protein inspection, the majority of the differentially regulated proteins identified in the WT strain were different from those detected in MacnA. However, this is commonly observed when proteomes of two different strains are not matched directly with each other (Yao *et al*., 2011; Xiao *et al*., 2011).

As expected, many of the significantly up- or downregulated spots were identified as proteins involved in sensing or preventing oxidative stress. Interestingly, several of them turned out to possess IRE motifs on their respective mRNAs (Table1 in Publication 2, Michta *et al*., 2014). This indicates that they might be targets for a direct post-transcriptional regulation by AcnA. The tellurium resistance protein SSQG_02339 and the translation elongation factor Tu SSQG_04757 were identified among the proteins with IRE motifs, which have putative functions in cellular stress defense. Moreover, they were differentially regulated in WT and MacnA due to oxidative stress, what provides a direct *in vivo* evidence for an AcnA-mediated regulation of these protein expressions upon oxidative stress.

Changes were detected also for several other proteins, which are involved in oxidative stress defense, such as a putative thioredoxin (SSQG_05458) (Zeller and Klug, 2006), a putative stress inducible protein (SSQG_00322) (Kvint *et al*., 2003; O'Toole *et al*., 2002; Boes *et al*., 2006), and a putative serine protease (SSQG_02132) (Clausen *et al*., 2002; Biswas *et al*., 2010). The downregulation of these proteins in MacnA indicates that *acnA* mutation is associated with the decreased production of anti-oxidative stress proteins what may significantly contribute to the impaired defense of the strain against free radicals. The

reduced expression of proteins with IREs may directly result from the lack of AcnA-mediated transcript stabilization.

Other significant changes caused by oxidative stress concerned proteins from carbon metabolism pathways, such as pentose phosphate pathway, glycolysis, TCA cycle and glycerol synthesis pathway. These data suggest carbon flux redistribution as an adaptation mechanism to this stressful condition. In the WT, the enzymes from pentose phosphate pathway (SSQG_00870 putative 6-phosphogluconate dehydrogenase) and TCA cycle (TBCG_03283 putative NADP-dependent isocitrate dehydrogenase (IDH-NADP)) were upregulated. Pentose phosphate pathway and TCA are especially important for NADPH generation. NADPH provides reducing equivalents for redox reactions protecting against ROS (Buchana and Balmer, 2005; Singh *et al*., 2007). Thus, upregulation of enzymes from both pathways probably leads to the increased NADPH level and contributes to the metabolic adaptation to oxidative stress. In contrary, in MacnA a downregulation of the putative IDH-NADP (SSQG_06852) was observed. This may lead to a cellular imbalance of reducing equivalents, which could contribute to the oxidative stress sensitivity of MacnA. However, none of these enzymes possesses an IRE motif. Thus, their regulation by AcnA may be only indirect. Also enzymes from glycolysis such as phosphopyruvate hydratase (SCO3096), phosphoglycerate kinase (SSQG_01870), and putative glyceraldehyde-3-phosphate dehydrogenase (GAPDH) (SSQG_01871, SSTG_00732) were differentially regulated by oxidative stress in WT. Changes in glycolytic enzymes due to oxidative stress and redirection of the carbohydrates flux towards the pentose phosphate pathway were shown previously for yeast cells (Ralser *et al*., 2007).

Another compound important for cellular response to oxidative stress is glycerol. It has been shown that glycerol is an efficient free radicals scavenger and regulates redox processes (Afzal *et al*., 2012). In MacnA the putative repressor of the glycerol catabolism pathway (SSQG_01539) was overexpressed. Consequently, the overexpression of the glycerol catabolism repressor may lead to an accumulation of glycerol and regeneration of reducing equivalents.

On the corresponding gene sequence of the phosphoglycerate kinase (SSQG_01870), the glyceraldehyde-3-phosphate dehydrogenase (SSQG_01871) and the putative glycerol operon regulatory protein (SSQG_01539) IRE motifs were identified, which suggests an AcnA-mediated regulation of the respective mRNAs.

Previous gel shift experiments showed that the *ftsZ*-IRE is a target for AcnA binding. In the proteomic analysis the cell division protein FtsZ (SSQG_02023) was significantly upregulated in the WT after MV application. Together these results strongly suggest an AcnA-mediated regulation of FtsZ expression. Changes were detected also for SepF1 (SSQG_01640) and SepF2 (SSQG_02020) which are putative cell division proteins associated with FtsZ. Both of them were downregulated under oxidative stress conditions in MacnA. Moreover, a secreted protein (SSQG_01691) similar to the sporulation control protein Spo0M of *B. subtilis* (Han *et al*., 1998) was upregulated in MacnA. This demonstrates that the regulation of proteins involved in cell division and sporulation processes is greatly changed by oxidative stress in *S. viridochromogenes*. However, in the case of the genes encoding SepF1, SepF2 or the Spo0M homologous protein no IRE elements were identified. Thus, the influence of the lack of AcnA regulation on their expression is indirect.

Taking together, many proteins from different metabolic pathways were identified in this global approach. Those proteins for which IRE motifs were identified on the corresponding mRNA sequences and which were differentially regulated in both strains provided a direct *in vivo* evidence for an AcnA-mediated regulation. The proteins with IRE elements but not identified in the proteomes of both strains need to be further confirmed in more direct approaches. The changed expression of proteins without IREs can be influenced by *acnA* mutation indirectly.

5. Discussion

5.1. Aconitase from *S. viridochromogenes* Tü494 is an RNA-binding protein and exhibits a regulatory function on post-transcriptional level

Many enzymes exert in the cell a second function, unrelated with their primary task. Such enzymes are called “moonlighting proteins” (Jefffery, 1999). These enzymes, except exhibiting a catalytic function, interfere with the regulation in bacteria. This regulation may occur by different mechanisms. For e.g. there are enzymes, represented by aconitase, which bind to IREs and control the gene expression on post-transcriptional level (Commichau and Stuelke, 2008). In another group there are enzymes that are additionally active as a DNA-binding transcription factors that repress the gene expression in absence of their substrates. To this group belongs e.g. PutA, which catalyses the degradation of proline to glutamate, but in bacteria, such as *E. coli* or *Salmonella enterica* may also act as a transcription repressor (Ling *et al*., 1994; Ostrovsky de Spicer *et al*., 1991). The third class of “moonlighting proteins” consists of enzymes that control the gene expression by signal-dependent phosphorylation of transcription regulators. The sugar-specific permeases serve as an example. As shown for *E. coli*, these permeases are involved in sugar transport but might also control the activity of transcription activators by phosphorylating them in response to the respective sugar (Amster-Choder and Wright, 1990). Finally, there are enzymes that control the activity of transcription factors by protein-protein interactions. It has been shown for *B. subtilis* that glutamine synthetase can also control gene expression through interaction with the transcription factor TnrA (Wray *et al*., 2001).

Two patterns of evolution of these bifunctional enzymes are especially important: the acquisition of DNA or RNA binding domains by enzymes and the separation of enzymatic and regulatory function via gene duplication. Proline dehydratase PutA provide an example for the acquisition of a DNA-binding domain. In many proteobacteria, including *E. coli*, the PutA protein is bifunctional because acts as an enzyme and additionally as a transcriptional repressor of the *put* operon. The regulatory function of PutA is possible due to acquisition of a specific RHH domain that enables the interaction with the

specific DNA. In contrast, in *Bradyrhizobium japonicum*, PutA does not posses DNA binding domain and, thus, exhibit only catalytic activity (Krishnan and Becker, 2005; Commichau and Stülke, 2008). *B. subtilis* uracil phosphoribosyltransferase is the example where two function of the protein have been separated by the gene duplication. In this bacterium there are two enzymes with uracil phosphoribosyltransferase activity but only one of them is involved in nucleotide biosynthesis. The other one acts as an RNA-binding termination protein that controls the expression of *pyr* operon (Turner *et al*., 1998; Commichau and Stülke, 2008).

Here, the "moonlighting" property of AcnA from *S. viridochromogenes* was investigated. The RNA-binding ability of aconitase was verified by the variety of shift experiments (Publication 1, Michta *et al*., 2012). These results indicated that AcnA from *S. viridochromogenes* might also have a regulatory function. Interestingly, the deletion of a part of an N-terminal conserved motif (amino acids 125-129), involved in regulatory function (Dupuy *et al*., 2006, Basilion *et al*., 1994), resulted in stronger aconitase binding to IRE hairpins. It is possible that this deletion introduces some conformational changes to the AcnA that enhances its RNA-binding. Furthermore, the catalytically inactive aconitase AcnA(C538A) was able to shift IREs, suggesting that the exchange of the cysteine involved in [4Fe-4S] coordination does not block the regulatory activity of AcnA. In *B. subtilis* the ACN_{C517A}, which was also mutated in a cysteine important for the cluster assembly, had lower affinity for IREs, however, the binding was still observed (Alén and Sonenshein, 1999). In contrary, the aconitase mutated in amino acids involved in RNA coordination (AcnA(R763E/Q767E)) was unable for IRE recognition and binding. Since this protein was also catalytically inactive, it can be concluded that some of the same amino acids are involved in both functions of AcnA. The same was suggested for IRP1 from yeast cells where it has been shown that even though the RNA-binding residues are not part of aconitase active site, their substitution can affect the catalytic function of IRP1 (Selezneva *et al*., 2013). The lack of shift formation between AcnA and *recA*-IRE where the stem and the loop were absent, showed that the presence of the secondary structure of IRE and the loop sequence are the IRE core components essential for AcnA binding.

Similarly, it has been described for eukaryotes that the central IRE element consists of the five unspecified bases forming stem, the key AGU nucleotides in the loop region and midstem 'C bulge' base (Henderson *et al*., 1994; Dandekar *et al*., 1991; Leipuviene and Theil, 2007). However, Goforth *et al*., 2010, have shown that in eukaryotes there are also other determinants outside the C bulge and the loop that determine aconitase binding affinity. Furthermore, they have shown that IRP1 binds to different IREs with different affinity, suggesting that a hierarchy of binding exists, which is important for differential translational control. It is known, that in prokaryotic cells, the loop sequence can differ from the consensus sequence of eukaryotes (Tang and Guest, 1999; Alén and Sonenshein, 1999; Banerjee *et al*., 2007). Additionally, instead of the typical 'C bulge' also an 'A bulge' can form a functional IRE sequence (Henderson *et al*., 1994). Whether other unpredicted regions of the IRE, apart from the loop and the bulge position, are important for aconitase binding in prokaryotic cells still needs to be elucidated. Interestingly, in this analysis the AcnA could not recognize any consensus IRE sequences in the case when IREs were synthesized as DNA instead of as RNA. Thus, it seems that the presence of uracil on the stem and/or loop provides some key bonds with AcnA.

RT-PCR analysis showed that the regulation by AcnA occurs on post-transcriptional level (Publication 1, Michta *et al*., 2012). In this experiment the transcript stability for *recA*-mRNA was significantly higher in the WT strain than in MacnA. This suggests that the *recA* transcript, which possesses an IRE-like structure at the 5' end, is stabilized by AcnA. Previously performed Western-blot experiment showed that the RecA protein amount was increased due to oxidative stress in the WT strain, whereas no RecA was detected in MacnA (Schad, 2010). These results directly show that AcnA stabilizes the *recA* transcript under oxidative stress conditions. This is stabilization on post-transcriptional level because any regulation on transcriptional level was excluded by adding to the cultures rifampicin, which is an RNA polymerase inhibitor. These results are especially significant because of the crucial role of RecA in response to stress. The recombinase A is involved in the bacterial SOS response where it cooperates with the UvrABC complex. This complex plays a role in DNA repair by excision of the nucleotide where the mutation has

occurred. Intriguingly, the IRE-like sequence was also identified on the 5' UTR of *uvrB*. The mechanism of *recA* transcript stabilization by AcnA might occur by binding to the 5' localized IRE what in consequence could protect the mRNA from digestion by impairing the activity of unspecific RNases. Interestingly, aconitase from *Caulobacter crescentus* has been shown to interact with RNases, such as PNPase, RNaseE and DEAD-box RNA helicase to form a degradosome (Hardwick *et al*., 2011). *S. viridochromogenes* contains homologues of PNPase, RNasaE, as well as DEAD-box RNA helicase. It is known that PNPase nonspecifically removes nucleotides from mRNA, but is stalled by double-stranded RNA structures such as a stem-loop. Perhaps aconitase is carried by degradosome only under particular conditions in order to direct the degradosome to double stranded RNA and thus unable its degradation activity.

Surprisingly, the proteomic analysis did not identify the RecA protein as significantly up or downregulated in none of the analyzed strains. Most likely it results from the limitation of the applied method. Astonishing may be also a fact that SodA, commonly known to be important for oxidative stress defense, was not identified in this analysis. This protein has previously been shown to be regulated by AcnA in *E. coli* (Tang *et al*., 2002). Here, the lack of SodA upregulation may be associated with the type of applied oxidative stress as observed before (Ballal and Manna, 2009; Karavolos *et al*., 2009). Furthermore, since no IRE motif was identified on the superoxide dismutase mRNA sequence in *S. viridochromogenes*, the expression of this protein is not expected to be directly regulated by AcnA. Nevertheless, further results of the proteomic analysis support the regulatory role of AcnA under oxidative stress (Publication 2, Michta *et al*., 2014). First, the SSQG_02339 encoding for tellurium resistance protein and SSQG_04757 encoding for elongation factor Tu, were identified as differentially expressed in the WT as well as in the MacnA due to oxidative stress treatment. Both of these proteins have previously been shown to play a role in defense against various stressful conditions (Anantharaman *et al*., 2012; Borsetti *et al*., 2005; Caldas *et al*., 1998) and both of them possess IRE motifs on their corresponding mRNAs. Moreover, the majority of the identified stress-related proteins turned out to possess IRE motifs on their corresponding

mRNAs, what also makes them putative targets for AcnA. The functionality of these IREs has still to be confirmed in gel shift analysis.

Interesting results were provided by an experiment, where the presence of artificial IREs led to an AcnA-mediated increase of the *prpA* transcript stability in *S. viridochromogenes*. Such artificial IRE motifs could be used as translational control elements. They could offer a possibility for reengineering the native translational regulation in *Streptomyces* cells for various purposes. The attempts to modulate the translation in *Streptomyces* has been done for instance by the usage of antisense RNA for influencing antibiotic production (D'Alia *et al*., 2010). The application of artificial IRE-Aconitase regulation system could offer a simple synthetic biology tool. Nevertheless, a repetition of the RT-PCR experiment for *prpA* transcript stability and further confirmation of the obtained results would be necessary. This could be done for instance in a similar RT-PCR approach by examining the expression level of the genes (*phsA*, *phsB*, *phsC* etc.) which are directly regulated by PrpA. Also the corresponding complementation of *ΔprpA* with 5' IRE *prpA* and the examination of its transcript stability should be performed. Alternatively, similar experiments could be performed in another *Streptomyces* strain, where the mutation of a regulatory gene clearly leads to the significant decrease of antibiotic production. In such a case, the bioassay analysis could provide direct evidence for stabilization of the corresponding mRNA by the presence of a 3' localized IRE motif.

In conclusion, aconitase from *S. viridochromogenes* is a "moonlighting" enzyme, which can efficiently control the expression of genes involved in DNA repair processes under oxidative stress conditions. In nature, such multifunctional enzymes, exhibiting regulatory functions by interacting with RNA but also with DNA or other proteins, allow for building a highly complex network that maintain the function and structure of the cell, while possessing at the same time the optimal number of protein encoding genes (Cieśla, 2006). The list of enzymes associated with RNA is long but in most of the cases the physiological relevance of such interaction remains unknown. The majority of such bifunctional enzymes interacting with RNA represent evolutionary relicts without further physiological functions. Aconitase is so far the best studied example of

bacterial “moonlighting” enzymes with RNA-binding activity (Cieśla, 2006; Commichau and Stuelke, 2008). Here, an evidence for physiological significance of AcnA-RNA interaction in *S. viridochromogenes* was provided.

5.2. The lack of the regulatory function of AcnA and accumulation of citrate contribute to the morphological defect of MacnA

The *S. viridochromogenes* aconitase mutant has been shown to have strong morphological and physiological defects (Schwartz *et al*., 1999). Similarly, *S. coelicolor*, *B. subtilis* and *S. aureus* strains bearing the *acnA* mutation have multiple defects in morphological and physiological development (Viollier *et al*., 2001a; Craig *et al*., 1997; Somerville *et al*., 2002). AcnA is one of the key enzymes in the TCA cycle. TCA provides ATP, reducing compounds and supplies α-ketoglutarate for the synthesis of glutamate. Thus, *acnA* mutation can arrest the flux through the TCA and in consequence lead to various metabolic dysfunctions. The exogenous medium complementation with L-glutamate, which can be converted to α-ketoglutarate, should restore the proper flux through TCA cycle and normal growth behavior. Since feeding with glutamate did not restore the normal growth, it was suggested that the morphological defect of MacnA does not result simply from the inactivation of TCA *per se* (Schwartz *et al*., 1999). Nevertheless, the lack of the catalytic function of AcnA contributes to the MacnA phenotype, since the complementation of the mutant with the *acnA* gene restored the normal growth but complementation with the catalytically inactive AcnA(C538A) did not (Schad, 2006). Furthermore, the *acnA* mutation in *S. coelicolor* led to citrate accumulation up to 14 mM, whereas it was not detected in the WT strain (Viollier *et al*., 2001a). It seems that for *S. coelicolor* an increased citrate concentration provides highly unfavorable conditions because its accumulation immediately induces the TamR transcription regulator which functions to alleviate the inhibitory effect of accumulated citrate (Huang and Grove, 2013). Also a *B. subtilis* aconitase deletion strain accumulated citrate in the culture supernatant (Craig *et al*., 1997). Thus, it was speculated that the pH drop, due to organic acids accumulation resulting from *acnA* mutation, can be the alternative reason for the defective growth of MacnA. In *S. coelicolor* and *S.*

viridochromogenes aconitase mutants the pH drop was observed (Viollier *et al*., 2001a; Schad, 2010). Nevertheless, it seems that the pH drop due to the medium acidification cannot be the main reason for the differentiation defect of MacnA because this strain exhibits the “bald” phenotype also on nonacidogenic medium sources or plates buffered to the neutral pH (Schwartz *et al*., 1999; Schad, 2010). This suggests that acidogenesis is the effect rather than the cause of the MacnA “bald” phenotype. It has been shown that bacterial cells can form oxygen gradients, such that even cells relatively close to the air-surface are in microaerobic environment (Wimpenny, 1982). Thus, accumulation of organic acids might be a consequence of limited oxygen availability in dense substrate mycelium. In the WT the aerial hyphae increase the oxygen availability, thus allow for the consumption of organic acids (Viollier *et al*., 2001b). Furthermore, it was documented for many *Streptomyces* that organic acid accumulation and medium acidification normally also occurs in the wild type strains (Doskocil *et al*., 1958; Hobbs *et al*., 1992; Madden *et al*., 1996). This however does not inhibit the growth because acidification of a glucose-based medium is followed by a cAMP-dependent metabolic switch that neutralizes the medium (Süsstrunk *et al*., 1998). In the current analysis, the development of *S. viridochromogenes* WT was inhibited only by 20 mM citrate but not by the same concentration of other organic acids (Publication 1, Michta *et al*., 2012). This supports the idea that it is not the medium acidification that causes the impaired growth of MacnA. At the same time, these data suggest that intra- or extracellular accumulation of citrate in *S. viridochromogenes acnA* mutant is at least in part responsible for its growth impairment. Thus, there must be another mechanism, apart from medium acidification, in which accumulated citrate contributes to the “bald” phenotype of MacnA. It was speculated that citrate is a strong chelator of divalent cations that are needed for sporulation what confers the mechanism underlying the differentiation defect in the *B. subtilis* aconitase mutant (Craig *et al*., 1997). The addition of Fe^{2+} and Mn^{2+} restored sporulation in the *B. subtilis* aconitase mutant. However, this was not the case for *S. viridochromogenes* (Schad, 2010). Also in the *S. coelicolor* aconitase mutant no restoration of growth was observed after the addition of Cu^{2+}, Mn^{2+}, Fe^{2+} (Viollier *et al*., 2001a). Probably, this was due to a variable

affinity of citrate to different divalent cations, which have diverse activities as cofactors. Furthermore, the toxicity of heavy metals at high concentrations might make it difficult to suppress the “bald” phenotype by supplementing the medium. Most likely this is also the reason why the growth of MacnA could not be restored by the addition of these cations. In conclusion, citrate accumulation contributes to some extend to the defective growth of MacnA, however, it is rather not the only reason. For the *S. coelicolor* double mutant (*acoA citA*) where the aconitase and in addition citrate synthase genes were mutated, the growth remained impaired. If citrate was responsible for the defective growth, the deletion of the citrate synthase gene should prevent citrate accumulation and restore the growth behavior. Since no restoration of growth was observed, a regulatory function of aconitase, independent of its role as an enzyme, was suggested (Viollier *et al*., 2001a). Also the complementation of MacnA with AcnA(Δ125-129) indicates that the lack of a regulatory function of AcnA contributes to the morphological defect of MacnA. This complementation resulted in an earlier sporulation and higher PTT production in comparison to the WT strain (Schad, 2010). This is possible since the AcnA(Δ125-129), which showed in shift experiments higher RNA-binding activity, may change the stability of mRNAs encoding the proteins involved in morphological differentiation.

5.3. The regulatory function of aconitase is involved in oxidative stress defense, cellular differentiation and presumably other pathways

The set of typical IREs with a CAGUG loop are localized in *S. viridochromogenes* genome in proximity of the genes involved in oxidative stress response or DNA repair, such as recombinase A (*recA*), excinuclease (*uvrB*), DNA replication initiator protein (*dnaA*), putative uracil-DNA glycosylase (*SSQG_01218*) (Sancar and Sancar, 1988) or tellurium resistance protein (*terD*) (Anantharaman *et al*., 2012). Also IRE-corresponding sequences with another loop variant CUGUG were found in proximity of several genes with a predicted role in oxidative stress, such as the putative FAD-binding oxidoreductase (*SSQG_00552*) or the MarR transcriptional regulator which is also known to be involved in oxidative stress response (*SSQG_03294*) (Bussmann *et al*., 2010).

Thus, the localization of IRE-corresponding sequences in the *S. viridochromogenes* genome may indicate the involvement of AcnA in oxidative stress defense. The functionality of several of these IREs was confirmed in shift experiments (Publication 1, Michta *et al*., 2012). A strong evidence for the role of AcnA as a 'survival enzyme' under oxidative stress has been shown for *E. coli* (Tang and Guest, 1999; Varghese *et al*., 2003; Tang *et al*., 2002). In this bacterium AcnA and AcnB regulate the superoxide dismutase (SodA) synthesis. SodA is the major enzyme in oxidative stress defense because it catalyzes the dismutation of the superoxide anion to oxygen and hydrogen peroxide, which is later decomposed by catalase. AcnA and AcnB have an opposite effect on the stability of the *sodA* transcript (Tang *et al*., 2002; Gardner and Fridovich, 1991; Gardner and Fridovich 1992; Bradbury *et al*., 1996). AcnA enhances the stability of the *sodA* transcript, whereas AcnB lowers its stability. Additionally, both aconitases interact with 3' IREs localized on the UTR of their own transcripts and stabilize them. In this way aconitases from *E. coli* provide very sensitive protection against oxidative stress (Tang *et al*., 2002). In the *S. viridochromogenes* genome only one gene (SSQG_06085) encoding for a functional aconitase is present. A similar gene product is resembled by Pmi (SSQG_01043). However, Pmi has no aconitase enzyme activity.

The high sensitivity of MacnA to oxidative stress caused by H_2O_2 suggests the involvement of AcnA in stress response. The hypersensitivity to hydrogen peroxide and methyl viologen of the aconitase mutant was also observed for *E. coli* (Tang, *et al*., 2002). In addition, MacnA showed an increased sensitivity to heat stress (Publication 1, Michta *et al*., 2012). Increased temperature promotes the formation of hydroxyl radicals. Perhaps, the lack of an AcnA-mediated regulation of genes involved in stress defense promotes the higher concentration of reactive oxygen species at 39°C, what could be the reason for the growth defect of the mutant. For *E. coli* it has been reported that heat stress induces the expression of enzymes, such as SodA, AhpC, Dps, which are involved in oxidative stress response (Lüders *et al*., 2009). AhpC codes for an alkyl hydroperoxide reductase, an enzyme that reduces organic peroxides. Dps is a stationary phase nucleoid protein that sequesters iron and protects DNA from damage and was shown to be involved in protection from multiple

stresses, including oxidative stress caused by treatment with hydrogen peroxide (Martinez and Kolter, 1997). Additionally, the level of SodA was increased due to aconitase binding to the *sodA* transcript under oxidative stress (Tang *et al*., 2002). In *S. viridochromogenes* it has been shown that the RecA protein is induced due to oxidative stress. The RecA protein turned out to be important also during heat stress defense (Duwat *et al*., 1995). Thus, it is possible that *E. coli* and perhaps also *S. viridochromogenes* use additionally a common pathway for oxidative and heat stress defense. Nevertheless, it is important to mention that any mutation in a gene from primary metabolism would probably lead to an increased sensitivity to any stressful condition. Thus, the conclusion about the role of AcnA in the oxidative stress response cannot be drawn only from the observation of heat and oxygen stress sensitivity of MacnA.

Interestingly, the promoter of *acnA* harbors sequences with a high similarity to the binding sites of SoxS (regulator of superoxide dismutase) and to the binding sites of the global regulators Fur and MarR that are known to play a role in iron and oxidative stress response, respectively (Muschko *et al*., 2002). Thus, the analysis of the AcnA promoter region provides a further hint about the role of this protein in oxidative stress defense.

AcnA seems to have a regulatory role also in the differentiation process. One of the IRE-corresponding sequences identified in the *S. viridochromogenes* genome was located on the 5' UTR of *ftsZ*. By gel shifts assays it has been shown that the *ftsZ*-IRE is a target for AcnA binding (Publication 1, Michta *et al*., 2012). FtsZ is a *Streptomyces* cell division protein, essential for the generation of spores (Flärdh and Buttner, 2009). Thus, it is possible that the lack of AcnA-mediated regulation is responsible for the lack of sporulation in the MacnA mutant. Interestingly, in the proteome analysis the FtsZ protein was identified in the WT strain but not in the mutant. The effect of an aconitase mutation on the differentiation process has been described for *B. subtilis* (Craig *et al*., 1997). In this bacterium, the CitB aconitase binds specifically to the 3' UTR of *gre*E encoding a transcription regulator of late sporulation genes. As a result, the *gre*E-dependent genes were downregulated (Serio *et al*., 2006).

Furthermore, it may be possible that AcnA regulation is involved in the metabolic switch from primary to secondary metabolism. This is supported by

the fact that the second maximum of AcnA activity correlates with the onset of secondary metabolism. Thus, it seems that AcnA plays an important role not only in morphological but also in physiological differentiation (Muschko *et al*., 2002).

In prokaryotic and eukaryotic organisms AcnA plays a role in cellular iron regulation. Thus, in many organisms the IRE motifs are localized in proximity of genes involved in iron metabolism. In *B. subtilis*, the IRE-like sequences were found on the 3' end of *goxD*, encoding an iron containing protein cytochrome aa_3 oxidase involved in electron transport, and between *feuA* and *feuB* genes, coding for receptors of iron. It has also been shown that these IRE sequences can be recognized and bound by the *B. subtilis* aconitase CitB (Alen and Sonenshein, 1999). *For M. tuberculosis*, the IREs were found on the 3' UTR of thioredoxin (*trxC*) and 5' UTR of the iron-dependent repressor and activator (*ideR*) mRNA. Mycobacterial aconitase Acn could bind to these IREs (Banerjee *et al*., 2007). Also in vertebrates the main function of the aconitase is the regulation of iron metabolism. For example, the human cytosolic IRP1 binds to the IREs of ferritin, which is an iron storage protein (Muckenthaler *et al*., 2008). In *S. viridochromogenes* only one IRE motif was found on the UTR of a gene involved in iron metabolism. This was an iron regulatory protein (SSQG_07448). Since the functionality of this IRE was not validated, it is unclear if *S. viridochromogenes* AcnA is directly involved in iron regulation. It is known that *S. coelicolor* possesses a number of genes encoding putative siderophores (Barona-Gómez *et al*., 2006). Perhaps the transport of iron occurs efficiently enough and the AcnA-mediated regulation of iron metabolism in *Streptomyces* is not needed. Also proteomic analysis did not identify any significant changes in regulation of proteins directly involved in Fe metabolism.

In this work, the regulatory function of aconitase on post-transcriptional level under oxidative stress conditions in *S. viridochromogenes* has been demonstrated. Furthermore, it has been found that the AcnA-IRE interaction is a functional cellular mechanism that allows the strain to adapt to unfavorable environmental conditions.

6. References

Afzal H., Sato D., Jeelani G., Soga T., Nozaki T. (2012). Dramatic increase in glycerol biosynthesis upon oxidative stress in the anaerobic protozoan parasite *Entamoeba histolytica*. PLoS. Negl. Trop. Dis. 6: 1831.

Alén C., Sonenshein A. L. (1999). *Bacillus subtilis* aconitase is an RNA-binding protein. Proc. Natl. Acad. Sci. U S A. 96: 10412-10417.

Alijah R., Dorendorf J., Talay S., Pühler A., Wohlleben W. (1991). Genetic analysis of the phosphinothricin-tripeptide biosynthetic pathway of *Streptomyces viridochromogenes* Tü494. Appl. Microbiol. Biotechnol. 34: 749-755.

Amster-Choder O., Wright A. (1990). Regulation of activity of a transcriptional anti-terminator in *E. coli* by phosphorylation *in vivo*. Science. 249: 540-542.

Anantharaman V., Iyer L. M., Aravind L. (2012). Ter-dependent stress response systems: novel pathways related to metal sensing, production of a nucleoside-like metabolite, and DNA-processing. Mol. Biosyst. 8: 3142-3165.

Ballal A., Manna A. C. (2009). Regulation of superoxide dismutase (*sod*) genes by SarA in *Staphylococcus aureus*. J. Bacteriol. 191: 3301-3310.

Banerjee S., Nandyala A. K., Raviprasad P., Ahmed N., Hasnain S. E. (2007). Iron-dependent RNA-binding activity of *Mycobacterium tuberculosis* aconitase. J. Bacteriol. 189: 4046-4052.

Barona-Gómez F., Lautru S., Francou F. X., Leblond P., Pernodet J. L, Challis G. L. (2006). Multiple biosynthetic and uptake systems mediate siderophore-dependent iron acquisition in *Streptomyces coelicolor* A3(2) and *Streptomyces ambofaciens* ATCC 23877. Microbiology. 152: 3355-3366.

Basilion J. P., Rouault T. A., Massinople C. M., Klausner R. D., Burgess W. H. (1994). The iron-responsive element-binding protein: localization of the RNA-binding site to the aconitase active-site cleft. Proc. Natl. Acad. Sci. U S A. 91: 574-578.

Bayer E., Gugel K. H., Hägele K., Hagenmaier H., Jessipow S. (1972). Metabolic products of microorganisms. Phosphinothricin and phosphinothricyl-alanyl-analine. Helv. Chim. Acta. 55: 224-239.

Bérdy J. (2005). Bioactive microbial metabolites. A personal view. J. Antibiot. 58: 1-26.

Biswas T., Small J., Vandal O., Odaira T., Deng H. Ehrt S., Tsodikov O. V. (2010). Structural insight into serine protease Rv3671c that Protects *M. tuberculosis* from oxidative and acidic stress. Structure. 18: 1353-1363.

Blodgett J. A., Zhang J. K., Metcalf W. W. (2005). Molecular cloning, sequence analysis, and heterologous expression of the phosphinothricin tripeptide biosynthetic gene cluster from *Streptomyces viridochromogenes* DSM 40736. Antimicrob. Agents. Chemother. 49: 230-240.

Boes N., Schreiber K., Härtig E., Jaensch L., Schobert M. (2006). The *Pseudomonas aeruginosa* universal stress protein PA4352 is essential for surviving anaerobic energy stress. J. Bacteriol. 188: 6529-6538.

Borsetti F., Tremaroli V., Michelacci F., Borghese R., Winterstein C. Daldal F., Zannoni D. (2005). Tellurite effects on *Rhodobacter capsulatus* cell viability and superoxide dismutase activity under oxidative stress conditions. Res. Microbiol. 156: 807-813.

Bradbury A. J., Gruer M. J., Rudd K. E., Guest J. R. (1996). The second aconitase (AcnB) of *Escherichia coli*. Microbiology. 142: 389-400.

Brown N. L., Stoyanov J. V., Kidd S. P., Hobman J. L. (2002). The MerR family of transcriptional regulators. FEMS Microbiol. Rev. 27: 145-163.

Buchanan B. B., Balmer Y. (2005). Redox regulation: a broadening horizon. Annu. Rev. Plant. Biol. 56: 187-220.

Burg R. W., Miller B. M., Baker E. E., Birnbaum J., Currie S. A., *et al*. (1979). Avermectins, new family of potent anthelmintic agents: producing organism and fermentation. Antimicrob. Agents. Chemother. 15: 361-367.

Bussmann M., Baumgart M., Bott M. (2010). RosR (Cg1324), a hydrogen peroxide-sensitive MarR-type transcriptional regulator of *Corynebacterium glutamicum*. J. Biol. Chem. 285: 29305-29318.

Caldas T. D., E. l. Yaagoubi A., Richarme G. (1998). Chaperone properties of bacterial elongation factor EF-Tu. J. Biol. Chem. 273: 11478-11482.

Chater K. F. (2006). *Streptomyces* inside-out: a new perspective on the bacteria that provide us with antibiotics. Philos. Trans. R. Soc. Lond. B. Biol. Sci. 361: 761-768.

Cieśla J. (2006). Metabolic enzymes that bind RNA: yet another level of cellular regulatory network? Acta. Biochim. Pol. 53: 11-32.

Clausen T., Southan C., Ehrmann M. (2002). The HtrA family of proteases: implications for protein composition and cell fate. Mol. Cell. 10: 443-455.

Commichau F. M., Stülke J. (2008). Trigger enzymes: bifunctional proteins active in metabolism and in controlling gene expression. Mol. Microbiol. 67: 692-702.

Craig J. E., Ford M. J., Blaydon D. C., Sonenshein A. L. (1997). A null mutation in the *Bacillus subtilis* aconitase gene causes a block in Spo0A-phosphate-dependent gene expression. J. Bacteriol. 179: 7351-7359.

D'Alia, D., Nieselt, K., Steigele, S., Muller, J., Verburg, I., and Takano, E. (2010). Noncoding RNA of glutamine synthetase I modulates antibiotic production in *Streptomyces coelicolor* A3(2). J. Bacteriol. 192: 1160–1164.

Dandekar T., Stripecke R., Gray N. K., Goossen B., Constable A., Johansson H. E., Hentze M. W. (1991). Identification of a novel iron-responsive element in murine and human erythroid delta-aminolevulinic acid synthase mRNA. EMBO J.10: 1903-1909.

Demple B. (1991). Regulation of bacterial oxidative stress genes. Annu. Rev. Genet. 25: 315-337.

Diddens H., Zähner H., Kraas E., Göhring W., Jung G. (1976). On the transport of tripeptide antibiotics in bacteria. Eur. J. Biochem. 66: 11-23.

Doskocil J., Sikyta B., Kasparova J., Doskocilova D., Zajicek J. (1958). Development of the culture of *Streptomyces rimosus* in submerged fermentation. J. Gen. Microbiol. 18: 302-312.

Dupuy J., Volbeda A., Carpentier P., Darnault C., Moulis J. M., Fontecilla-Camps J. C. (2006). Crystal structure of human iron regulatory protein 1 as cytosolic aconitase. Structure. 14: 129-139.

Duwat P., Sourice S., Ehrlich S. D., Gruss A. (1995). *recA* gene involvement in oxidative and thermal stress in *Lactococcus lactis*. Dev. Biol. Stand. 85: 455-467.

Ensign J. C. (1978). Formation, properties, and germination of actinomycete spores. Annu. Rev. Microbiol. 32: 185-219.

Eys S., Schwartz D., Wohlleben W., Schinko E. (2008). Three thioesterases are involved in the biosynthesis of phosphinothricin tripeptide in *Streptomyces viridochromogenes* Tü494. Antimicrob. Agents. Chemother. 52: 1686-1696.

Flärdh K., Buttner M. J. (2009). *Streptomyces* morphogenetics: dissecting differentiation in a filamentous bacterium. Nat. Rev. Microbiol. 7: 36-49.

Gardner P. R., Fridovich I. (1991). Superoxide sensitivity of the *Escherichia coli* aconitase. J. Biol. Chem. 266: 19328-19333.

Gardner P. R., Fridovich I. (1992). Inactivation-reactivation of aconitase in *Escherichia coli*. A sensitive measure of superoxide radical. J. Biol. Chem. 267: 8757-8763.

Glazebrook M. A., Doull J. L., Stuttard C., Vining L. C. (1990). Sporulation of *Streptomyces venezuelae* in submerged cultures. J. Gen. Microbiol. 136: 581-8.

Goforth J. .B, Anderson S. A., Nizzi C. P., Eisenstein R. S. (2010). Multiple determinants within iron-responsive elements dictate iron regulatory protein binding and regulatory hierarchy. RNA. 16: 154-169.

Gräfe U. Biochemie der Antibiotika. Struktur-Biosynthese-Wirkmechanismus. (1992). Spektrum Akademischer Verlag, Heidelberg.

Gruer M. J., Artymiuk P. J., Guest J. R. (1997). The aconitase family: three structural variations on a common theme. Trends Biochem. Sci. 22: 3-6.

Han W. D., Kawamoto S., Hosoya Y., Fujita M., Sadaie Y. *et al*. (1998). A novel sporulation-control gene (*spo0M*) of *Bacillus subtilis* with a sigmaH-regulated promoter. Gene 217: 31-40.

Hara O., Murakami T., Imai S., Anzai H., Itoh R., *et al*. (1991). The bialaphos biosynthetic genes of *Streptomyces viridochromogenes*: cloning, heterospecific expression, and comparison with the genes of *Streptomyces hygroscopicus*. J. Gen. Microbiol. 137: 351-359.

Hardwick S. W., Chan V. S., Broadhurst R. W., Luisi B. F. (2011). An RNA degradosome assembly in *Caulobacter crescentus*. Nucleic Acids Res. 39: 1449-1459.

Heinzelmann E., Kienzlen G., Kaspar S., Recktenwald J., Wohlleben W., *et al*. (2001). The phosphinomethylmalate isomerase gene *pmi*, encoding an aconitase-like enzyme, is involved in the synthesis of phosphinothricin tripeptide in *Streptomyces viridochromogenes*. Appl. Environ. Microbiol. 67: 3603-3609.

Henderson B. R., Menotti E., Bonnard C., Kühn L. C. (1994). Optimal sequence and structure of iron-responsive elements. J. Biol. Chem., 269: 1781–1789.

Hobbs G., Obanye A. I., Petty J., Mason J. C., Barratt E., *et al*. (1992). An integrated approach to studying regulation of production of the antibiotic methylenomycin by *Streptomyces coelicolor* A3(2). J. Bacteriol. 174: 1487-1494.

Hodgson, D. A. (2000). Primary metabolism and its control in streptomycetes: a most unusual group of bacteria. Adv. Microb. Physiol. 42: 47-238.

Huang H., Grove A. (2013). The transcriptional regulator TamR from *Streptomyces coelicolor* controls a key step in central metabolism during oxidative stress. Mol. Microbiol. 87: 1151-1166.

Jeffery C. J. (1999). Moonlighting proteins. Trends Biochem. Sci. 24: 8-11.

Karavolos M. H., Horsburgh M. J., Ingham E., Foster, S. J. (2009) Role and regulation of the superoxide dismutases of *Staphylococcus aureus*. Microbiology. 149: 2749-2758.

Keating T. A, Walsh C. T. (1999). Initiation, elongation, and termination strategies in polyketide and polypeptide antibiotic biosynthesis. Curr. Opin. Chem. Biol. 3: 598-606.

Kiley P. J., Beinert H. (1998). Oxygen sensing by the global regulator, FNR: the role of the iron-sulfur cluster. FEMS Microbiol. Rev. 22: 341-352.

Koglin A., Löhr F., Bernhard F., Rogov V. V., Frueh D. P., *et al*. (2008). Structural basis for the selectivity of the external thioesterase of the surfactin synthetase. Nature. 454: 907-911.

Kondo Y. T., Shomura Y., Ogawa T., Tsuruoka H., Watanabe K., *et al*. (1973). Studies on a new antibiotic SF-1293. Isolation and physic-chemical and biological characterization of SF- 1293 substances. Sci. Rep. Meiji. Seika. 13: 34-41.

Kopp F., Marahiel M. A. (2007). Macrocyclization strategies in polyketide and nonribosomal peptide biosynthesis. Nat. Prod. Rep. 24: 735-749.

Krishnan N., Becker D. F. (2005). Characterization of a bifunctional PutA homologue from Bradyrhizobium japonicum and identification of an active site residue that modulates proline reduction of the flavin adenine dinucleotide cofactor. Biochemistry. 44: 9130-9139.

Kumada Y., Anzai H., Takano E., Murakami T., Hara O., *et al*. (1988). The bialaphos resistance gene (*bar*) plays a role in both self-defense and bialaphos biosynthesis in *Streptomyces hygroscopicus*. J. Antibiot. 41: 1838-1845.

Kvint K., Nachin L., Diez A., Nyström T. (2003). The bacterial universal stress protein: function and regulation. Curr. Opin. Microbiol. 6: 140-145.

Lauble H., Kennedy M. C. , Beinert H., Stout C. D. (1992). Crystal structures of aconitase with isocitrate and nitroisocitrate bound. Biochemistry. 31: 2735-2748.

Lauble H., Kennedy M. C., Beinert H., and Stout C. D. (1994). Crystal structures of aconitase with Trans-aconitate and nitrocitrate bound. J. Mol. Biol. 237: 437–451.

Leipuviene R., Theil E. C. (2007). The family of iron responsive RNA structures regulated by changes in cellular iron and oxygen. Cell. Mol. Life Sci. 64: 2945-2955.

Ling M., Allen S. W., Wood J. M. (1994). Sequence analysis identifies the proline dehydrogenase and delta 1-pyrroline-5-carboxylate dehydrogenase domains of the multifunctional *Escherichia coli* PutA protein. J. Mol. Biol. 243: 950-956.

Lloyd S. J., Lauble H., Prasad G. S., Stout C. D. (1999). The mechanism of aconitase: 1.8 A resolution crystal structure of the S642a: citrate complex. Protein Sci. 8: 2655-2662.

Lüders S., Fallet C., Franco-Lara E. (2009). Proteome analysis of the *Escherichia coli* heat shock response under steady-state conditions. Proteome Sci. 7:36.

Madden T., Ward J. M., Ison A. P. (1996). Organic acid excretion by *Streptomyces lividans* TK24 during growth on defined carbon and nitrogen sources. Microbiology. 142: 3181-3185.

Martinez A., Kolter R. (1997). Protection of DNA during oxidative stress by the nonspecific DNA-binding protein Dps. J. Bacteriol. 179: 5188-5194.

Massilamany C., Gangaplara A., Gardner D. J., Musser J. M., Steffen D., *et al*. (2011). TCA cycle inactivation in *Staphylococcus aureus* alters nitric oxide production in RAW 264.7 cells. Mol. Cell. Biochem. 355: 75-82.

McCarthy A. J., Williams S. T. (1992). Actinomycetes as agents of biodegradation in the environment-a review. Gene. 115: 189-192.

Méndez C., Braña A. F., Manzanal M. B., Hardisson C. (1985). Role of substrate mycelium in colony development in *Streptomyces*. Can. J Microbiol. 31: 446-450.

Messner K. R., Imlay J. A. (1999). The identification of primary sites of superoxide and hydrogen peroxide formation in the aerobic respiratory chain and sulfite reductase complex of *Escherichia coli*. J. Biol. Chem. 274: 10119-10128.

Minotti G., Menna P., Salvatorelli E., Cairo G., Gianni L. (2004). Anthracyclines: molecular advances and pharmacologic developments in antitumor activity and cardiotoxicity. Pharmacol. Rev. 56: 185-229.

Muckenthaler M. U., Galy B., Hentze M. W. (2008). Systemic iron homeostasis and the iron-responsive element/iron-regulatory protein (IRE/IRP) regulatory network. Annu. Rev. Nutr. 28: 197-213.

Muschko K., Kienzlen G., Fiedler H. P., Wohlleben W., Schwartz D. (2002). Tricarboxylic acid cycle aconitase activity during the life cycle of *Streptomyces viridochromogenes* Tü494. Arch. Microbiol. 178: 499-505.

Muschko K. (2005). Untrsuchungen zur Regulation der Antibiotikabiosynthese von Phosphinothricintripeptide (PTT) aus *Streptomyces viridochromogenes*. Dissertation, University of Tübingen.

Nett M., Ikeda H., Moore B. S. (2009). Genomic basis for natural product biosynthetic diversity in the actinomycetes. Nat. Prod. Rep. 26: 1362-1384.

Ostrovsky de Spicer P., O'Brien K., Maloy S. (1991). Regulation of proline utilization in *Salmonella typhimurium*: a membrane-associated dehydrogenase binds DNA *in vitro*. J. Bacteriol. 173: 211-219.

O'Toole R., Smeulders M. J., Blokpoel M. C., Kay E. J., Lougheed K. *et al*. (2003). A two-component regulator of universal stress protein expression and adaptation to oxygen starvation in *Mycobacterium smegmatis*. J. Bacteriol. 185: 1543-1554.

Pohl E., Haller J. C., Mijovilovich A., Meyer-Klaucke W., Garman E., *et al*. (2003). Architecture of a protein central to iron homeostasis: crystal structure and spectroscopic analysis of the ferric uptake regulator. Mol. Microbiol. 47: 903-915.

Ralser M., Wamelink M. M., Kowald A., Gerisch B., Heeren G., *et al*. (2007). Dynamic rerouting of the carbohydrate flux is key to counteracting oxidative stress. J. Biol. 6: 10.

Revill W. P., Bibb M. J., Hopwood D. A. (1996). Relationships between fatty acid and polyketide synthases from *Streptomyces coelicolor* A3(2): characterization of the fatty acid synthase acyl carrier protein. J. Bacteriol. 178: 5660-5667.

Sancar A., Sancar G. B. (1988). DNA repair enzymes. Annu. Rev. Biochem. 57: 29-67.

Sánchez S., Chávez A., Forero A., García-Huante Y., Romero A. *et al*. (2010). Carbon source regulation of antibiotic production. J. Antibiot. 63: 442-459.

Schad K. (2006). Charakterisirung der Primaer- und Sekundaerstoffwechselaconitasen AcnA and Pmi in *Streptomyces viridochromogenes* Tü 494. Diplomarbeit. University of Tübingen.

Schad K. (2010). Die Rolle der Aconitase AcnA in der Abwehr von oxidativem Stress und in der morphologischen Differenzierung von *Streptomyces viridochromogenes* Tü494. Doktorarbeit. University of Tübingen.

Schinko E., Schad K., Eys S., Keller U., Wohlleben W. (2009). Phosphinothricin-tripeptide biosynthesis: an original version of bacterial secondary metabolism? Phytochemistry. 70: 1787-800.

Schwartz D., Alijah R., Nussbaumer B., Pelzer S., Wohlleben W. (1996). The peptide synthetase gene *phsA* from *Streptomyces viridochromogenes* is not juxtaposed with other genes involved in nonribosomal biosynthesis of peptides. Appl. Environ. Microbiol. 62: 570-577.

Schwartz D., Berger S., Heinzelmann E., Muschko K., Welzel K., *et al*. (2004). Biosynthetic gene cluster of the herbicide phosphinothricin tripeptide from *Streptomyces viridochromogenes* Tü494. Appl. Environ. Microbiol. 70: 7093-7102.

Schwartz D., Kaspar S., Kienzlen G., Muschko K., Wohlleben W. (1999). Inactivation of the tricarboxylic acid cycle aconitase gene from *Streptomyces viridochromogenes* Tü494 impairs morphological and physiological differentiation. J. Bacteriol. 181: 7131-7135.

Selezneva A. I., Walden W. E., Volz K. W. (2013). Nucleotide-specific recognition of iron-responsive elements by iron regulatory protein 1. J. Mol. Biol. 425: 3301-3310.

Serio A. W., Pechter K. B., Sonenshein A. L. (2006). *Bacillus subtilis* aconitase is required for efficient late-sporulation gene expression. J. Bacteriol. 188: 6396-6405.

Singh R., Mailloux R. J., Puiseux-Dao S., Appanna V. D. (2007). Oxidative stress evokes a metabolic adaptation that favors increased NADPH synthesis and decreased NADH production in *Pseudomonas fluorescens.* J. Bacteriol. 189: 6665-6675.

Somerville G. A., Chaussee M. S., Morgan C. I., Fitzgerald J. R., Dorward D., *et al*. (2002). *Staphylococcus aureus* aconitase inactivation unexpectedly inhibits post-exponential-phase growth and enhances stationary-phase survival. Infect. Immun. 70: 6373-6382.

Somerville G., Mikoryak C. A., Reitzer L. (1999). Physiological characterization of *Pseudomonas aeruginosa* during exotoxin A synthesis: glutamate, iron limitation, and aconitase activity. J. Bacteriol. 181: 1072-1078.

Stachelhaus T., Mootz H. D., Bergendahl V., Marahiel M. A. (1998). Peptide bond formation in nonribosomal peptide biosynthesis. Catalytic role of the condensation domain. J. Biol. Chem. 273: 22773-22781.

Strieker M., Tanović A., Marahiel M. A. (2010). Nonribosomal peptide synthetases: structures and dynamics. Curr. Opin. Struct. Biol. 20: 234-240.

Süsstrunk U., Pidoux J., Taubert S., Ullmann A., Thompson C. J. (1998). Pleiotropic effects of cAMP on germination, antibiotic biosynthesis and morphological development in *Streptomyces coelicolor*. Mol. Microbiol. 30: 33-46.

Tang Y., Guest J. R. (1999). Direct evidence for mRNA binding and post-transcriptional regulation by *Escherichia coli* aconitases. Microbiology. 145: 3069-3079.

Tang Y., Guest J. R., Artymiuk P. J., Green J. (2005). Switching aconitase B between catalytic and regulatory modes involves iron-dependent dimer formation. Mol. Microbiol. 56: 1149-1158.

Tang Y., Guest J. R., Artymiuk P. J., Read R. C., Green J. (2004). Post-transcriptional regulation of bacterial motility by aconitase proteins. Mol. Microbiol. 51: 1817-1826.

Tang Y., Quail M. A., Artymiuk P. J., Guest J. R., Green J. (2002). *Escherichia coli* aconitases and oxidative stress: post-transcriptional regulation of *sodA* expression. Microbiology. 148: 1027-1037.

Thompson C. J., Movva N. R., Tizard R., Crameri R., Davies J. E., *et al*. (1987). Characterization of the herbicide-resistance gene bar from *Streptomyces hygroscopicus*. EMBO J. 6: 2519-2523.

Turner R. J., Bonner E. R., Grabner G. K., Switzer R. L. (1998). Purification and characterization of Bacillus subtilis PyrR, a bifunctional pyr mRNA-binding attenuation protein/uracil phosphoribosyltransferase. J. Biol. Chem. 273: 5932-5938.

Umezawa H., Aoyagi T., Morishima H., Kunimoto S., Matsuzaki M. (1970). Chymostatin, a new chymotrypsin inhibitor produced by actinomycetes. J Antibiot. 23: 425-427.

Umezawa H., Maeda K., Takeuchi T., Okami Y. (1966). New antibiotics, bleomycin A and B. J. Antibiot. 19: 200-209.

van Wezel G. P., McDowall K. J. (2011). The regulation of the secondary metabolism of *Streptomyces*: new links and experimental advances. Nat. Prod. Rep. 28: 1311-1333.

Varghese S., Tang Y., Imlay J. A. (2003). Contrasting sensitivities of *Escherichia coli* aconitases A and B to oxidation and iron depletion. J. Bacteriol. 185: 221-230.

Vézina C., Kudelski A., Sehgal S. N. (1975). Rapamycin (AY-22,989), a new antifungal antibiotic. I. Taxonomy of the producing streptomycete and isolation of the active principle. J. Antibiot. 28: 721-726.

Viollier P. H., Minas W., Dale G. E., Folcher M., Thompson C. J. (2001b). Role of acid metabolism in *Streptomyces coelicolor* morphological differentiation and antibiotic biosynthesis. J. Bacteriol. 183: 3184-3192.

Viollier P. H., Nguyen K. T., Minas W., Folcher M., Dale G. E., Thompson C. J. (2001a). Roles of aconitase in growth, metabolism, and morphological differentiation of *Streptomyces coelicolor*. J. Bacteriol. 183: 3193-3203.

Watve M. G., Tickoo R., Jog M. M., Bhole B. D. (2001). How many antibiotics are produced by the genus *Streptomyces*? Arch. Microbiol. 176: 386-90.

Williams C. H., Stillman T. J., Barynin V. V., Sedelnikova S. E., Tang Y., *et al*. (2002). *E. coli* aconitase B structure reveals a HEAT-like domain with implications for protein–protein recognition. Nature Structural Biology, 9: 447–452.

Wilson T. J., Bertrand N., Tang J. L., Feng J. X., Pan M. Q., *et al*. (1998). The *rpfA* gene of *Xanthomonas campestris* pathovar campestris, which is involved in the regulation of pathogenicity factor production, encodes an aconitase. Mol. Microbiol. 28: 961-970.

Wimpenny J. W. T. (1982). Responses of microorganisms to physical and chemical gradients. Philos. Trans. R. Soc. Lond. 297: 497-515.

Wohlleben W., Arnold W., Broer I., Hillemann D., Strauch E., (1988). Nucleotide sequence of the phosphinothricin N-acetyltransferase gene from *Streptomyces viridochromogenes* Tü494 and its expression in *Nicotiana tabacum*. Gene. 70: 25-37.

Wray L. V. Jr., Zalieckas J. M., Fisher S. H. (2001). *Bacillus subtilis* glutamine synthetase controls gene expression through a protein-protein interaction with transcription factor TnrA. Cell. 107: 427-435.

Xiao M., Xu P., Zhao J., Wang Z., Zuo F., *et al*. (2011) Oxidative stress-related responses of *Bifidobacterium longum* subsp. *longum* BBMN68 at the proteomic level after exposure to oxygen. Microbiolgy. 6: 1573-1588.

Yao Y., Sun H., Xu F., Zhang X., Liu S. (2011). Comparative proteome analysis of metabolic changes by low phosphorus stress in two *Brassica napus* genotypes. Planta. 233: 523-537.

Yasutake Y., Yaoa M., Sakaia N., Kiritaa T., and Tanaka I. (2004). Crystal structure of the *Pyrococcus horikoshii* isopropylmalate isomerase small subunit provides insight into the dual substrate specificity of the enzyme. Journal of Molecular Biology. 344: 325–333.

Zeller T., Klug G. (2006). Thioredoxins in bacteria: functions in oxidative stress response and regulation of thioredoxin genes. Naturwissenschaften. 93: 259-266.

7. List of publications

1. Michta E., Schad K., Blin K., Ort-Winklbauer R., Röttig M., Kohlbacher O., Wohlleben W., Schinko E., Mast Y. (2012).
The bifunctional role of aconitase in *Streptomyces viridochromogenes* Tü494. Environ. Microbiol. 14: 3203-3219.

2. Michta E., Ding W., Zhu S., Blin K., Ruan H., Wang R., Wohlleben W., Mast Y. (2014).
Proteomic approach to reveal the regulatory function of aconitase AcnA in oxidative stress response in the antibiotic producer *Streptomyces viridochromogenes* Tü494. PLoS One. 9:e87905.

environmental microbiology

Environmental Microbiology (2012) doi:10.1111/1462-2920.12006

The bifunctional role of aconitase in *Streptomyces viridochromogenes* Tü494

Ewelina Michta,[1] Klaus Schad,[1] Kai Blin,[1,2] Regina Ort-Winklbauer,[1] Marc Röttig,[2] Oliver Kohlbacher,[2] Wolfgang Wohlleben,[1] Eva Schinko[1] and Yvonne Mast[1]*

[1]*Interfakultäres Institut für Mikrobiologie und Infektionsmedizin (IMIT), Mikrobiologie/Biotechnologie, Fakultät für Biologie, Eberhard-Karls-Universität Tübingen, Auf der Morgenstelle 28, 72076 Tübingen, Germany.*

[2]*Angewandte Bioinformatik, Wilhelm-Schickard-Institut für Computerwissenschaften, Eberhard-Karls-Universität Tübingen, Sand 14, 72076 Tübingen, Germany.*

Summary

In many organisms, aconitases have dual functions; they serve as enzymes in the tricarboxylic acid cycle and as regulators of iron metabolism. In this study we defined the role of the aconitase AcnA in *Streptomyces viridochromogenes* Tü494, the producer of the herbicide phosphinothricyl-alanyl-alanine, also known as phosphinothricin tripeptide or bialaphos. A mutant in which the aconitase gene *acnA* was disrupted showed severe defects in morphology and physiology, as it was unable to form any aerial mycelium, spores nor phosphinothricin tripeptide. AcnA belongs to the iron regulatory proteins (IRPs). In addition to its catalytic function, AcnA plays a regulatory role by binding to iron responsive elements (IREs) located on the untranslated region of certain mRNAs. A mutation preventing the formation of the [4Fe-4S] cluster of AcnA eliminated its catalytic activity, but did not inhibit RNA-binding ability. *In silico* analysis of the *S. viridochromogenes* genome revealed several IRE-like structures. One structure is located upstream of *recA*, which is involved in the bacterial SOS response, and another one was identified upstream of *ftsZ*, which is required for the onset of sporulation in streptomycetes. The functionality of different IRE structures was proven with gel shift assays and specific IRE consensus sequences were defined. Furthermore, RecA was shown to be upregulated on post-transcriptional level under oxidative stress conditions in the wild-type strain but not in the *acnA* mutant, suggesting a regulatory role of AcnA in oxidative stress response.

Received 26 July, 2012; accepted 24 September, 2012. *For correspondence. E-mail yvonne.mast@biotech.uni-tuebingen.de; Tel. (+49) (0) 70712973204; Fax (+49) (0) 7071295979.

Introduction

Streptomycetes are Gram-positive soil bacteria with a complex life cycle. The differentiation process starts with an arthrospore, which subsequently forms a branched substrate mycelium. Detrimental environmental conditions or the depletion of nutrients induce the development of an aerial mycelium from the substrate mycelium. To aid in dispersal, some of the aerial hyphae are constricted to mononuclear spores. Streptomycetes also undergo a physiological differentiation and produce a great variety of secondary metabolites, including antibiotics.

Streptomyces viridochromogenes Tü494 produces the antibiotic phosphinothricin tripeptide (PTT), which consists of the non-proteinogenic amino acid phosphinothricin linked to two alanine residues (Bayer *et al.*, 1972). Phosphinothricin is industrially produced as Basta® or Liberty® and used as an important herbicide in agriculture. The gene cluster associated with PTT biosynthesis has been identified (Strauch *et al.*, 1988; Alijah *et al.*, 1991) and sequenced (Schwartz *et al.*, 2004; Blodgett *et al.*, 2005), and the function of several enzymes has been elucidated (Schwartz *et al.*, 1996; Heinzelmann *et al.*, 2001; Blodgett *et al.*, 2007; Eys *et al.*, 2008).

One of the identified enzymes, Pmi, catalyses the isomerization of phosphinomethylmalate to isophosphinomethylmalate, a process that resembles the isomerization of citrate to isocitrate in the tricarboxylic acid (TCA) cycle that is catalysed by AcnA. However, both enzymes are highly specific for their reactions (Heinzelmann *et al.*, 2001). Pmi and AcnA have an overall identity of approximately 52% and consist of four domains that are arranged around a [4Fe-4S] cluster (Heinzelmann *et al.*, 2001). Therefore, it is likely that AcnA and Pmi from *S. viridochromogenes* evolved through duplication of an ancestral aconitase gene (Heinzelmann *et al.*, 2001; Schinko *et al.*, 2009). AcnA has high similarity to proteins of the iron regulatory protein (IRP) group (Schinko *et al.*, 2009). The aconitase mutant strain MacnA (formerly designated AcoA; Table 1 and Schwartz *et al.*, 1999) exhibited the bald phenotype on agar medium (Schwartz *et al.*, 1999),

Table 1. Bacterial strains and plasmids.

Bacterial strains and plasmids	Relevant genotype and phenotype	Source reference
Streptomyces viridochromogenes		
Tü494	PTT producing wild-type	Bayer *et al.* (1972)
MacnA	gene interruption of *acnA*: *aphII*; bald phenotype, (formerly designated AcoA)	Schwartz *et al.* (1999)
Streptomyces lividans		
T7	*tsr*, T7-RNA-polymerase gene	Fischer (1996)
E. coli		
XL1 Blue	*recA*1 *end* A1 *gyrA*96 *thi*-1 *hsd*R17 *sup*E44 *rel*A1 *laq*[F', *pro*AB *lacI*^{q} ZΔ M15 Tn*10*(*tet*r)]	Bullock *et al.* (1987)
B. subtilis		
ATCC6051	Wild-type	American Type Culture Collection
Plasmids		
pK18/19	pUC-derivative, *aphII*, *lacZ*'- complementation system	Pridmore (1987)
pSET152	*am*^{r}, *lacZ*$^{+}$, *rep*^{puc}, *oriT*, *int*ϕ^{c31}	Bierman *et al.* (1992)
pRSETB	T7 promoter expression system, 6xHis-tag, *bla*	Invitrogen
pJOE890	pUC derivative, positive selection system, *bla*, 2 multiple cloning sites, 2 *ter*	J. Altenbuchner, pers. comm.
pDRIVE	*lacZ*'' – complementation system, *bla*, *kan*, multiple cloning sites	Qiagen
pGM9	*Streptomyces* vector, replicon of pSG5, *tsr*, *ble*	Muth *et al.* (1989)
pEH98	pK18 derivative carrying the inducible *tipA*-promoter	E. Schinko, pers. comm.
pKS1	pDrive carrying the *acnA*-gene	This study
pKS2	pJOE890 carrying the *C538A*$^{1+2}$ fragment	This study
pKS3	pDrive derivative carrying *Δ125–129*$^{1+2}$	This study
pKS4	pDrive carrying *acnA2(Δ125–129)*	This study
pKS5	pDrive carrying *R763E/Q767E*$^{1+2}$	This study
pKS6	pRSETB carrying the *hisacnA* gene	This study
pKS7	pRSETB carrying the *hisacnA1(C538A)* gene	This study
pKS8	pRSETB carrying the *hisacnA2(Δ125–129)* gene	This study
pKS9	pRSETB carrying the *hisacnA3(R762E/Q766E)* gene	This study
pKS10	pDrive carrying the promoter region of *acnA* (*pacnA*)	This study
pKS16	Fusion of pKS6 with pGM9	This study
pKS17	Fusion of pKS7 with pGM9	This study
pKS18	Fusion of pKS8 with pGM9	This study
pKS19	Fusion of pKS9 with pGM9	This study
pKS20	pEH98 carrying the *hisacnA* gene	This study
pKS21	pEH98 carrying *hisacnA1(C538A)*	This study
pKS22	pEH98 carrying *hisacnA2(Δ125–129)*	This study
pKS23	pEH98 carrying *hisacnA3(R763E/Q767E)*	This study
pKS24	pSET152 carrying *hisacnA*	This study
pKS25	pSET152 carrying *hisacnA1(C538A)*	This study
pKS26	pSET152 carrying *hisacnA 2(Δ125–129)*	This study
pKS27	pSET152 carrying *hisacnA3(R763E/Q767E)*	This study
pKS28	pSET152 carrying *hisacnA* and *pacnA*	This study
pKS29	pSET152 carrying *hisacnA1(C538A)* and *pacnA*	This study
pKS30	pSET152 carrying *hisacnA2(Δ125–129)* and *pacnA*	This study
pKS31	pSET152 carrying *hisacnA3(R763E/Q767E)* and *pacnA*	This study

which is characterized by the lack of aerial mycelium formation and sporulation and shows only retarded growth in liquid medium. MacnA was also defective in PTT production, demonstrating that AcnA not only affects morphological but also physiological differentiation. Similar effects of TCA cycle enzymes on differentiation and antibiotic production have been observed in *Streptomyces coelicolor* (Viollier *et al*., 2001a,b) and *Streptomyces noursei* (Jonsbu *et al*., 2001). Such pleiotropic effects of mutations in aconitase genes are not unique to streptomycetes; they have also been reported for *Pseudomonas aeruginosa*, *Staphylococcus aureus* and *Xanthomonas campestris* (Wilson *et al*., 1998; Somerville *et al*., 1999; 2002).

Aconitases are a class of trigger enzymes, which in addition to their metabolic function act as important regulators in response to iron scarcity or oxidative stress (Commichau and Stülke, 2008). For example, one of the best studied aconitases is human cytosolic IRP1, which has aconitase activity and besides this functions also as a regulatory protein in iron metabolism (Muckenthaler *et al*., 2008). Under iron sufficiency conditions, IRP1 is active as an aconitase; however, when the iron concentration decreases, the [4Fe-4S] cluster is disassembled, and the enzyme loses its aconitase activity. The resulting apo-enzyme undergoes structural changes (Dupuy *et al*., 2006) that open a cleft for the binding of specific sequences known as iron responsive elements (IREs). IREs form stem-loop structures at the 5′- or 3′-untranslated regions (UTRs) of mRNA transcripts such as ferritin. The binding of IRP1 to the 5′ UTR blocks translation, whereas binding at the 3′ end stabilizes the transcript and enhances translation (Muckenthaler *et al*., 2008). The *Escherichia coli* aconitases AcnA and AcnB also function as post-transcriptional regulators via site-specific binding to their own mRNA (Tang and Guest, 1999). Additionally, they have positive (AcnA) and negative (AcnB) effects on the stability of the superoxide dismutase (SodA) transcript (Tang *et al*., 2002). For *Mycobacterium tuberculosis* and *Bacillus subtilis* aconitases, a stress-dependent binding to IRE-like structures of genes involved in iron metabolism (Alén and Sonenshein, 1999; Banerjee *et al*., 2007) or sporulation (Serio and Sonenshein, 2006; Serio *et al*., 2006) have been shown. Moreover, aconitases can also regulate bacterial motility, as demonstrated in *Salmonella enterica* serovar Typhimurium LT2 (Tang *et al*., 2004).

The morphological and physiological defects of MacnA, which could not be fully restored by complementation with TCA cycle intermediates, suggest a regulatory function for the *S. viridochromogenes* aconitase AcnA (Schwartz *et al*., 1999). In this paper, we demonstrate that in addition to its catalytic function, AcnA acts as a post-transcriptional regulator. Several IRE-like structures were identified in the *S. viridochromogenes* genome by computational analysis and their functionality was validated in gel shift assays. Moreover, the analysis of RecA regulation as well as the analysis of sporulation initiation in different complemented MacnA strains supported the regulatory function for AcnA in the stress response of streptomycetes.

Results

The aconitase mutant MacnA has a severe growth defect

MacnA is unable to differentiate into aerial mycelium and to sporulate. The growth defect is accompanied by a physiological defect as MacnA fails to produce any PTT (Schwartz *et al*., 1999). This phenotype was observed even on media with mannitol as non-acidogenic carbon source, where pH should remain near neutrality, which corresponds to what was described for the *S. coelicolor* aconitase mutant *acoA* (Viollier *et al*., 2001a). These results suggest that the growth defects of the aconitase mutants are not only caused by acidogenesis. Exogenous complementation with glutamate, which can easily be converted into α-ketoglutarate, only partially restored the normal growth behaviour, indicating that the phenotype of MacnA is not the result of the missing reaction product of aconitase (Schwartz *et al*., 1999). To test if the intracellular accumulation of citrate – the aconitase substrate – caused the differentiation defect, the WT strain was plated on yeast malt (YM) agar plates with increasing citrate concentrations, assuming that citrate is transported into the cell via citrate transporters. In *S. viridochromogenes* at least two putative citrate transporters have been identified (SSQG_01282 and SSQG_01602). When grown with 2 mM of trisodium citrate, the *S. viridochromogenes* WT showed a normal morphological development, characterized by the formation of a substrate mycelium, which merges into an aerial mycelium and finally results in the production of green spores. The supply of 10 mM of trisodium citrate led to the formation of only substrate and aerial mycelium, whereas no spore production was detected. With 20 mM trisodium citrate the WT strain even failed to develop any aerial hyphae corresponding to the general phenotype of the MacnA mutant (Fig. 1A). In contrast, when other organic acids (e.g. sodium acetate; succinic acid, disodium salt) were added to the medium in the same concentrations, growth was normal and only spore formation was impaired at 20 mM of the respective organic acid (Fig. S1). Thus, high citrate concentrations severely impair the morphological development of *S. viridochromogenes* and an increased citrate concentration is at least partially responsible for the defective differentiation of MacnA.

To further analyse if the growth defect of MacnA arises from a pH decrease due to organic acid accumulation, as

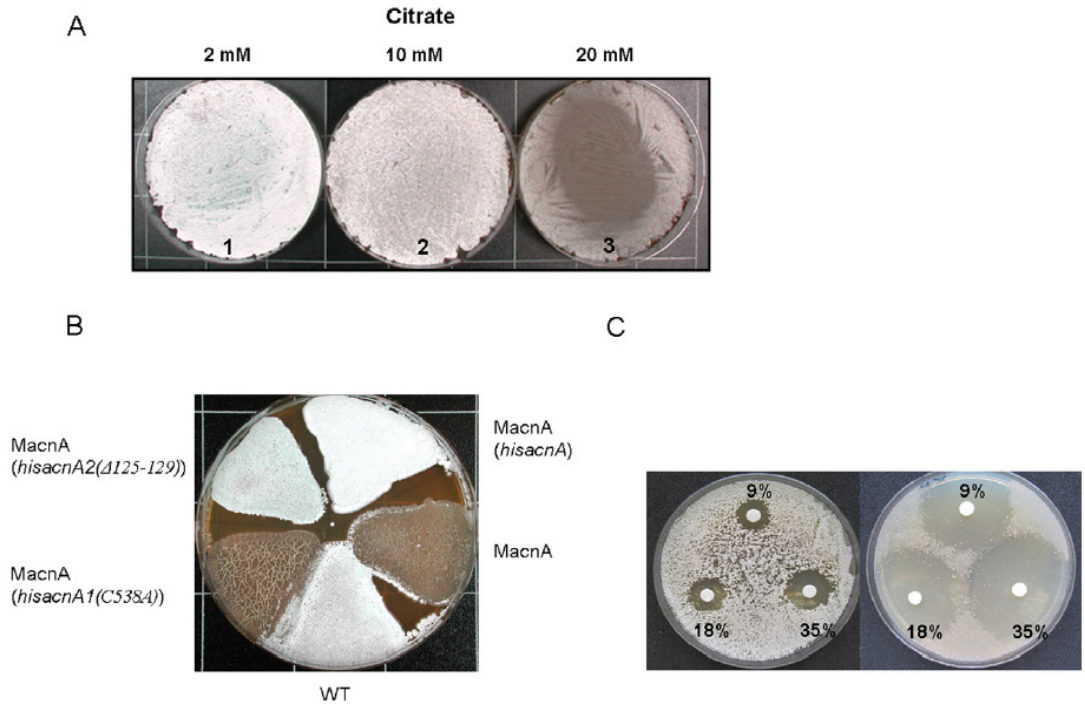

Fig. 1. A. Phenotypic comparison of *S. viridochromogenes* WT grown for 6 days in YM medium with different concentrations of citrate [(1) 2 mM, (2) 10 mM, (3) 20 mM]. Spores are visible by a green, aerial mycelium by a white, and substrate mycelium by a brown colour.
B. Phenotypic comparison of MacnA strains complemented with the different mutated aconitase genes *hisacnA*, *hisacnA*1(C538A), and *hisacnA*2(Δ125–129).
C. Susceptibility of WT and MacnA to oxidative stress. WT and MacnA were streaked on YM agar plates and incubated for 36 h. Filter plates containing 20 µl of different H_2O_2 concentrations (9%, 18% or 35% H_2O_2) were placed on the plates, and the inhibition zones indicating sensitivity to H_2O_2 were photographed after a further 36 h.

reported previously for several mutants showing the bald phenotype (Süsstrunk *et al*., 1998), the *S. viridochromogenes* WT and MacnA were grown in glucose-containing medium. Here, MacnA showed a steady decrease in pH to 4.5, while the WT strain had only a temporary pH decrease (data not shown). To test if external pH influences *S. viridochromogenes* development, the WT was cultivated on media with different pHs. On neutral pH the WT strain showed normal growth, whereas it was unable to differentiate on plates buffered at a pH lower than 5.0. In contrast, MacnA already demonstrated morphological defects on plates buffered at neutral pH (data not shown). This suggests that the low pH cannot be the sole reason for the defective differentiation of MacnA.

Furthermore, because of citrate being a chelator of divalent cations, its accumulation would interfere with the natural ion balance in the cell and impair the cellular metabolism since divalent cations serve as cofactors for several enzymatic reactions. Divalent cations have also been previously described to be essential for the activation of sporulation in *B. subtilis* (Craig *et al*., 1997).

In summary, the morphological defects of MacnA may be caused by several factors, which probably correlate with each other: deletion of aconitase most likely results in an extensive citrate accumulation, which may impair the cellular metabolism in high concentrations. Furthermore, it probably leads to an increase of organic acid production in general and thus to a decrease in the intracellular pH, as reported previously (Viollier *et al*., 2001a). Besides, the citrate may capture divalent cations needed for various enzymatic reactions. Another explanation for the growth defect of MacnA may lie in the regulatory role of AcnA (see below).

Identification of a catalytically active amino acid in AcnA

The amino acids specifically required for substrate recognition, catalysis and [4Fe-4S] cluster assembly are known

Table 2. Conserved amino acids involved in the catalytic and regulatory function of AcnA.

	Bovine aa position	AcnA aa position
[4Fe-4S]-Cluster		
Cys	358	472
Cys	421	538
Cys	424	541
Asp	258	296
Asp	446	576
Substrate recognition		
Glu	72	84
Ser	166	204
Arg	447	571
Arg	452	576
Arg	580	748
Ser	643	817
Arg	644	818
Catalysis		
Asp	100	123
His	101	124
Asp	165	203
His	147	176
Glu	262	300
His	167	205
Ser	642	816
RNA-binding		
Arg	728	763
Arg/Glu	R732	Q767
RNA-binding motif		
IRE-BP	DLVIDHSIQVD	
AcnA	ELVIDHSVIAD	

for the bovine mitochondrial aconitase (ACO2; Accession number Z49931; Table 2) (Lauble *et al.*, 1992). The respective residues in *S. viridochromogenes* AcnA were identified by comparing the amino acid sequences of the two proteins. Three cysteine residues involved in the coordination of the [4Fe-4S] cluster are known to be essential for the catalytic activity of ACO2 (Lauble *et al.*, 1992). To generate an enzymatically inactive version of *S. viridochromogenes* AcnA, Cys538 was mutated to an alanine residue using site-directed mutagenesis (HisacnA1(C538A)) (Fig. 2A). HisacnA1(C538A) and HisacnA were heterologously expressed in *S. lividans* T7 and purified as His-tagged proteins (Fig. 2B). After dialysis the specific activities of the mutated aconitases were determined. Whereas HisacnA had an enzymatic activity of approximately 12 U mg^{-1} protein, HisacnA1(C538A) showed no enzymatic activity at all (Fig. 2C), demonstrating that Cys538 is essential for the catalytic function of AcnA. To analyse the effects of the mutation of AcnA on growth and PTT production, *hisacnA* and *hisacnA1(C538A)* were expressed in a Δ*acnA* background. This was accomplished using the integrative plasmid pSET152 carrying the mutated *acnA* genes under the control of the native *acnA* promoter (*pacnA*). As expected, introduction of the *hisacnA* gene into MacnA (MacnA(*hisacnA*)) restored normal growth behaviour (Fig. 1B) and PTT production to the WT level (Fig. S2). In contrast, introduction of *hisacnA1(C538A)* did not rescue the growth defect of MacnA (Fig. 1B) and resulted in only a slight increase in PTT production (Fig. S2). This shows that the loss of the catalytic function of AcnA is one reason for the growth and physiological defect of MacnA.

apo-AcnA is an RNA binding protein

In order to analyse the regulatory function of HisacnA, the protein was purified and used in gel shift assays with the Cy5-labelled, 44 bp IRE structure of human ferritin (*hfer*, Fig. 3), which has been successfully used as a reference for the analysis of aconitase–RNA interactions (Banerjee *et al.*, 2007). Here, HisacnA was only able to bind to *hfer* in its apo-form, which is devoid of the [4Fe-4S] cluster. In contrast, HisacnA with the reactivated [4Fe-4S] cluster did not form a binding complex with the *hfer* IRE sequence (Fig. 4A). To verify the specificity of the HisacnA–IRE binding, increasing concentrations of unlabelled *hfer* RNA were added to the protein-RNA incubation mixture, which resulted in a decrease of Cy5-*hfer*-HisAcnA complex formation since the unlabelled *hfer* RNA displaced the Cy5-labelled *hfer* RNA from the apo-HisacnA protein in a concentration dependent manner (Fig. 4B). As a negative control, the binding of apo-HisacnA to a 50 bp internal fragment of *hrdB* mRNA was analysed, which lacks any IRE-like structure. No complex formation was detected with *hrdB* and apo-HisacnA (Fig. 4C), demonstrating that binding of aconitase is IRE-sequence specific. Altogether, these results suggest that AcnA has a RNA-binding ability in its apo-form, which is IRE-sequence specific.

Putative RNA-binding residues in AcnA are involved in catalysis

AcnA shows around 50% sequence identity to IRP1 and aconitases of *B. subtilis* and *M. tuberculosis*, whereas it is only little identical to *E. coli* aconitases (25% AcnA, 16% AcnB). To investigate the regulatory function of AcnA on a molecular level, the sequences of AcnA and IRP1 were compared since IRP1 is the best studied aconitase. High sequence conservation was observed for a region of AcnA, which aligns with the IRE-binding region of IRP1 (Fig. 5A and B; Table 2). Specific residues were identified that may be responsible for the coordination of the negatively charged RNA backbone to the apo-AcnA protein (Fig. 5C). Two of the identified residues, Arg763 and Gln767, are likely to be important for binding (Table 2) as homologous residues in rabbit IRP1 (Arg728 and Arg732) and CitB from *B. subtilis* (Arg740 and Gln744) are critical for the interaction of the IRPs with their RNA targets (Kaldy *et al.*, 1999; Serio *et al.*, 2006). To analyse the regulatory function of these residues in AcnA, the

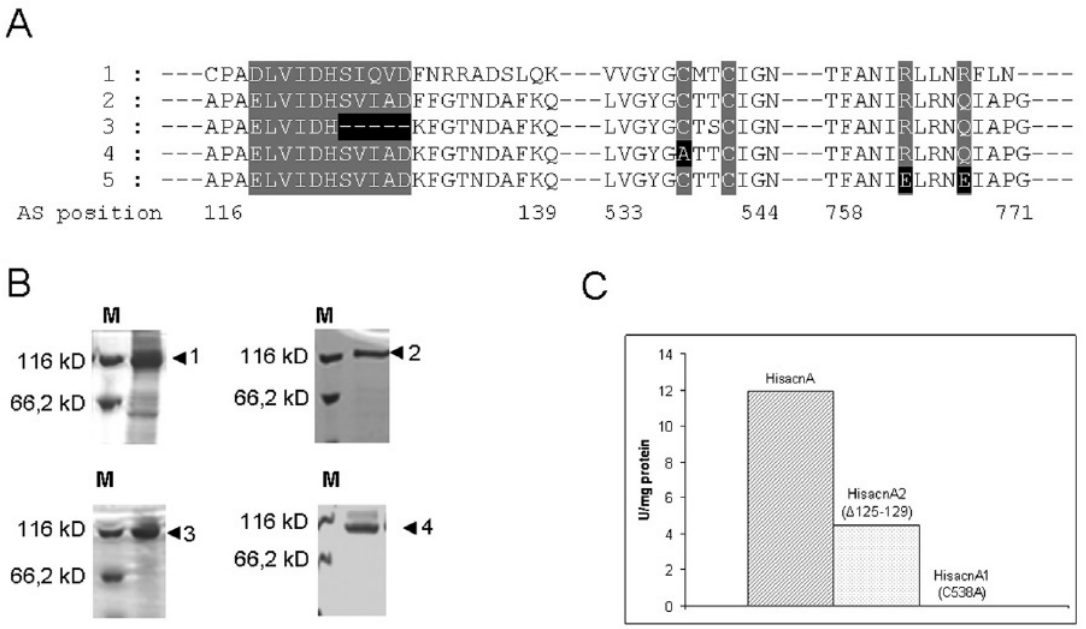

Fig. 2. A. Schematic presentation of the differences in the regulatory and catalytically important residues of IRP1 and the mutated AcnA variants. Lane 1, IRP1; lane 2, HisacnA; lane 3, HisacnA2(Δ125–129); lane 4, HisacnA1(C538A); lane 5, HisacnA3(R763E/Q767E). Grey boxes mark the conserved IRE-binding motifs, two of the conserved cysteines necessary for [4Fe-4S] cluster formation, and the conserved Arg and Gln residues involved in RNA binding. Black boxes highlight the introduced mutations.
B. SDS-PAGE of the purified HisAcnA variants. Lane M, protein molecular weight marker; lane 1, HisacnA; lane 2, HisacnA2(Δ125–129); lane 3, HisacnA1(C538A); lane 4 HisacnA3(R763E/Q767E). All proteins have a size of approximately 100 kDa.
C. Aconitase activity (U mg^{-1} protein) of purified HisacnA, HisacnA2(Δ125–129), and HisacnA1(C538A). The activities were measured at OD_{240}. Aconitases were assayed in a 225 μl reaction mixture containing 50 mM NaCl and 30 mM trisodium citrate.

respective DNA codons were mutated to triplets encoding glutamate residues using site-directed mutagenesis (HisacnA3(R763E/Q767E)). In addition, we identified an amino acid sequence in AcnA (amino acids 119–129; Table 2) that was previously shown to be important for IRE binding in the human iron-responsive element-binding protein (IRE-BP) (Basilion *et al.*, 1994). To analyse its function, the sequence was partially deleted in HisacnA2(Δ125–129) using a recombinant PCR approach (Fig. 2A).

HisacnA3(R763E/Q767E) and HisacnA2(Δ125–129) were heterologously expressed and purified from *S. lividans* T7 (Fig. 2B). Both proteins were assayed for their enzymatic activity. While HisacnA2(Δ125–129) was active (approximately 4.5 U mg^{-1} protein), albeit at a lower level than HisacnA (approximately 12 U mg^{-1} protein; Fig. 2C),

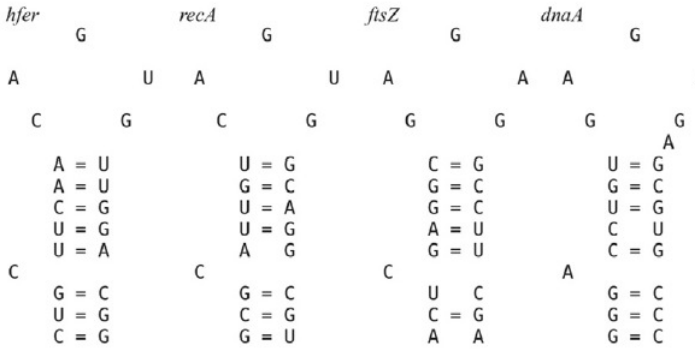

Fig. 3. IRE-like hairpin structures from humans and streptomycetes. *hfer*, IRE-structure from human ferritin; *recA*, *ftsZ*, and *dnaA*, IRE-like structures from *S. viridochromogenes*.

HisacnA3(R763E/Q767E) displayed no enzymatic activity (data not shown). Apparently, the amino acids Arg763 and Gln767 are essential for aconitase activity, whereas the sequence motif consisting of Ser125/Val126/Ile127/Ala128/Asp129 is dispensable for the catalytic function of AcnA. The fact that predicted RNA-binding residues are needed for the catalytic function of the aconitase is not surprising since also previous structural analyses of IRE-BP have suggested that the enzymatic active-site cleft of this protein provides at least part of the RNA binding site (Basilion *et al.*, 1994).

Arg763 and Gln767, but not Cys538 are important for the binding to IRE-like structures

To determine if the IRE-binding activity is interconnected with the catalytic function of AcnA, the catalytically inactive HisacnA1(C538A) was assayed for *hfer*-binding activity. Here, only a weak binding was observed with HisacnA1(C538A) and *hfer* in gel shift assays (Fig. 4D), suggesting the exchange of the cysteine in the [4Fe-4S] cluster did not completely block the regulatory activity of AcnA. Similar results have been obtained using the *B. subtilis* aconitase ACN_{C517A} that also was mutated in one of the cysteines important for [4Fe-4S] cluster assembly and had a lower affinity for the IRE sequence than the wild-type aconitase (Alén and Sonenshein, 1999). In contrast, apo-HisacnA3(R763E/Q767E), which was mutated in the amino acids that are responsible for the coordination of the RNA, could not bind to the IRE-like structure at all (Fig. 4E). Therefore, HisacnA3(R763E/Q767E) probably is regulatory inactive. Surprisingly, the binding to the IRE hairpin structure of apo-HisacnA2(Δ125–129), which was deleted for a portion of the putative IRE-binding region, was even stronger in comparison with apo-HisacnA (Fig. 4D). Probably, the deletion of the five amino acids led to a conformational change of the AcnA protein that is beneficial for its RNA-binding ability. Interestingly, complementation of MacnA with *hisacnA2(Δ125–129)* resulted in a strain that sporulated earlier (Fig. 1B) and had an increased PTT production (Fig. S2) compared with MacnA(*hisacnA*). This change in sporulation may be interconnected with the improved RNA-binding ability of HisacnA2(Δ125–129) because one of the suggested AcnA targets is involved in *Streptomyces* spore formation (see *ftsZ* IRE below).

Identification of IRE-like structures in the UTRs of various S. viridochromogenes *genes*

To identify the target genes for the AcnA-IRE mediated regulation, a computational search for conserved IRE-like structures in *S. viridochromogenes*, *S. coelicolor*, *S. avermitilis* and *S. griseus* was performed using the SPIRE algorithm (see *Experimental procedures*). Here, the known eukaryotic (Henderson *et al.*, 1994; Butt *et al.*, 1996; Walden *et al.*, 2006) as well as prokaryotic IRE sequence motives (Alén and Sonenshein, 1999; Tang and Guest, 1999; Banerjee *et al.*, 2007) were used for the search of IRE motives in streptomycetes. The programme also allowed variance in sequence composition and secondary structure folding. A putative IRE sequence with high similarity to *hfer* IRE was identified in front of *recA* (encoding recombinase A), *uvrB* (encoding an excinuclease), and *SSQG_01218* (putative uracil-DNA glycosylase), all of which are genes of the DNA repair pathway and known to be involved in oxidative stress response (Sancar and Sancar, 1988). Another typical IRE sequences with the CAGUG loop sequence was identified in front of *terD*, which encodes a tellurium resistance protein (Table 3). Because variation was allowed, structures that were not perfectly identical to the IRE consensus loop sequence were also identified. For example, hairpins with a GAGAG loop instead of the typical CAGUG loop were found in the 5′ UTR in front of the translational start codon of *ftsZ*, which codes for a cell division protein, involved in spore wall formation of *Streptomyces* (Flärdh, 2003), as well as in front of *dnaA*, encoding a DNA replication initiator protein (Zakrzewska-Czerwińska *et al.*, 2000). Another difference in the IRE-like structure of *dnaA* is the atypical A instead of the typical C in the bulge region (Fig. 3). It has been shown before that also an 'A bulge' can be part of a functional IRE sequence (Henderson *et al.*, 1994). However, here it is not clear if the A codon really forms the bulge *in vivo* or if maybe the following C residue or even a 2 bp nucleotide is used for the bulge formation. The GAGAG loop was also identified in front of *rpsQ* (ribosomal protein S17) and *thrS* (threonyl-t-RNA synthetase), which have predicted functions in transcription and translation. *SSQG_06118* (putative thiolase), *SSQG_03986* (putative subunit of pyruvate dehydrogenase complex), *SSQG_06761* (putative polyprenyl synthetase), and *gltB* (subunit of glutamate synthase), next to IRE-like motifs, are all putatively involved in bacterial metabolism (Table 3). As another loop variant CUGUG was identified, which is located in the 5′ UTR in front of *SSQG_00552*, encoding a putative FAD-binding oxidoreductase, which has a predicted function in oxidative stress response. IRE sequences were also identified in the 3′ UTRs downstream of several genes. Two of them encode putative regulators (*SSQG_07448* and *SSQG_03294*), of which *SSQG_07448* codes for an IRP, suggesting that AcnA might be involved in regulation of iron metabolism. *SSQG_03294* encodes a MarR family transcriptional regulator. Interestingly, the promoter region of *acnA* contains a binding site for MarR, which is a global transcriptional regulator known to be involved in oxidative stress response (Muschko *et al.*, 2002; Bussmann *et al.*, 2010).

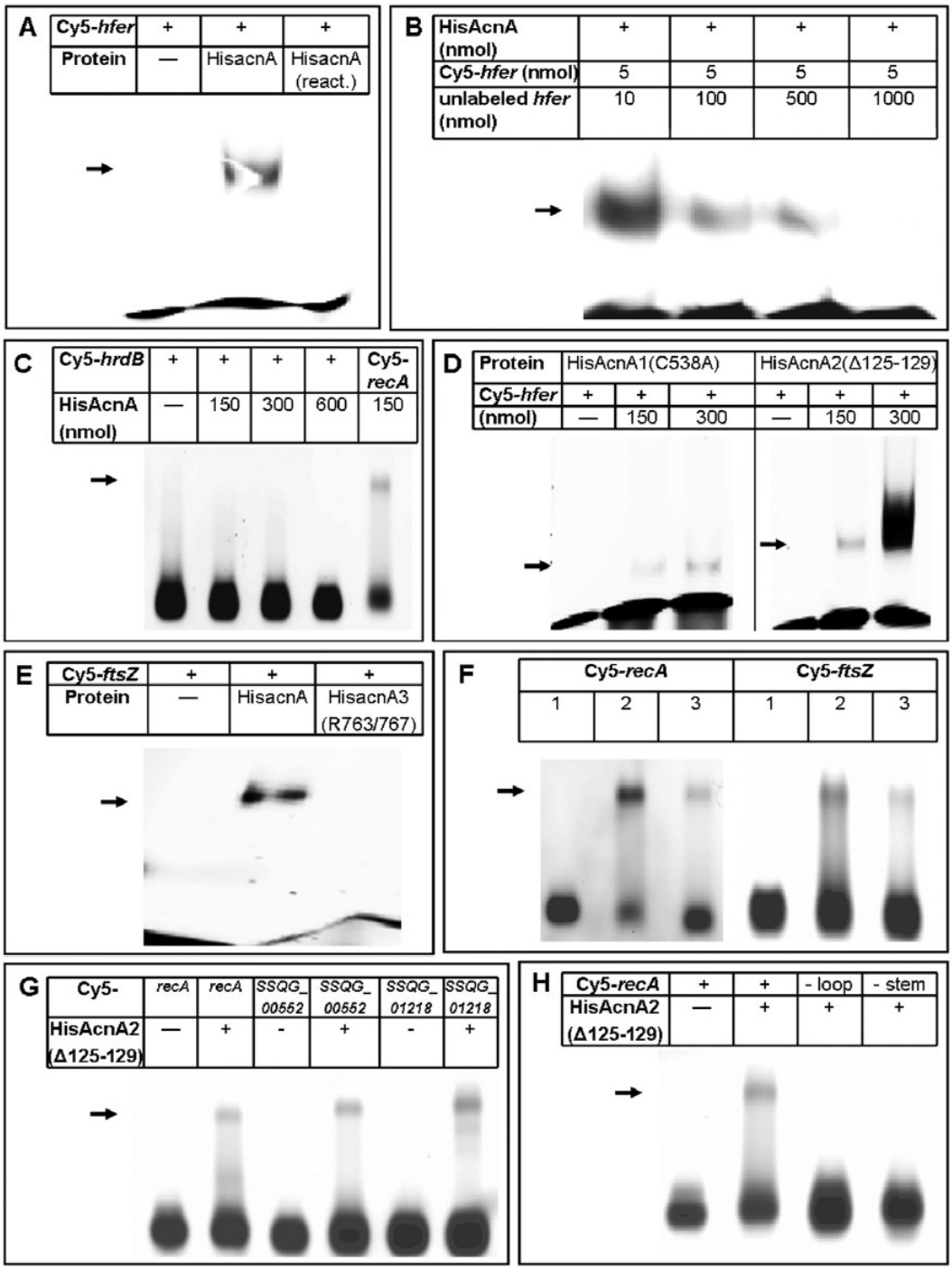

Fig. 4. Gel shift assays with IRE-like structures and purified HisAcnA proteins.
A. RNA containing IRE of human ferritin (*hfer*) together with oxidized or reactivated (react.) HisacnA.
B. RNA containing IRE of human ferritin (*hfer*) together with apo-HisacnA and increasing concentrations of unlabelled specific *hfer* RNA.
C. internal *hrdB* RNA fragment with increasing concentrations of apo-HisAcnA, RNA containing the IRE-like structure of *recA* was used as a positive control.
D. RNA containing *hfer*-IRE together with increasing concentrations of apo-HisacnA1(C538A) and apo-HisacnA2(Δ125–129) respectively, on two seperate gels.
E. RNA containing IRE-like structure of *ftsZ* together with apo-HisacnA and apo-HisacnA3(Q763E/R767E) respectively.
F. gel shifts with RNA containing IRE-like structures of *recA* and *ftsZ* together with water (1), apo-HisacnA (2), and apo-HisacnA2(Δ125–129) (3) respectively.
G. RNA containing IRE-like structures of *recA*, *SSQG_00552*, and *SSQG_01218* together with apo-HisacnA2(Δ125–129) respectively. Arrows show shifted bands.
H. RNA containing IRE-like structure of *recA*, *recA* without loop (– loop), and *recA* without stem sequence (– stem) together with apo-HisacnA2(Δ125–129) respectively.

Another IRE was identified downstream of *SSQG_00660* encoding a glutamate racemase, which besides is function in D-glutamate synthesis for cell wall biosynthesis is involved in gyrase inhibition and in this way may coordinate DNA replication and cell division (Sengupta *et al.*, 2008). *SSQG_03723* containing an IRE at the 3′ UTR codes for an ATP-dependent RNA helicase HrpA, involved in mRNA processing (Koo *et al.*, 2004) (Table 3). Generally, the identified IRE sequences at the 3′ UTRs were located farther from the transcriptional stop codon of the

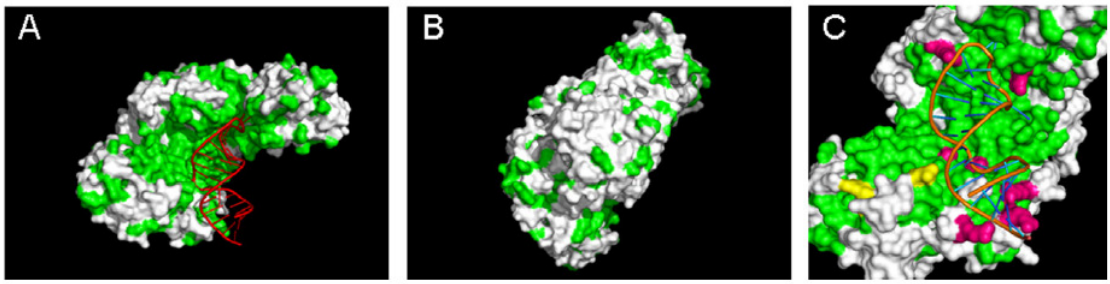

Fig. 5. Schematic presentation of the conserved protein regions in AcnA. AcnA was modelled according to the known structure of rabbit IRP1.
A. Front view.
B. Back view.
C. View of the putative RNA-binding region.
Variable residues (grey), perfectly conserved residues (green) and arginines presumably involved in coordinating the RNA (pink) are indicated. Mutated residues in AcnA3(R763E/Q767E) are highlighted (yellow).

Table 3. Identified hairpin loops in the genome of *S. viridochromogenes*.

Annotation in the *Streptomyces viridochromogenes* locus	Gene	Function	Sequence (loop region)	Localization[a]	
SSQG_00660	*n. n.*	Glutamate racemase	CAGUG	3′	86 bp
SSQG_00725	*terD*	Tellurium resistance	CAGUG	5′	64 bp
SSQG_01895	*uvrB*	Excinuclease	CAGUG	5′	21 bp
SSQG_03294	*n. n.*	MarR family transcriptional regulator	CAGUG	3′	137 bp
SSQG_03986	*n. n.*	Putative subunit of pyruvate dehydrogenase complex	CAGUG	5′	15 bp
SSQG_05803	*recA*	Recombinase A	CAGUG	5′	57 bp
SSQG_07448	*n. n.*	Iron regulatory protein	CAGUG	3′	157 bp
SSQG_03723	*n. n.*	ATP-dependent RNA helicase HrpA	CUGUG	3′	91 bp
SSQG_01405	*thrS*	Threonyl-t-RNA synthetase	GAGAG	5′	4 bp
SSQG_01968	*gltB*	Subunit of glutamate synthase	GAGAG	5′	60 bp
SSQG_02023	*ftsZ*	Cell division	GAGAG	5′	9 bp
SSQG_03923	*dnaA*	DNA replication initiation	GAGAG	5′	4 bp
SSQG_04780	*rpsQ*	Ribosomal protein S17	GAGAG	5′	6 bp
SSQG_06118	*n. n.*	Putative thiolase	GAGAG	5′	5 bp
SSQG_06761	*n. n.*	Putative polyprenyl synthetase	GAGAG	5′	93 bp

a. Distance of the IRE-like structure from the start or stop codon.

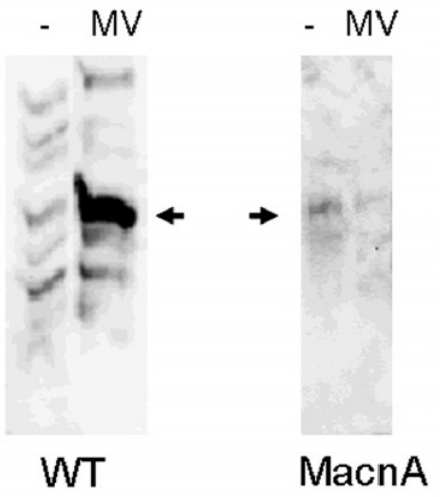

Fig. 6. Immunoblot analysis of RecA expression in WT *S. viridochromogenes* and MacnA. Cell-free extracts were separated using SDS-PAGE and RecA was detected using an *S. coelicolor* RecA antibody that also binds to *S. viridochromogenes* RecA. Oxidative stress was simulated by the addition of the oxidative stress reagent methyl viologen (MV). –, without methyl viologen; MV, with methyl viologen. The arrows point to the RecA protein band.

respective gene than the IREs at the 5′ UTR in respect to the transcriptional start codon.

apo-AcnA has an IRE-sequence specific RNA-binding ability

To analyse if the identified IRE motifs with the different loop sequences are really bound by the AcnA protein, gel shift assays with apo-HisAcnA and apo-HisacnA2(Δ125–129) were performed together with RNA fragments containing the *recA* and *ftsZ* IRE-like sequences of *S. viridochromogenes* respectively. apo-HisacnA2(Δ125–129) was used as this protein always showed the best shift performance (see above). All structures formed a complex with apo-HisacnA as well as with apo-HisacnA2(Δ125–129) (Fig. 4F). Here, the apo-HisacnA proteins did not prefer the GAGAG loop of *ftsZ* or the CAGUG loop of *recA* in the IRE-like structure since both RNAs were recognized equally. Besides that, the RNA fragment containing the *SSQG_00552* IRE-sequence with a CUGUG loop and six different RNAs harbouring a CAGCG loop (data not shown) were analysed in gel shifts with apo-HisacnA(Δ125–129). In these assays only the *SSQG_00552* RNA led to a shift, whereas all the RNAs with the CAGCG loop did not shift (data not shown). Also here the CUGUG loop was not preferred over the CAGUG loop as the *SSQG_00552* RNA was bound with an equal efficiency as the control RNAs *recA* and *SSQG_01218* (Fig. 4G). Furthermore, these data clearly show that CAGCG is not a functional IRE loop sequence. From these results we suggest a conserved IRE loop motif, which may consist of a SWGWG (S = G or C; W = A or U) pentanucleotide. Thus, all the genes harbouring an IREs sequence with a GAGUG, GAGAG, or CUGUG loop (Table 3) are presumably post-transcriptionally regulated by AcnA.

To further analyse if the stem and the loop structures of IRE sequences are important for AcnA binding, gel shift assays were performed with apo-HisacnA2(Δ125–129) and *recA* RNAs, where the loop and stem sequences were each exchanged by sequences that cannot form such secondary structures (*recA-loop* and *recA-stem* respectively). Here, only the native *recA* RNA sequence was bound by apo-HisacnA(Δ125–129), whereas the RNAs without stem or loop structures showed no shifted band (Fig. 4H), illustrating that both secondary structures are essential for AcnA binding.

RecA is post-transcriptionally upregulated under oxidative stress conditions

Since binding of apo-HisAcnA to the *recA* RNA was successfully shown in gel shift assays, we analysed whether AcnA is really involved in the post-transcriptional regulation of RecA synthesis. Therefore, we aimed to assess the amount of RecA protein in the WT and the MacnA mutant strain after applying oxidative stress to the cells. For these analyses *S. viridochromogenes* WT and MacnA were grown in YM medium to the mid-exponential phase, when rifampicin was added to the cultures. Rifampicin is a RNA-polymerase specific inhibitor and was used to exclude any regulatory effects on transcriptional level. Each culture was supplemented with methyl viologen as an oxidative stress inducer to induce a transition of AcnA into its regulatory active apo-form. The addition of methyl viologen clearly resulted in a higher RecA protein level in the WT strain, while no difference in RecA amount was observed for the MacnA mutant (Fig. 6). Furthermore, RT-PCR experiments showed that the *recA* transcript amount is significantly decreased in MacnA compared with the WT, suggesting that the *recA* transcript is stabilized by AcnA (Fig. S3). This supports the potential post-transcriptional regulatory role of AcnA in the synthesis of RecA under oxidative stress conditions.

MacnA is sensitive to oxidative and temperature stress

To analyse the physiological influence of oxidative stress on *S. viridochromogenes* WT and MacnA growth, both strains were exposed to different concentrations of

hydrogen peroxide in a filter plate assay (Fig. 1C). The inhibition zones caused by hydrogen peroxide were approximately 2.5 times larger in MacnA compared with the WT strain. To some extent the higher sensitivity of MacnA to hydrogen peroxide may be associated with the regulatory role of AcnA in oxidative stress response, as previously shown for *E. coli* aconitase A (Tang *et al.*, 2002). Since an increased temperature correlates with the formation of hydroxyl radicals (Lüders *et al.*, 2009), we also tested the heat stress resistance of the WT and the MacnA mutant strain by incubating them at 27°C, 37°C and 39°C. While the WT strain showed little or no sensitivity towards high temperatures, MacnA was unable to grow at 39°C (data not shown). Generation of hydroxyl radicals at high temperatures could be one explanation for this phenotype. However, since the MacnA mutant grows much slower than the WT, which probably results from its impaired cellular metabolism, any kind of stress condition may harm the mutant more than the WT strain. Thus, the stress sensitivity of MacnA cannot directly be assigned to the regulatory function of AcnA in oxidative stress response.

Discussion

Aconitases have a central role in carbon metabolism. Therefore, various aconitase-deficient strains, such as of *S. aureus* and *B. subtilis* have multiple defects in morphological and physiological differentiation (Craig *et al.*, 1997; Somerville *et al.*, 2002). Similarly, the aconitase mutant of *S. viridochromogenes*, MacnA, is impaired in differentiation and showed the bald phenotype (Schwartz *et al.*, 1999). In this study, we demonstrate that the differentiation defect of MacnA is linked to the loss of the catalytic function of AcnA, which catalyses the conversion of citrate to isocitrate. This is suggested since the expression of catalytically inactive but regulatory active HisacnA1(C538A) in MacnA did not lead to any improvement in morphological differentiation. Similar results were obtained after expression of catalytically inactive HisacnA3(R763E/R767E) in MacnA. The morphological development of *S. viridochromogenes* WT is inhibited by the exogenous addition of 20 mM citrate, suggesting that the differentiation defect of MacnA is the result of an increase of the citrate level. In further support of this, citrate accumulation up to 14 mM was observed in an aconitase mutant of *S. coelicolor*, while no citrate was detectable in WT *S. coelicolor* (Viollier *et al.*, 2001b). The ability of citrate to chelate divalent ions has been suggested to be the mechanism underlying the differentiation defect of a *B. subtilis* aconitase mutant. Craig *et al.* speculated that divalent cations, which are needed as cofactors in a phosphorelay system involved in the initiation of sporulation, would be sequestered by citrate (Craig *et al.*, 1997). Indeed, it has been shown that addition of Fe^{2+} and Mn^{2+} partially restored sporulation of the *B. subtilis* aconitase mutant. In our study however, the addition of iron ions to WT *S. viridochromogenes* growing on plates with 20 mM citrate did not prevent the differentiation defect (K. Schad, unpublished). Similarly, no increase in differentiation was observed following the addition of several divalent cations to the *S. coelicolor* aconitase mutant (Viollier *et al.*, 2001b).

Alternatively, it has been proposed that a pH decrease, caused by the accumulation of organic acids due to the block of the TCA cycle, might be the reason for the differentiation defect. In fact, low pHs block the differentiation process of the *S. viridochromogenes* WT. In a *S. coelicolor* aconitase mutant, the pH steadily decreased over the course of growth, and pH values less than 5.0 have been reported to retard *S. coelicolor* growth (Viollier *et al.*, 2001a,b). The cultivation of this mutant on plates buffered at neutral pH did not restore colony development (Viollier *et al.*, 2001b). The same was found for the *S. viridochromogenes* MacnA strain, suggesting that the pH decrease is not the only reason for the differentiation defect. These observations indicate that low pHs may only partially be the reason for the growth defect of the aconitase mutants. Altogether, the growth defect of MacnA may come from a combination of several aspects, which to some extent correlate with each other (high citrate concentration, low pH, cation chelation, regulation). Previous studies on the *S. viridochromogenes* aconitase have suggested an additional regulatory function of AcnA that is similar to that reported for IRPs (Schwartz *et al.*, 1999). It might be that this regulatory function of AcnA is in part involved in morphological differentiation. This is assumed since the expression of HisacnA2(Δ125–129), which is deleted in a predicted RNA-binding sequence resulted in an earlier sporulation of the strain. This phenotypical effect may be due to the improved IRE binding of HisacnA2(Δ125–129), which probably (de)stabilizes respective mRNAs involved in morphological development.

Here we provide new results that highlight the regulatory function of AcnA. HisacnA can bind to the consensus IRE of human ferritin (*hfer*). The binding of HisacnA to *hfer* only occurred in its apo-form that lacked the [4Fe-4S] cluster. This conformational change presumably occurs upon iron starvation or oxidative stress, which leads to a disassembly of the [4Fe-4S] cluster. The resulting apoenzyme undergoes structural changes in such a way that a cleft is opened within the aconitase, which is necessary for the binding to IRE-like stem-loop RNA structures (Dupuy *et al.*, 2006).

In vertebrates the main function of the IRP–IRE system is the regulation of iron metabolism (Muck-

enthaler *et al.*, 2008). Similarly, the aconitase of the Gram-positive actinobacterium *M. tuberculosis* is involved in the regulation of iron metabolism. The mycobacterial aconitase has been shown to bind to IRE-like structures in the UTRs of the mRNA of an iron-containing enzyme (*trxC*) and an iron-dependent regulator (*ideR*) (Banerjee *et al.*, 2007). Whether the *S. viridochromogenes* aconitase AcnA is involved in iron response remains unclear since no IRE-like structures have been found in the UTRs of genes known to be involved in iron metabolism. Perhaps streptomycetes do not need to regulate iron metabolism through AcnA because they (at least *S. coelicolor*) harbour a number of genes encoding putative siderophores (Barona-Gómez *et al.*, 2006), and therefore can transport iron quite efficiently under different environmental conditions. However, AcnA seems to be involved in oxidative stress response, because several IRE motifs were identified in the UTRs of genes involved in oxidative stress defence and regulation, such as *recA*, *uvrB*, *dnaA* and *SSQG_01218*, and their functionality was affirmed in gel shift assays. Furthermore, oxidative stress increased the amount of RecA protein in the *S. viridochromogenes* WT. This regulation obviously occurred on post-transcriptional level since the cultures examined for RecA expression were blocked in transcription by the addition of the RNA polymerase inhibitor rifampicin. Thus, AcnA promotes an increase in the amount of RecA protein in response to oxidative stress, which, in turn, is required to deal with the DNA damage caused by oxidative stress. However, how this regulation occurs on molecular level is still to be elucidated. Furthermore, the MacnA mutant showed an increased sensitivity to hydrogen peroxide. This impairment could be a hint that AcnA is involved in oxidative stress response. In addition, MacnA showed an increased susceptibility to heat stress. Lüders *et al.* reported that heat stress induced the expression of SodA, AhpC and Dps, which are enzymes known to be involved in oxidative stress response in *E. coli.* Interestingly, the SodA level is increased in *E. coli* by the binding of apo-AcnA to the *sodA* transcript under oxidative stress conditions (Tang *et al.*, 2002). Therefore, it is possible that, in addition or alternatively to the well-known heat shock regulation, *E. coli* uses a pathway for heat stress response similar to that of oxidative stress response. Another explanation for the heat sensitivity of MacnA is that the formation of hydroxyl radicals is increased at elevated temperatures (Lüders *et al.*, 2009). Since AcnA is involved in the oxidative stress defense, the higher concentration of hydroxyl radicals at 39°C could be responsible for the inability of the mutant MacnA to grow under heat stress. This is supported by the higher sensitivity of a *Lactococcus lactis recA* mutant to heat stress (Duwat *et al.*, 1995). However, as the mutation of any important primary metabolism gene will probably lead to a higher sensitivity of the respective mutant, the heat and oxygen stress sensitivity of MacnA cannot be regarded as an evidence for AcnAs role in oxidative stress response.

In addition to their probable role in the regulation of oxidative stress, aconitases seem to have a regulatory function in other pathways, including the onset of sporulation. Interestingly, one of the identified *S. viridochromogenes* hairpin structures is located in the 5′ UTR of *ftsZ*, and specific binding of HisacnA could be demonstrated. FtsZ is a cell division protein involved in the formation of septal crosswalls in aerial hyphae, finally leading to the generation of spores. *ftsZ* in streptomycetes is tightly regulated and possesses three different promoters (Flärdh *et al.*, 2000). The identified hairpin structure at the 5′ UTR is present in each *ftsZ* transcript and therefore possibly provides an additional regulatory element. In this regard, it is interesting that the phenotype of an *acnA* mutant is comparable to that of an *ftsZ* mutant of *S. coelicolor* (McCormick *et al.*, 1994), which is also defective in sporulation. The multiple effects of mutations in aconitases on differentiation have been described for various bacteria (Craig *et al.*, 1997; Wilson *et al.*, 1998; Somerville *et al.*, 2002). In a *citB* (aconitase) mutant of *B. subtilis*, *gerE*-dependent genes are down regulated (Serio *et al.*, 2006). CitB is specifically involved in binding to a hairpin structure at the 3′ UTR of *gerE*, which encodes a transcriptional regulator that regulates the expression of the alternative sigma factor σ_K. σ_K in turn regulates many genes that are important for the onset of sporulation.

Interestingly, the identified upstream regions of *recA*, *dnaA* and *ftsZ* harbouring IRE sequences were found to be highly conserved among several analysed differentiating actinomycetes (such as *S. viridochromogenes*, *S. griseus*, *S. coelicolor*, *S. avermitilis* . . .), whereas no such conserved region and no IRE motif was found in the respective upstream regions of the non-differentiating actinomycetes *Amycolatopsis japonicum* and *Actinoplanes friuliensis*. This indicates that in these strains there may be another way of regulation, which is aconitase-independent.

In this paper we provided evidence for a regulatory function of AcnA under stress conditions on the post-transcriptional level. This includes AcnA-binding to IRE-like structures in the UTRs of specific genes under oxidative stress conditions and thus altering their mRNA stability. In this way AcnA regulates the protein amount of several genes that are involved in sporulation like *ftsZ*, and in the DNA repair like *recA* and *uvrB*, allowing the cell to rapidly adapt to changing environmental conditions.

Experimental procedures

Bacterial strains, plasmids, growth conditions and analysis of PTT production

The bacterial strains and plasmids used in this work are listed in Table 1. The morphological and physiological properties of wild-type *S. viridochromogenes* Tü494 (WT), the *acnA* mutants and the complemented derivatives were examined on YM medium (Schwartz *et al.*, 1996). Cultivation was carried out at 30°C; liquid cultures were incubated in 100 ml of medium in an orbital shaker (180 r.p.m.) in 500 ml Erlenmeyer flasks with steel springs. Spores were isolated as previously described (Kieser *et al.*, 2000). PTT production was analysed in a previously described biological assay (Eys *et al.*, 2008) using *B. subtilis* ATCC6051 and *E. coli* XL1 blue (Bullock *et al.*, 1987) as test organisms.

Amplification, cloning, restriction mapping and in vitro *manipulation of DNA*

For the amplification of DNA fragments by PCR, the following reaction mixture was used: 0.5 μg of template DNA; 1.0 μg of each primer; 10 μl of 10× reaction buffer (containing 20 mM $MgCl_2$), 5% dimethylsulphoxide; 0.2 mM deoxynucleoside triphosphates; and 1 μl of polymerase (either *Taq* polymerase or ProofStart polymerase; Qiagen, Hilden, Germany) (Table S1). After an initial denaturation step (5 min at 98°C), 25 cycles of amplification (1 min 30 s at 94°C; 1 min 30 s at the specific annealing temperature of the primer pair; 2 min at 72°C) were performed. DNA isolation methods have been performed as described previously (Kieser *et al.*, 2000). The restriction nucleases were purchased from various suppliers and used as recommended by the manufacturer. Transformation of *E. coli* was carried out using the $CaCl_2$ method (Sambrook *et al.*, 1989). *Escherichia coli* XL1 Blue (Bullock *et al.*, 1987) cells were used for standard cloning experiments. Cloning constructs were sequenced to verify that no mutations were introduced during PCR.

Identification of IRE-like structures

To identify conserved putative IRE-like sequences, the genomes of *S. viridochromogenes* (GenBank NZ_GG657757), *S. avermitilis* (GenBank NC_003155), *S. coelicolor* (GenBank NC_003888), and *S. griseus* (GenBank NC_010572) were screened using a newly developed algorithm called SPIRE (Search for Prokaryote IRE).

The SPIRE algorithm

SPIRE is a sequence-based approach to identify IRE-like sequences in prokaryote genome data. IRE-like sequences are defined as sequences occurring in the up- or downstream untranslated region of genes that match the RNA pattern $BN_1N_2N_3N_4N_5LLLLLXM_5M_4M_3M_2M_1$, where B is the bulge position, which can be either C or A; N and M are pairing bases with identical indices; L is one of the five loop sequence bases, and X is an optional sixth base in the loop. The loop region reported for eukaryotes is CAGUG (Walden *et al.*, 2006). Based on binding affinity studies by Henderson and colleagues (1994) and Butt and colleagues (1996), as well as by reported binding sequences from *B. subtilis* (Alén and Sonenshein, 1999) and *M. tuberculosis* (Banerjee *et al.*, 2007), SPIRE searches for the additional loop sequences CAGCG, GAGAG, UAGUA, CAAUG, and CCGUG. Conserved IRE-like sequences can be identified by cross-checking against other genomes. A further filter optionally can remove hypothetical proteins.

SPIRE algorithm implementation

SPIRE is implemented using computational biology routines from BioPython (Cock *et al.*, 2009). In a first step, the regular expressions (ClA). . .. (CAGUG|CAAUG|GAGAG|UAGUA|CAGCG|CUGUG) and (CACAG|CACUG|CAUUG|CUCUC|UACUA|CGCUG). . .. (G|U) are used to search for bulge and loop matches on the forward and reverse strand respectively. SPIRE then checks if the regular expression matches fold to IRE-like stem-loop structures. When checking the fold, SPIRE allows for five or six bases in the loop region, as well as one mismatch in the stem. SPIRE allows to filter for hits that are located in the untranslated regions up to 200 bases up- or downstream of a gene, but can also consider all possible hits. To identify conserved IRE-like sequences, SPIRE can be run on reference genomes, using the output to build a BLAST database of IRE-like sequences. SPIRE then utilizes these BLAST database to filter for IRE-like sequences that show a significant similarity to IRE-like sequences from the reference genomes. The significance is assumed for BLAST hits with an *E*-value below 0.04. The hypothetical protein filter removes all hits where the neighbouring gene's product is annotated with the string 'hypothetical protein'. The used implementation of SPIRE is available at (http://www.uni-tuebingen.de/en/32760)

Analysis of the protein-specific RNA-binding region

To visualize the conservation of the RNA-binding region, the conserved residues of AcnA were each mapped to a template crystal structure of rabbit IRP1 (PDB-id 2IPY). The mapping was performed by aligning the protein sequence of AcnA to the template sequence. The mapped structures were rendered in PyMOL (Delano, 2002).

Amplification and cloning of acnA

The native *acnA* gene was amplified using primers P1 and P2 (Table S1); amplification with these primers produced PCR fragments with synthetic BamHI and HindIII restriction sites at the 5′ and 3′ ends respectively. The 2.7 kb PCR fragments were cloned into the PCR cloning vector pDrive (Qiagen) to generate the plasmid pKS1. From pKS1, *acnA* was isolated as a 2.8 kb BamHI/HindIII fragment that was subsequently cloned into pRSETB (digested with BglII and HindIII) to generate *acnA* with an N-terminal *his*-tag sequence (pKS6).

Site-specific mutagenesis of acnA

The mutagenesis of *acnA* was achieved using a recombinant PCR approach, as previously described (Heinzelmann *et al.*, 2003). To replace cysteine 538 in the catalytic centre of AcnA with alanine, the primers P3–P6 were designed. The primers P4 and P5 were complementary and mediated the exchange of cysteine to alanine at the genetic level ($TGC_{1612-14} \rightarrow GCT$). In the first step, the fragments *C538A*^{1} (913 bp) and *C538A*^{2} (584 bp) were amplified using P3/P4 or P5/P6. In the second step both fragments were used together with P3 and P6 to produce the 1.5 kb *C538A*$^{1+2}$ fragment. *C538A*$^{1+2}$ was cloned into EcoRV-digested pJOE890, generating pKS2. From pKS2, *C538A*$^{1+2}$ was isolated as a 1.0 kb BstXI-digested fragment and cloned into the BstXI-digested pKS6 (see above), generating the plasmid pKS7 with the *hisacnA1*(C538A) gene.

For the partial deletion of the putative IRE-binding motif in AcnA, primers P1, P7, P8, and P9 were used. Fragment 1, *Δ125–129*^{1}, containing the first 0.9 kb of *acnA*, was amplified using the primers P1 and P7. The second fragment, *Δ125–129*^{2} (1.5 kb), was amplified using the primers P8 and P9. Primers P7 and P8 were complementary and characterized by the deletion of codons 125–129 of *acnA*. In the second PCR step, both fragments were used with the primers P1 and P9 to generate the *Δ125–129*$^{1+2}$ (1.9 kb) fragment. *Δ125–129*$^{1+2}$ was cloned into pDRIVE to produce pKS3. The WT fragment in pKS1 was exchanged with the *Δ125–129*$^{1+2}$ fragment, using BamHI and NcoI restriction sites, to generate pKS4 containing the *acnA2(Δ125–129)* gene. *acnA2(Δ125–129)* was then isolated as 2.8 kb fragment from pKS4 by digestion with BamHI and HindIII and cloned into BglII/HindIII-digested pRSETB to generate pKS8.

In order to change Arg763 and Gln767 to glutamate residues, we created *R763E/Q767E*$^{1+2}$ using the fragments *R763E/Q767E*^{1} (amplified with primers P10 and P11) and *R763E/Q767E*^{2} (amplified with primers P12 and P13) and primers P10 and P13, as described above. *R763E/Q767E*$^{1+2}$ was cloned into pDrive generating pKS5. The *R763E/Q767E*$^{1+2}$ fragment was isolated from pKS5 by digestion with PfoI and BbsI and used to replace the WT fragment in pKS6 to generate pKS9 carrying *hisacnA3(R763E/Q767E)*.

Complementation of the MacnA mutant

For the complementation of MacnA, the native and the mutated *acnA* genes were isolated as NdeI/HindIII fragments from pKS6, pKS7, pKS8 or pKS9 and cloned into NdeI/HindIII-digested pEH98, generating pKS20, pKS21, pKS22 and pKS23 respectively. From these plasmids the *acnA*-fragments were isolated as EcoRI and XbaI fragments and then cloned into the integrative pSET152 vector, generating pKS24, pKS25, pKS26 and pKS27 respectively. In the next cloning step, the native *acnA* promoter (*pacnA*) was cloned in front of the various *acnA* genes to approximate the basal expression level. *pacnA* was amplified using primers P18 and P19 and cloned into pDrive to produce pKS10. From pKS10 the 1.1 kb *pacnA* fragment was isolated following digestion with EcoRI and BglII and cloned into EcoRI/BglII-digested pKS24, pKS25, pKS26, or pKS27, generating pKS28, pKS29, pKS30, and pKS31 respectively. These constructs were used for genetic complementation of MacnA.

Overexpression and purification of recombinant HisacnA, HisacnA1(C538A), HisacnA2(Δ125–129), and HisacnA3(R763E, Q767E)

To achieve expression in *Streptomyces lividans* T7, the plasmids pKS6, pKS7, pKS8 and pKS9 were fused to pGM9 (Muth *et al.*, 1989) using the HindIII restriction site in the plasmids. The resulting plasmids (pKS16, pKS17, pKS18 and pKS19 respectively) were directly used for transformation of *S. lividans* T7 protoplasts. The purification of the His-tagged proteins from *S. lividans* T7 was performed using a previously described procedure (Heinzelmann *et al.*, 2001). The collected fractions were analysed using standard 10% SDS-PAGEs. Size estimation was performed using the Unstained Protein Molecular Weight Marker (Fermentas, Burlington, Canada). The gels were stained with Coomassie brilliant blue and the fractions containing the mutated AcnA proteins were pooled. The pooled fractions were dialysed against 50 mM $NaHPO_4$, pH 8.0, and the protein concentrations were estimated using the BCA Protein Assay Kit (Thermo Scientific, Rockford, USA). The protein was stored at 4°C for no longer than 4 days and used for enzymatic tests or gel shift assays.

Reactivation of aconitase proteins

The activation of the aconitases was achieved under reducing conditions (1 mM DTT) by the addition of 0.5 mM $NH_4Fe(SO_4)_2$ and incubation on ice for 30 min. The reactivated protein was directly used for further experiments.

Aconitase enzyme test

Aconitases catalyse the isomerization of citrate to isocitrate via the intermediate *cis*-aconitate. During the aconitase reaction an equilibration of citrate, *cis*-aconitate, and isocitrate (89.5:4.3:6.2) is adjusted. The aconitase assay is based on the measurement of *cis*-aconitate at OD_{240}. The activities of purified AcnA and the mutated derivatives were measured at OD_{240}. Aconitases were assayed in a 225 µl reaction mixture containing 50 mM NaCl and 30 mM trisodium citrate. Specific aconitase activity was evaluated as described previously (Muschko *et al.*, 2002).

Gel shift assays

Cy5-labelled RNA with the IRE-like sequence from *hfer*, *recA*, *ftsZ*, *SSQG_01218 SSQG_00552*, or *hrdB* (Table S1) were commercially synthesized by Integrated DNA Technologies (IDT DNA, Leuven, Belgium). For gel shift assays with *recA* and *ftsZ*, the *S. coelicolor* IRE sequences were used because in the beginning of this work the *S. viridochromogenes* genome was not yet available. The sequence of the *ftsZ* RNA fragment was 100% identical to that of *S. viridochromogenes*, while the *recA*-sequence had four base substitutions that are not involved in the formation of the hairpin structure. All other IRE sequences were from *S. viridochromogenes*. A

total of 0.5 μg of RNA was incubated with purified protein (0.1–4 μg) in a gel shift assay containing 10 mM Tris-HCl (pH 8.0), 50 mM KCl, and 10% glycerol. Under these conditions the HisAcnA proteins were in the oxidized and thus regulatory active form, since the imidazol used for protein purification acts as an oxidizing agent and leads to a disassembly of the [4Fe-4S] cluster. Non-specific binding was prevented by the addition of a 100-fold excess of yeast tRNA (Sigma-Aldrich, Munich, Germany). The reactions were incubated for 15 min at room temperature and loaded on a 6% non-denaturing Tris-glycine polyacrylamide gel. RNA bands were visualized by fluorescence imaging using a Typhoon Trio+ Variable Mode Imager (GE Healthcare, Munich, Germany).

Immunoblot analysis of RecA expression

Precultures of *S. viridochromogenes* WT and MacnA were grown in 100 ml Erlenmeyer flasks at 27°C for 7 h in an orbital shaker (180 r.p.m.). Ten millilitres of each preculture was transferred to two Erlenmeyer flasks both containing 100 ml fresh YM medium. A *S. lividans recA* mutant (Vierling *et al.*, 2001) and *S. lividans* WT induced for RecA expression served as controls (data not shown). Transcription in the bacteria was subsequently arrested by the addition of rifampicin (0.2 mg ml^{-1}). One of each main culture was supplemented with methylviologen dichloride hydrate (0.2 mM) as an oxidative stress inducer. The cells were then incubated for 90 min and afterwards harvested by centrifugation (10 min, 5000 *g*). Cell pellets were resuspended in lysis buffer and disrupted using a French Press Cell (Aminco, Silver Springs, Maryland, USA). Cell-free extracts were recovered by centrifugation at 13000 *g* for 20 min at 4°C. The protein concentration was assayed using the BCA Protein Assay Kit (Thermo Scientific) and equal concentrations of the protein were stored at –20°C. Immunoblots were performed using a Perfect Blue Semi-Dry Electro Blotter (PEQLAB Biotechnologie GmbH, Erlangen, Germany). Immunoblot analysis was carried out using a rabbit anti-RecA antibody (S. Vierling and G. Muth, unpubl. data) and a secondary horseradish peroxidise-conjugated anti-rabbit antibody (Amersham, Freiburg, Germany). Bands were visualized using ECL Western Blotting Detection Reagents (Amersham, Freiburg, Germany).

RT-PCR analysis of recA

For RT-PCR experiments, the *S. viridochromogenes* WT and the MacnA mutant were grown in HM-medium at 30°C. Because WT and MacnA mutant strains showed different growth rates, samples were taken for different time points and DNA concentration of the biomass was estimated as described before (Herbert *et al.*, 1971) to ensure that the strains were in a comparable growth status. Prior to sample harvest, cells were treated with rifampicin (0.2 mg ml^{-1}) to exclude any regulatory effects on transcriptional level. Furthermore, respective cell lines were left untreated for 90 min as a control, whereas others were treated with heat stress at 39°C and oxidative stress (addition of 0.2 mM methyl viologen) for 90 min respectively. The 48 h sample of the WT and the 96 h sample of MacnA were used for RT-PCR analyses. RNA isolation and RT-PCR was performed as described previously (Amin *et al.*, 2011) with *recA*-specific internal primers. As a positive control, cDNA was amplified from the major vegetative sigma factor (*hrdB*) transcript, which is produced constitutively.

Acknowledgements

This research was supported by grants from the Deutsche Forschungsgemeinschaft (SPP1152: Wo 485/7-1,2,3) and the BMBF (GenBioCom #0315585A). We would like to thank Günther Muth for providing the anti-RecA antibody and for helpful discussions.

References

Alén, C., and Sonenshein, A.L. (1999) *Bacillus subtilis* aconitase is an RNA-binding protein. *Proc Natl Acad Sci USA* **96:** 10412–10417.

Alijah, R., Dorendorf, J., Talay, S., Pühler, A., and Wohlleben, W. (1991) Genetic analysis of the phosphinothricin-tripeptide biosynthetic pathway of *Streptomyces viridochromogenes* Tü494. *Appl Microbiol Biotechnol* **34:** 749–755.

Amin, R., Reuther, J., Bera, A., Wohlleben, W., and Mast, Y. (2011) A novel GlnR target gene, *nnaR*, is involved in nitrate/nitrite assimilation in *Streptomyces coelicolor*. *Microbiology* **158:** 1172–1182.

Banerjee, S., Nandyala, A.K., Raviprasad, P., Ahmed, N., and Hasnain, S.E. (2007) Iron-dependent RNA-binding activity of *Mycobacterium tuberculosis* aconitase. *J Bacteriol* **189:** 4046–4052.

Barona-Gómez, F., Lautru, S., Francou, F.X., Leblond, P., Pernodet, J.L., and Challis, G.L. (2006) Multiple biosynthetic and uptake systems mediate siderophore-dependent iron acquisition in *Streptomyces coelicolor* A3(2) and *Streptomyces ambofaciens* ATCC 23877. *Microbiology* **152:** 3355–3366.

Basilion, J.P., Rouault, T.A., Massinople, C.M., Klausner, R.D., and Burgess, W.H. (1994) The iron-responsive element-binding protein: localization of the RNA-binding site to the aconitase active-site cleft. *Proc Natl Acad Sci USA* **91:** 574–578.

Bayer, E., Gugel, K.H., Hägele, K., Hagenmaier, H., Jessipow, S., König, W.A., and Zähner, H. (1972) Stoffwechselprodukte von Mikroorganismen. 98. Phosphinothricin und Phosphinothricyl-Alanyl-Alanin. *Helv Chim Acta* **55:** 224–239.

Bierman, M., Logan, R., O'Brien, K., Seno, E.T., Nagaraja-Rao, R., and Schoner, B.E. (1992) Plasmid cloning vectors for the conjugal transfer of DNA from *Escherichia coli* to *Streptomyces* sp. *Gene* **116:** 43–49.

Blodgett, J.A., Zhang, J.K., and Metcalf, W.W. (2005) Molecular cloning, sequence analysis, and heterologous expression of the phosphinothricin tripeptide biosynthetic gene cluster from *Streptomyces viridochromogenes* DSM 40736. *Antimicrob Agents Chemother* **49:** 230–240.

Blodgett, J.A., Thomas, P.M., Li, G., Velasquez, J.E., van der Donk, W.A., Kelleher, N.L., and Metcalf, W.W. (2007) Unusual transformations in the biosynthesis of the antibiotic phosphinothricin tripeptide. *Nat Chem Biol* **3:** 480–485.

Bullock, W.O., Fernandez, J.M., and Short, J.M. (1987) XL1-Blue, a high efficiency plasmid transforming *recA Eschrichia coli* strain with beta galactosidase selection. *Focus* **5:** 376–378.

Bussmann, M., Baumgart, M., and Bott, M. (2010) RosR (Cg1324), a hydrogen peroxide-sensitive MarR-type transcriptional regulator of *Corynebacterium glutamicum*. *J Biol Chem* **285:** 29305–29318.

Butt, J., Kim, H.Y., Basilion, J.P., Cohen, S., Iwai, K., Philpott, C.C., *et al.* (1996) Differences in the RNA binding sites of iron regulatory proteins and potential target diversity. *Proc Natl Acad Sci USA* **93:** 4345–4349.

Cock, P.J.A., Antao, T., Chang, J.T., Chapman, B.A., Cox, C.J., Dalke, A., *et al.* (2009) Biopython: freely available Python tools for computational molecular biology and bioinformatics. *Bioinformatics* **25:** 1422–1423.

Commichau, F.M., and Stülke, J. (2008) Trigger enzymes: bifunctional proteins active in metabolism and in controlling gene expression. *Mol Microbiol* **67:** 692–702.

Craig, J.E., Ford, M.J., Blaydon, D.C., and Sonenshein, A.L. (1997) A null mutation in the *Bacillus subtilis* aconitase gene causes a block in Spo0A-phosphate-dependent gene expression. *J Bacteriol* **179:** 7351–7359.

Delano, W.L. (2002) The Pymol molecular graphics system [WWW document]. URL http://www.pymol.org.

Dupuy, J., Volbeda, A., Carpentier, P., Darnault, C., Moulis, J.M., and Fontecilla-Camps, J.C. (2006) Crystal structure of human iron regulatory protein 1 as cytosolic aconitase. *Structure* **14:** 129–139.

Duwat, P., Sourice, S., Ehrlich, S.D., and Gruss, A. (1995) *recA* gene involvement in oxidative and thermal stress in *Lactococcus lactis*. *Dev Biol Stand* **85:** 455–467.

Eys, S., Schwartz, D., Wohlleben, W., and Schinko, E. (2008) Three thioesterases are involved in the biosynthesis of phosphinothricin tripeptide in *Streptomyces viridochromogenes* Tü494. *Antimicrob Agents Chemother* **52:** 1686–1696.

Fischer, J. (1996) Entwicklung eines regulierbaren Expressionssystems zur effizienten Synthese rekombinanter Proteine in *Streptomyces lividans*. PhD Thesis. Stuttgart, Germany, University of Stuttgart.

Flärdh, K. (2003) Growth polarity and cell division in *Streptomyces*. *Curr Opin Microbiol* **6:** 564–571.

Flärdh, K., Leibovitz, E., Buttner, M.J., and Chater, K.F. (2000) Generation of a non-sporulating strain of *Streptomyces coelicolor* A3(2) by the manipulation of a developmentally controlled *ftsZ* promoter. *Mol Microbiol* **38:** 737–749.

Heinzelmann, E., Kienzlen, G., Kaspar, S., Recktenwald, J., Wohlleben, W., and Schwartz, D. (2001) The phosphinomethylmalate isomerase gene *pmi*, encoding an aconitase-like enzyme, is involved in the synthesis of phosphinothricin tripeptide in *Streptomyces viridochromogenes*. *Appl Environ Microbiol* **67:** 3603–3609.

Heinzelmann, E., Berger, S., Puk, O., Reichenstein, B., Wohlleben, W., and Schwartz, D. (2003) A glutamate mutase is involved in the biosynthesis of the lipopeptide antibiotic friulimicin in *Actinoplanes friuliensis*. *Antimicrob Agents Chemother* **47:** 447–457.

Henderson, B.R., Menotti, E., Bonnard, C., and Kuhn, L.C. (1994) Optimal sequence and structure of iron-responsive elements. Selection of RNA stem-loops with high affinity for iron regulatory factor. *J Biol Chem* **269:** 17481–17489.

Herbert, D., Phipps, P.J., and Strange, R.E. (1971) Chemical analysis of microbial cells. In *Methods in Microbiology*. Norris, J.R., and Ribbons, D.W. (eds). London, UK: Academic Press, pp. 209–344.

Jonsbu, E., Christensen, B., and Nielsen, J. (2001) Changes of in vivo fluxes through central metabolic pathways during the production of nystatin by *Streptomyces noursei* in batch culture. *Appl Microbiol Biotechnol* **56:** 93–100.

Kaldy, P., Menotti, E., Moret, R., and Kühn, L.C. (1999) Identification of RNA-binding surfaces in iron regulatory protein-1. *EMBO J* **18:** 6073–6083.

Kieser, T., Bibb, M.J., Buttner, M.J., Chater, K.F., and Hopwood, D.A. (2000) *Practical* Streptomyces *Genetics*. Norwich, UK: The John Innes Foundation.

Koo, J.T., Choe, J., and Moseley, S.L. (2004) HrpA, a DEAH-box RNA helicase, is involved in mRNA processing of a fimbrial operon in *Escherichia coli*. *Mol Microbiol* **6:** 1813–1826.

Lauble, H., Kennedy, M.C., Beinert, H., and Stout, C.D. (1992) Crystal structures of aconitase with isocitrate and nitroisocitrate bound. *Biochemistry* **31:** 2735–2748.

Lüders, S., Fallet, C., and Franco-Lara, E. (2009) Proteome analysis of the *Escherichia coli* heat shock response under steady-state conditions. *Proteome Sci* **7:** 1–15.

McCormick, J.R., Su, E.P., Driks, A., and Losick, R. (1994) Growth and viability of *Streptomyces coelicolor* mutant for the cell division gene *ftsZ*. *Mol Microbiol* **14:** 243–254.

Muckenthaler, M.U., Galy, B., and Hentze, M.W. (2008) Systemic iron homeostasis and the iron-responsive element/iron-regulatory protein (IRE/IRP) regulatory network. *Annu Rev Nutr* **28:** 197–213.

Muschko, K., Kienzlen, G., Fiedler, H.P., Wohlleben, W., and Schwartz, D. (2002) Tricarboxylic acid cycle aconitase activity during the life cycle of *Streptomyces viridochromogenes* Tü494. *Arch Microbiol* **178:** 499–505.

Muth, G., Nussbaumer, B., Wohlleben, W., and Pühler, A. (1989) A vector system with temperature sensitive replication for gene disruption and mutational cloning in streptomycetes. *Mol Gen Genet* **219:** 341–348.

Pridmore, R.D. (1987) New and versatile cloning vectors with kanamycin-resistance marker. *Gene* **56:** 309–312.

Sambrook, J., Fritsch, T., and Maniatis, T. (1989) *Molecular Cloning. A Laboratory Manual. 2. Auflage*. New York, NY, USA: Cold Spring Harbor Laboratory Press.

Sancar, A., and Sancar, G.B. (1988) DNA repair enzymes. *Annu Rev Biochem* **57:** 29–67.

Schinko, E., Schad, K., Eys, S., Keller, U., and Wohlleben, W. (2009) Phosphinothricin-tripeptide biosynthesis: an original version of bacterial secondary metabolism? *Phytochemistry* **70:** 1787–1800.

Schwartz, D., Alijah, R., Nussbaumer, B., Pelzer, S., and Wohlleben, W. (1996) The peptide synthetase gene *phsA* from *Streptomyces viridochromogenes* is not juxtaposed with other genes involved in nonribosomal biosynthesis of peptides. *Appl Environ Microbiol* **62:** 570–577.

Schwartz, D., Kaspar, S., Kienzlen, G., Muschko, K., and Wohlleben, W. (1999) Inactivation of the tricarboxylic acid cycle aconitase gene from *Streptomyces viridochromoge-*

nes Tü494 impairs morphological and physiological differentiation. *J Bacteriol* **181:** 7131–7135.
Schwartz, D., Berger, S., Heinzelmann, E., Muschko, K., Welzel, K., and Wohlleben, W. (2004) Biosynthetic gene cluster of the herbicide phosphinothricin tripeptide from *Streptomyces viridochromogenes* Tü494. *Appl Environ Microbiol* **70:** 7093–7102.
Sengupta, S., Ghosh, S., and Nagaraja, V. (2008) Moonlighting function of glutamate racemase from *Mycobacterium tuberculosis*: racemization and DNA gyrase inhibition are two independent activities of the enzyme. *Microbiology* **154:** 2796–2803.
Serio, A.W., and Sonenshein, A.L. (2006) Expression of yeast mitochondrial aconitase in *Bacillus subtilis*. *J Bacteriol* **188:** 6406–6410.
Serio, A.W., Pechter, K.B., and Sonenshein, A.L. (2006) *Bacillus subtilis* aconitase is required for efficient late-sporulation gene expression. *J Bacteriol* **188:** 6396–6405.
Somerville, G., Mikoryak, C.A., and Reitzer, L. (1999) Physiological characterization of *Pseudomonas aeruginosa* during exotoxin A synthesis: glutamate, iron limitation, and aconitase activity. *J Bacteriol* **181:** 1072–1078.
Somerville, G.A., Chaussee, M.S., Morgan, C.I., Fitzgerald, J.R., Dorward, D.W., Reitzer, L.J., and Musser, J.M. (2002) *Staphylococcus aureus* aconitase inactivation unexpectedly inhibits post-exponential-phase growth and enhances stationary-phase survival. *Infect Immun* **70:** 6373–6382.
Strauch, E., Wohlleben, W., and Pühler, A. (1988) Cloning of a phosphinothricin N-acetyltransferase gene from *Streptomyces viridochromogenes* Tü494 and its expression in *Streptomyces lividans* and *Escherichia coli*. *Gene* **63:** 65–74.
Süsstrunk, U., Pidoux, J., Taubert, S., Ullmann, A., and Thompson, C.J. (1998) Pleiotropic effects of cAMP on germination, antibiotic biosynthesis and morphological development in *Streptomyces coelicolor*. *Mol Microbiol* **30:** 33–46.
Tang, Y., and Guest, J.R. (1999) Direct evidence for mRNA binding and post-transcriptional regulation by *Escherichia coli* aconitases. *Microbiology* **145:** 3069–3079.
Tang, Y., Quail, M.A., Artymiuk, P.J., Guest, J.R., and Green, J. (2002) *Escherichia coli* aconitases and oxidative stress: post-transcriptional regulation of *sodA* expression. *Microbiology* **148:** 1027–1037.
Tang, Y., Guest, J.R., Artymiuk, P.J., Read, R.C., and Green, J. (2004) Post-transcriptional regulation of bacterial motility by aconitase proteins. *Mol Microbiol* **51:** 1817–1826.
Vierling, S., Weber, T., Wohlleben, W., and Muth, G. (2001) Evidence that an additional mutation is required to tolerate insertional inactivation of the *Streptomyces lividans recA* gene. *J Bacteriol* **183:** 4374–4381.
Viollier, P.H., Minas, W., Dale, G.E., Folcher, M., and Thompson, C.J. (2001a) Role of acid metabolism in *Streptomyces coelicolor* morphological differentiation and antibiotic biosynthesis. *J Bacteriol* **183:** 3184–3192.
Viollier, P.H., Nguyen, K.T., Minas, W., Folcher, M., Dale, G.E., and Thompson, C.J. (2001b) Roles of aconitase in growth, metabolism, and morphological differentiation of *Streptomyces coelicolor*. *J Bacteriol* **183:** 3193–3203.
Walden, W.E., Selezneva, A.I., Dupuy, J., Volbeda, A., Fontecilla-Camps, J.C., Theil, E.C., and Volz, K. (2006) Structure of dual function iron regulatory protein 1 complexed with ferritin IRE-RNA. *Science* **314:** 1903–1908.
Wilson, T.J., Bertrand, N., Tang, J.L., Feng, J.X., Pan, M.Q., Barber, C.E., *et al*. (1998) The *rpfA* gene of *Xanthomonas campestris pathovar campestris*, which is involved in the regulation of pathogenicity factor production, encodes an aconitase. *Mol Microbiol* **28:** 961–970.
Zakrzewska-Czerwińska, J., Jakimowicz, D., Majka, J., Messer, W., and Schrempf, H. (2000) Initiation of the *Streptomyces* chromosome replication. *Antonie Van Leeuwenhoek* **78:** 211–221.

Supporting information

Additional Supporting Information may be found in the online version of this article:

Fig. S1. Phenotypic comparison of *S. viridochromogenes* WT grown for 6 days in YM medium with different concentrations (2 mM, 10 mM, 20 mM) of (A) tri-sodium citrate, (B) sodium acetate, and (C) succinic acid, disodium salt.
Fig. S2. Analysis of PTT production of the *S. viridochromogenes* WT, the MacnA mutant, the *hisacnA* complemented MacnA mutant (MacnA(*hisacnA*)), the *hisacnA1(C538A)* complemented MacnA mutant (MacnA(*hisacnA1*)), and the *hisacnA2(Δ125–129)* complemented MacnA mutant (MacnA-(*hisacnA2*)) in a biological assay against *B. subtilis*.
Fig. S3. Transcriptional analysis of *recA* in the *S. viridochromogenes* WT and the MacnA mutant (two upper rows). *hrdB* was used as negative control (two lower rows). The wild-type sample was collected at 48 h and the MacnA sample at 96 h, when both strains were in a comparable growth status. First line: samples treated with the oxygen stress inducer methyl viologen; second line: samples treated with heat stress; third line: samples without stress treatment; fourth line: control – genomic DNA.
Table S1. Primer sequences, amplified fragments, PCR conditions, and IRE sequences.

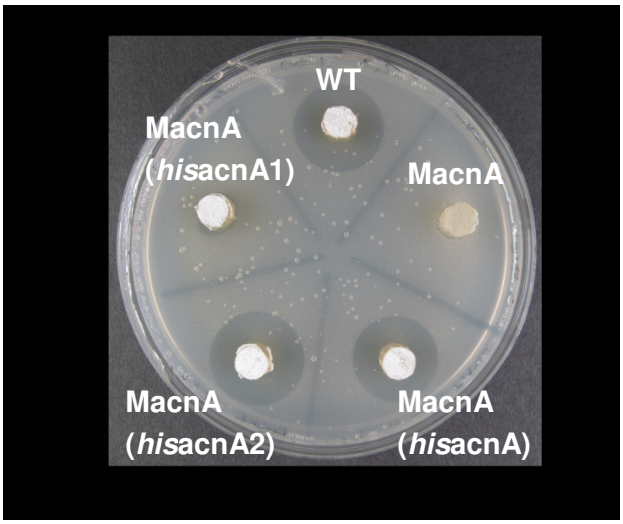

Supporting information, Fig.S2. Analysis of PTT production of the *S. viridochromogenes* WT, the MacnA mutant, the hisacnA complemented MacnA mutant (MacnA(hisacnA)), the hisacnA1(C538A) complemented MacnA mutant (MacnA(hisacnA1)), and the hisacnA2(Δ125–129) complemented MacnA mutant (MacnA(hisacnA2)) in a biological assay against *B. subtilis*.

Supporting information, Table S1. Primer sequences, amplified fragments, PCR conditions, and IREs.

Primer	**Primer sequence (5'→3')**	**Properties***
P1	AT**GGATCC**GTGTCGGCGAACAGCTTCGACG	BamHI restriction site
P2	AT**AAGCTT**CTTACTTGCGGATCAGGCTGCG	HindIII restriction site
P3	CGGCTTCAAGCTGAC	-
P4	CGGAGTTGCCGATGCAGGTGGT**AGC**GCCGTAG CCGACGAGGTTGAAGC	Exchange of GCA for AGC
P5	GCTTCAACCTCGTCGGCTACGGC**GCT**ACCACCT GCATCGGCAACTCCG	Exchange of TGC for GCT
P6	TGTCGGCCTTGATCG	-
P7	CGTGCCGAACTTGT- GGTCGATGACCAGCTCGGC	Deletion of CGGCGATGACGGAGT
P8	GTCATCGACC- ACAAGTTCGGCACGAACGACGC	Deletion of ACTCCGTCATCGCCG
P9	GGCCAGATGTCCTTCAG	-
P10	ACTTCTCCGAGAAGCTCGAGCTC	-
P11	CGTGCCCGGCGCGATCT**C**GTTGCGCAG**CTC**GAT GTTGGCGAACG	Exchange of G for C and GCG for CTC
P12	CGTTCGCCAACATC**GAG**CTGCGCAAC**G**AGATCG	Exchange of CGC for GAG and C for G

	CGCCGGGCACG	
P13	ATGCGGACGACCGCGTCGAACTC	-
P18	ATGAATTCCGTACGGCAGCTTGAAC	-
P19	ATGTGGTCGGGCGGTGATGTTCG	-

Fragment	**Primer**	**Annealing temp (°C)**	**Polymerase**	**Template**
acnA (2.8 kb)$^{+}$	P1 and P2	64	*Taq*	genomic DNA of Tü494
C538A^{1} (0.9 kb)$^{+}$	P3 and P4	54	*Taq*	genomic DNA of Tü494
C538A^{2} (0.5 kb)$^{+}$	P5 and P6	52	ProofStart	genomic DNA of Tü494
C538A^{1+2} (1.5 kb)$^{+}$	P3 and P6	46	ProofStart	*C538A^{1}+ C538A^{2}*
Ä125–129^{1} (0.4 kb)$^{+}$	P1 and P7	68	*Taq*	genomic DNA of Tü494
Ä125–129^{2} (1.5 kb)$^{+}$	P8 and P9	54	*Taq*	genomic DNA of Tü494
Ä125–129^{1+2} (1.9 kb)*	P1 and P9	46	ProofStart	*Ä125–129^{1}+ Ä125–129^{2}*
R763E/Q767E^{1} (1.2 kb)$^{+}$	P10 and P11	62	*Taq*	genomic DNA of Tü494
R763E/Q767E^{2} (0.4 kb)$^{+}$	P12 and P13	62	*Taq*	genomic DNA of Tü494
R763E/Q767E^{1+2} (1.6 kb)$^{+}$	P10 and P13	64	*Taq*	*R763E/Q767E^{1}+ R763E/Q767E^{2}*

IRE	**RNA Sequence (5'→3')**
hfer	AAUUCGGGAGAGGAUCCUGCUUCAACAGUG CUUGGACGGAUCCA
recA	GACCCGCAUCGGGGCCCAUUGUCAGUG GCAGGCAUUAGCGUCUUUGACGU
ftsZ	CGGCCGGGCGACACGUAACUCGAGGCGAGAG GCCUUCGACGUGGCAGCAC
hrdB	CCAGGAGGGCAACCUCGGUCUGAUCCGCGCGG UGGAGAAGUUCGACUACA
recA-loop	GCGUCGGGCGCAUUGUCCCCGCACCGGUUAGC GUCUU
recA-stem	GCGUCGGGGCGCAAAAACAGUGAAAAACGUU AGCGUCUU

SSQG_01218	CGGGGCUUCCCGGGCACGUUGUCAGUGGUCGCC GGUAGGUUCUGAGGCCU CUUCCCGGGCACGUUGUCAGUGGUCGCCGGUAGGUUCUGA
SSQG_00552	CGACGAGGGCCUGCUCCUGCUGCUGUGCGGCGCGUGGAACC AGGUGGUCC CGAGGGCCUGCUCCUGCUGCUGUGCGGCGCGUGGAACCAG

*The properties are underlined in the primer sequence; IRE motive is underlined in the RNA sequence

+ expected size of PCR fragment

OPEN ACCESS Freely available online

PLOS ONE

Proteomic Approach to Reveal the Regulatory Function of Aconitase AcnA in Oxidative Stress Response in the Antibiotic Producer *Streptomyces viridochromogenes* Tü494

Ewelina Michta[1], Wei Ding[2], Shaochun Zhu[2], Kai Blin[1], Hongqiang Ruan[2], Rui Wang[2,3], Wolfgang Wohlleben[1], Yvonne Mast[1]*

1 Department of Microbiology/Biotechnology, Interfaculty Institute of Microbiology and Infection Medicine, Eberhard Karls University of Tübingen, Tübingen, Germany, **2** Shanghai Applied Protein Technology Co., Ltd., Shanghai, China, **3** Key Laboratory of Synthetic Biology, Institute of Plant Physiology and Ecology, Shanghai Institutes for Biological Sciences, Chinese Academy of Sciences, Shanghai, China

Abstract

The aconitase AcnA from the phosphinothricin tripeptide producing strain *Streptomyces viridochromogenes* Tü494 is a bifunctional protein: under iron-sufficiency conditions AcnA functions as an enzyme of the tricarboxylic acid cycle, whereas under iron depletion it is a regulator of iron metabolism and oxidative stress response. As a member of the family of iron regulatory proteins (IRP), AcnA binds to characteristic iron responsive element (IRE) binding motifs and post-transcriptionally controls the expression of respective target genes. A *S. viridochromogenes* aconitase mutant (MacnA) has previously been shown to be highly sensitive to oxidative stress. In the present paper, we performed a comparative proteomic approach with the *S. viridochromogenes* wild-type and the MacnA mutant strain under oxidative stress conditions to identify proteins that are under control of the AcnA-mediated regulation. We identified up to 90 differentially expressed proteins in both strains. *In silico* analysis of the corresponding gene sequences revealed the presence of IRE motifs on some of the respective target mRNAs. From this proteome study we have *in vivo* evidences for a direct AcnA-mediated regulation upon oxidative stress.

Citation: Michta E, Ding W, Zhu S, Blin K, Ruan H, et al. (2014) Proteomic Approach to Reveal the Regulatory Function of Aconitase AcnA in Oxidative Stress Response in the Antibiotic Producer *Streptomyces viridochromogenes* Tü494. PLoS ONE 9(2): e87905. doi:10.1371/journal.pone.0087905

Editor: Vladimir N. Uversky, University of South Florida College of Medicine, United States of America

Received October 18, 2013; **Accepted** December 30, 2013; **Published** February 3, 2014

Funding: This research was supported by grants from the Deutsche Forschungsgemeinschaft (SPP1152: Wo 485/7-1,2,3) and the Federal Ministry of Education and Research (GenBioCom #0315585A). EM acknowledges the scholarship Aufenthalt für anwendungsorientierte Biowissenschaftler(innen) und Biotechnolog(inn)en in Shanghai und Jiangsu/China from the ministry of Baden-Württemberg. The funders had no role in study design, data collection and analysis, decision to publish, or preparation of the manuscript.

Competing Interests: The authors declare that Shanghai Applied Protein Technology Co., Ltd does not have any competing interests in terms of employment, consultancy, patents, products in development or marketed products. The authors have the following interests: Authors WD, SZ, HR, RW are employed by commercial company Shanghai Applied Protein Technology Co., Ltd. There are no patents, products in development or marketed products to declare. This does not alter the authors' adherence to all the PLOS ONE policies on sharing data and materials, as detailed online in the guide for authors.

* E-mail: yvonne.mast@biotech.uni-tuebingen.de

Introduction

Streptomyces are gram-positive soil bacteria that undergo a complex life cycle where morphological differentiation is strongly coordinated with secondary metabolites production [1]. *Streptomyces viridochromogenes* Tü494 is the producer of the herbicide antibiotic phosphinothricin tripeptide (PTT). In this strain the function of the protein AcnA was analyzed in detail previously, because it represents a nodal point between primary and secondary metabolism [2–4]. It has been shown before that an *S. viridochromogenes* aconitase mutant (MacnA) is unable to form any aerial mycelium, spores nor PTT [3]. Furthermore, this mutant is highly sensitive to oxidative stress [5]. As reported for *Escherichia coli* aconitase A this oxidative stress hypersensitivity is not due to the lack of a citric acid cycle function *per se*, but to some extent may be associated with the loss of the regulatory function of AcnA [6]. The AcnA enzymes from *E. coli* and *S. viridochromogenes* both belong to the same family of iron regulatory proteins (IRPs).

One of the best studied aconitases is the human cytosolic iron regulatory protein 1 (IRP1). Under normal physiological conditions IRP1 functions as a tricarboxylic acid cycle (TCA) enzyme and converts citrate to isocitrate. However, under iron deficiency or oxidative stress conditions, the 4Fe-4S cluster in the catalytic center of IRP1 is disassembled and the protein undergoes conformational changes, resulting in the catalytically inactive apo-enzyme [7] that becomes open and accessible for the binding of sequences known as iron responsive elements (IREs) [8]. IREs form stem-loop structures at the 5′ or 3′ end of untranslated regions (UTRs) of mRNA transcripts such as that of the iron-storage protein ferritin. For IRP1 it has been shown that the binding to the 5′ UTR inhibits translation by blocking the mRNA-ribosome complex formation, while binding at the 3′ UTR protects the mRNA from degradation by RNases, which stabilizes the transcript and in this way stimulates translation [7]. In prokaryotic cells, there is no evidence so far that the binding of

aconitase to the 5′ or 3′ ends of mRNA exerts different effects on translation.

The major regulatory role of IRP1 in eukaryotes is to control iron homeostasis by binding to mRNAs such as that of the iron-storage protein ferritin. For several bacterial species, e.g. *E. coli*, *Mycobacterium tuberculosis*, and *Bacillus subtilis*, also a stress-dependent binding of aconitase to IRE-like structures of genes involved in oxidative stress has been reported [6,9–12]. Oxidative stress has a broad influence on cellular metabolism. Notably, the reactivity of H_2O_2 with iron in the Fenton reaction connects oxidative stress and cellular iron metabolism. In this reaction Fe^{2+} generates highly reactive hydroxyl radicals, which quickly abstract H-atoms from most organic molecules [13].

A regulatory function of aconitase in oxidative stress control is also ascribed for AcnA of *S. viridochromogenes* Tü494. In a related paper, we presented *in vitro* shift experiments that proved the binding of apo-AcnA to different IRE structures, such as that of *recA*, which is crucial for the cellular SOS response. Furthermore, by immunoblot analysis we found that RecA expression is upregulated under oxidative stress conditions in the wild-type strain (WT) but not in the aconitase mutant MacnA, which demonstrates that AcnA is a post-transcriptional regulator of RecA expression under oxidative stress [5].

In the current study we used a proteomic approach to investigate the regulatory function of AcnA under oxidative stress conditions. We also aimed to identify enzymes that are crucial for the *S. viridochromogenes* oxidative stress adaptation. Besides that we tried to explore the changes in protein expression that may be associated with the impaired defense of the aconitase mutant MacnA against free radicals.

Materials and Methods

Bacterial strains, plasmids and growth conditions

For preparation of cell extracts applied for proteome analyses, the *S. viridochromogenes* WT and previously described aconitase mutant strain MacnA [3] were each grown in 100 ml of S-medium at 27°C on an orbital shaker (180 rpm) in 500 ml Erlenmeyer flasks with steel springs to the mid-exponential growth phase. Because WT and MacnA mutant strains showed different growth rates, samples were taken for different time points and DNA concentration of the biomass was estimated as described before [14] to ensure that the strains were in a comparable growth status (Fig. S1). Each culture was supplemented with 0.2 mM methyl viologen dichloride hydrate (MV). MV is an inducer of oxidative stress and initiates the transition of AcnA into its regulatory active apo-form. Cultures were incubated with MV on an orbital shaker (180 rpm) for 90 min at 27°C. Subsequently, identical amounts of mycelium from each strain were harvested by centrifugation (10 min, 5000 rpm). The cell pellets were washed twice with S-medium and then used for proteome analysis. As control, MV-untreated samples were used.

In silico analysis for identification of IRE sequences

To identify putative IRE sequences of genes encoding proteins identified in the proteomic analysis, the bioinformatical tool SPIRE was used (http://www.unituebingen.de/en/32760). The SPIRE algorithm and its implementation in searching for conserved IRE-like stem-loop structures has been described previously [5].

2D electrophoresis

Sample preparation. 100 mg of mycelium from each culture was ground in liquid nitrogen and then dissolved in 2D lysis buffer (8 M urea, 150 mM Tris/HCl pH 8, 4% CHAPS, 40 mM DTT). Protease inhibitor cocktail (Sigma) (sample:protease ratio = 25:1) was added to prevent proteolytic degradation. To increase the lysis efficiency, samples were incubated for 45 min at 35°C (incubation temperature should not exceed 37°C because the urea of the lysis buffer causes protein modifications changing the molecular weight). After incubation the samples were sonicated on ice and centrifuged (45 min, 14000 g, 4°C). Protein concentrations were estimated by Bradford assay [15].

Protein separation. 100 µg of protein from each sample was applied for analytical gels (used for image analysis and spot quantification) and 400 µg for preparative gels (used for spots excision). The total volume of each sample was made up to 250 µl with rehydratation buffer (330 mM urea, 1.3 mM CHAPS, 0.0045% bromophenol blue). The protein mixture was applied to Immobiline DryStrip strips (13 cm, pH 4–7; GE Healthcare). Isoelectric focusing (IEF) was performed with an Ettan IPGphor II apparatus (GE Healthcare) with following steps: 30 V for 12 h, 500 V for 1 h, 1000 V for 1 h, and 8000 V for 8 h. After IEF, each strip was equilibrated with a reducing equilibration buffer (6 M urea, 50 mM Tris/HCl pH 8.8, 30% glycerol, 2% SDS, 1% DTT) for 15 min followed by the incubation with an alkylating equilibration buffer (6 M urea, 50 mM Tris/HCl pH 8.8, 30% glycerol, 2% SDS, 1% iodoacetamide) for another 15 min. The strips were placed on the top of 12.5% SDS-PAGE gels and sealed with 0.5% agarose. Separation of the proteins in the second dimension occurred at 30 mA per gel in an Ettan DALT six instrument (GE Healthcare) until the bromophenol blue reached the bottom of the gel. Gels were fixed overnight in a mixture of 10% ethanol and 10% acetic acid. Analytical and preparative gels were stained with silver solution and scanned with Typhoon FLA9000 Variable Mode Imager (GE Healthcare) (Fig. S2).

Protein identification. To exclude artefacts caused by electrophoresis conditions, 2D analytical gels were run in triplicate. Spot detection, quantification, and matching were performed using Image Master 2D Platinum software version 5.0 according to the manufacturer's instruction (GE Healthcare). Spots were quantified calculating the relative spot volumes (ratio of individual spot volume and total volume of all spots). Significantly changed proteins between treated and control sample were defined as proteins that were more or less abundant by a ratio of 1.1. Spots of interest, identified by Image Master, were manually matched to the analytical gels and excised. The digestion in trypsin solution (Promega) was performed overnight at 37°C. The tryptic peptides were extracted with 60% acetonitrile and 0.1% trifluoroacetic acid. The dry peptide samples were reconstituted in 2 µl of standard diluent (acetonitrile to water ratio = 20:80), spotted on a 384-well Opti-TOF stainless steel plate, covered with 0.6 µl of matrix (5 mg/ml α-cyano-4-hydroxycinnamic acid in 50% acetonitrile and 0.1% trifluoroacetic acid) and air dried. MS and MS/MS data for protein identification were obtained by using MALDI-TOF-TOF instrument (4800 proteomics analyzer; Applied Biosystems). Combined peptide mass fingerprinting and MS/MS queries were performed using the MASCOT search engine 2.2 (Matrix Science, Ltd.) embedded into GPS-Explorer Software 3.6 (Applied Biosystems) on the NCBI database where the taxonomy was set to: Bacteria (Table S1). Only proteins with the GPS Explorer protein confidence index ≥95% were assumed to be significant ($p<0.05$) and successfully identified. The spots that did not fulfill this criterion were excluded from the results.

Results and Discussion

Identification of differentially expressed proteins in *S. viridochromogenes* WT and MacnA

To investigate the potential regulatory role of aconitase in oxidative stress defense in *Streptomyces viridochromogenes* Tü494 and to reveal the cellular mechanisms underlying the oxygen stress sensitivity in the aconitase mutant MacnA, a proteomic comparison between the *S. viridochromogenes* wild-type (WT) strain and MacnA under oxidative stress condition was performed. WT and MacnA were grown in liquid cultures to the mid-exponential growth phase, where each culture was supplemented with methyl viologen (MV). MV is an inducer of oxidative stress and also leads to the disassembly of holo-AcnA into its regulatory active apo-AcnA form [9]. The cytoplasmic fractions of both cultures were used for proteomic analysis. Fractions that were not treated with MV served as controls. To better distinguish between significant changes related to the aconitase mutation and changes related to oxidative stress response, the up- or downregulated proteins were identified separately for the WT strain and the MacnA mutant after oxidative stress treatment. This was conducted by comparison of the two-dimensional polyacrylamide gel electrophoresis (2D-PAGE) image of the MV-treated WT strain sample with the 2D-PAGE image of the MV-untreated WT strain sample (Fig. S2 A, B). The same was done for the mutant strain MacnA (Fig. S2 C, D). Thus, whenever a protein is described below to be up- or downregulated, this is in comparison to the control sample (MV-untreated) of the respective strain.

In the WT strain, 62 protein spots with significant differences in the expression level due to oxidative stress application were detected and identified by MALDI TOF/TOF. Among them 37 were upregulated and 25 were downregulated. In the MacnA strain, 27 proteins were differentially expressed as a consequence of oxidative stress treatment and identified by MALDI TOF/TOF: 16 among them were upregulated and 11 were downregulated. Some of the identified proteins, which are discussed below, occurred as multiple spots on the gel, which may be due to post-translation modifications.

The majority of the differentially regulated proteins identified in the WT strain were different from those detected in MacnA. This is because the respective 2D gels were not matched with each other by the proteome imaging program because then it would not be possible to distinguish between influence of oxidative stress from influence of *acnA* mutation. Also in other proteomic studies, where oxidative stress was investigated in different strains, it has been observed that just very few (if any) of the same proteins were identified in all analyzed gels [16,17]. Proteins that were identified as up- or downregulated in one strain but their expression was not, or differentially, changed in the respective other strain after oxidative stress application, were considered to be affected by AcnA. The proteins that were similarly expressed in both strains due to oxidative stress exposure were considered to be independent from AcnA regulation.

All identified proteins, could be assigned to different metabolic pathways such as: carbon metabolism, fatty acid metabolism, amino acid biosynthesis, phosphate uptake and phosphate metabolism, protein synthesis and turnover, DNA synthesis, proteins involved in control of energy status, and proteins induced in response to stress conditions (Table S1). However, no polypeptides were identified, which are directly involved in iron metabolism. This corresponds to the observations from our previous analysis of *S. viridochromogenes* where nearly no IRE-like structures have been found in the UTRs of genes known to be involved in iron metabolism [5].

As expected, many of the identified proteins were related to cellular stress response and several of them were found to possess predicted IRE motifs on their respective mRNAs (Table S1 and 1), which points to a direct post-transcriptional regulation by AcnA. Especially two proteins with putative functions in cellular stress defense (tellurium resistance protein SSQG_02339 and translation elongation factor Tu SSQG_04757) were differentially regulated due to oxidative stress treatment in the WT and the MacnA mutant (see below). Both harbor predicted IRE motifs on their corresponding transcript sequence. Thus, these data provide a direct *in vivo* evidence for an AcnA-mediated regulation upon oxidative stress.

For differentially expressed proteins where no IRE motif was identified on the associated mRNA sequence, the regulation was regarded to be mediated only indirectly by AcnA (Table 2). In such a case AcnA could control the expression of another regulator, which itself directly regulates the respective gene expression. One example of such a regulator could be represented by MarR. The *S. viridochromogenes marR* mRNA sequence has been shown to harbor a predicted IRE element at its 3′ end [5] and thus may be a target of AcnA. MarR is a global regulator and known to be involved in the regulation of a variety of cellular processes including that of stress responses [18]. Thus, this regulator could be a tie point in such a predicted regulatory cascade. However, it also cannot be excluded that the dissimilar expression is based on different physiological preconditions of both strains.

Aconitase affects expression of proteins involved in cellular protection against oxidative damage

Three proteins (SSQG_03555, SSQG_00725, and SSQG_02339) annotated as putative tellurium resistance proteins, were found to be upregulated in the WT strain under oxidative stress conditions (Table S1). Tellurium resistance proteins represent a family of bacterial stress proteins that mediate resistance to tellurite (TeO_3^{-2}) and other xenobiotic toxic compounds, pore-forming colicins and several bacteriophages [19]. Tellurite acts as a strong oxidizing agent and its reactivity leads to the generation of reactive oxygen species (ROS) in the cytoplasm [20]. For the tellurium resistance protein SCO2368 from *S. coelicolor*, which shares 92% amino acid sequence identity to SSQG_02339, it has been shown that the level of protein increased during incubation of the bacterial cells with plant material. In these analyses a simultaneous increase of superoxide dismutase was observed. Therefore it was suggested that plant material provides some kind of oxidative stress [21,22]. A similar concomitant increase of tellurium resistance protein and superoxide dismutase was observed for *Frankia* cells incubated with root exudates of *Alnus glutinosa* [23]. Moreover, the induction of tellurium resistance due to oxidative stress (also due to MV supplementation) has been shown for *Rhodobacter capsulatus* [24]. Interestingly, we found putative IRE sequences in front of the genes encoding two out of the three identified tellurium resistance proteins (SSQG_02339, SSQG_00725), suggesting that their expression might be directly controlled by AcnA (Table 1). In particular, protein SSQG_02339 with the predicted IRE motif was found to be upregulated in the WT strain but downregulated in the MacnA. This result indicates that AcnA positively regulates the expression of SSQG_02339 under oxidative stress conditions. A congeneric upregulation of superoxide dismutase was not observed in *S. viridochromogenes*, which may be associated with the type of oxidative stress supply as observed before [25,26]. Furthermore, as no IRE motif was identified on the superoxide dismutase mRNA sequence, the expression of this protein is not expected to be directly regulated by AcnA.

Table 1. Proteins directly regulated by AcnA.

Locus	function	loop sequence of IRE	localization	distance in bp*	fold change	p-value
WT						
SSQG_00725	Tellurium resistance protein	CAGUG	5′	64	1.62	0.05
SSQG_01870	Phosphoglycerate kinase	CAGCG	5′	97	1.65	0.05
SSQG_01871	Glyceraldehyde-3-phosphate dehydrogenase	CAGCG	3′	35	1.46	0.02
SSQG_02023	Cell division protein FtsZ	GAGAG	5′	9	1.61	0.03
SSQG_02339	Tellurium resistance protein	GGGAG	3′	100	1.99	0.15
SSQG_03372	Glutathione peroxidase	CAGGG	5′	169	1.99	0.00
SSQG_03670	Phosphate-binding protein PstS	CAGGG	5′	155	0.49	0.07
SSQG_04757	Translation elongation factor Tu	GAGAG	5′	84	0.61	0.01
SSQG_04757	Translation elongation factor Tu	GAGAG	5′	84	0.56	0.04
SSQG_04757	Translation elongation factor Tu	GAGAG	5′	84	1.60	0.07
SSQG_04792	Adenylate kinase	CUGUG	3′	79	2.23	0.02
SSQG_05742	1-deoxy-D-xylulose 5-phosphate reductoisomerase	CAGGG	5′	181	3.05	0.06
SSQG_05905	Conserved hypotetical protein	GAGAG	5′	182	1.54	0.01
MacnA						
SSQG_00322	Stress inducible protein	CAGCG	3′	119	0.72	0.03
SSQG_01539	Glycerol operon regulatory protein	GAGAG	5′	90	1.59	0.11
SSQG_02132	Serine protease	CAGGG	3′	33	0.67	0.10
SSQG_02132	Serine protease	CAGGG	3′	44	0.67	0.10
SSQG_02339	Tellurium resistance protein	GGGAG	3′	100	0.41	0.00
SSQG_04757	Translation elongation factor Tu	GAGAG	5′	84	1.38	0.06
SSQG_04757	Translation elongation factor Tu	GAGAG	5′	84	1.29	0.04
SSQG_04757	Translation elongation factor Tu	GAGAG	5′	84	1.55	0.34

*Distance of the IRE-like motifs in base pairs from start or stop codon.
doi:10.1371/journal.pone.0087905.t001

The putative stress inducible protein SSQG_00322 belongs to the universal stress protein family Usp and was downregulated in MacnA due to oxidative stress treatment. In *E. coli* the production of Usp proteins is stimulated by a broad range of conditions including starvation for carbon, antibiotic treatment, heat or oxidative stress, etc. [27]. Furthermore, Usp expression was increased in hypoxic cells of *Mycobacterium tuberculosis* and *Mycobacterium smegmatis* [28,29] and also was important for *Pseudomonas aeruginosa* survival under anaerobic energy stress [30]. However, the exact biological function of these proteins is not known so far. Interestingly, at the 3′ end of the Usp encoding gene sequence in *S. viridochromogenes* an IRE motif was identified, which hints to a post-transcriptional regulation by AcnA. Thus, the observed downregulation of SSQG_00322 in the MacnA mutant might be due to the lack of an AcnA-mediated regulation.

An IRE motif was also identified upstream of a gene, encoding a putative glutathione peroxidase (SSQG_03372). The respective protein was significantly upregulated in the WT strain upon MV treatment. Glutathione peroxidases are among the critical enzymes that are needed to maintain the cytoplasmic redox potential and to protect organisms from oxidative damage [31].

The protein SSQG_05458 that codes for a putative thioredoxin was found to be significantly downregulated in MacnA in response to oxidative stress conditions. Thioredoxins are small redox proteins, which function as antioxidants by directly reducing hydrogen peroxide and also disulfide bonds formed by ROS [32]. The role of thioredoxins in oxidative stress response has been described for several bacteria, such as *E. coli*, *Mycobacterium leprae*, *Helicobacter pylori*, or *S. coelicolor* [33–36]. Normally, the level of thioredoxin is expected to increase after oxidative stress treatment. Interestingly, in our MacnA mutant the level of SSQG_05458 strongly decreased under such conditions.

A putative serine protease (SSQG_02132) was found to be downregulated upon MV treatment in MacnA and the respective mRNA sequence turned out to possess two IRE motifs (Table 1). Both are located in close proximity of the translational stop codon. The presence of two IRE motifs located so closely to each other is rather seldom observed. Perhaps two IRE motifs at the 3′ end provide stronger aconitase binding and consequently a better transcript stabilization and protection. Serine proteases have already been shown to play a role in protection against oxidative damage [37,38]. However, the mechanism of this protection is not fully understood. For the HtrA family of serine proteases of Gram-negative bacteria it was assumed that they degrade an excess of misfolded or denaturated proteins [39].

In conclusion, many of the identified proteins turned out to have a function in sensing, preventing or overcoming oxidative stress. This gives us a general view of which proteins are crucial for *S. viridochromogenes*' adaptation to oxidative stress conditions and also a notion about the cellular preconditions that may underlay the high oxygen stress sensitivity of the *S. viridochromogenes* aconitase mutant. For example, the downregulation of proteins such as thioredoxin (SSQG_05458), stress inducible protein (SSQG_00322), and tellurium resistance protein (SSQG_02339) may significantly contribute to the impaired defense of MacnA against free radicals.

Table 2. Proteins indirectly regulated by AcnA.

Locus	function	fold change	p-value
WT			
FrEUN1fDRAFT_6253	RNA binding S1 domain protein	1.28	0.04
FrEUN1fDRAFT_6253	RNA binding S1 domain protein	1.83	0.11
ThimaDRAFT_4816	translation elongation factor G	0.59	0.07
HMPREF1013_05577	50S ribosomal protein L5	1.94	0.03
SP187300_0321	50S ribosomal protein L5 (BL6)	3.23	0.10
Niako_6338	tRNA uridine 5-carboxymethylaminomethyl modification enzyme MnmG	1.82	0.17
SCO4729	DNA-directed RNA polymerase subunit alpha	1.70	0.11
SSQG_04836	chaperonin GroL	1.22	0.00
SSQG_04836	chaperonin GroL	1.85	0.01
SSQG_04185	chaperone DnaK	1.52	0.04
SSQG_04185	chaperone DnaK	2.19	0.13
SSQG_05867	protease	1.36	0.13
SSQG_03555	tellurium resistance protein	1.68	0.04
SSQG_03555	tellurium resistance protein	2.10	0.02
SSQG_00870	6-phosphogluconate dehydrogenase NAD-binding protein	1.65	0.02
SSQG_00870	6-phosphogluconate dehydrogenase NAD-binding protein	1.66	0.02
TBCG_03283	isocitrate dehydrogenase [NADP] Icd1	1.66	0.12
SSQG_02359	3-oxoacyl-[acyl-carrier-protein] synthase 2	4.24	0.09
CV_2767	aspartate-semialdehyde dehydrogenase	1.80	0.02
BURMUCGD1_1985	putative cellulose synthase operon protein C	1.54	0.04
FraEul1c_1109	guanosine pentaphosphate synthetase I/polyribonucleotide nucleotidyltransferase	2.52	0.01
SSQG_03741	phosphoribosylaminoimidazole-succinocarboxamide synthetase	1.61	0.02
RS9917_04255	hypothetical protein RS9917_04255	1.74	0.01
SSQG_05193	conserved hypothetical protein	1.98	0.10
SSQG_02286	conserved hypothetical protein	2.03	0.17
SSQG_04729	conserved hypothetical protein	4.20	0.00
G11MC16DRAFT_3049	conserved hypothetical protein	1.64	0.07
SSQG_03600	conserved hypothetical protein	1.79	0.02
FrEUN1fDRAFT_6253	RNA binding S1 domain protein	0.59	0.07
SSQG_04836	chaperonin GroL	0.61	0.09
BBAL3_51	TldD/PmbA family	0.69	0.03
SSTG_00732	glyceraldehyde-3-phosphate dehydrogenase, type I	0.55	0.08
SCO3096	phosphopyruvate hydratase (enolase)	0.52	0.02
SCO3096	phosphopyruvate hydratase (enolase)	0.51	0.01
CV_2767	aspartate-semialdehyde dehydrogenase	0.61	0.13
SSQG_01989	bifunctional HisA/TrpF protein	0.68	0.03
APM_0032	conjugative relaxase domain protein	0.63	0.09
APM_0032	conjugative relaxase domain protein	0.48	0.02
SSQG_03895	single-strand binding protein	0.31	0.02
SSQG_01951	two-component system response regulator	0.51	0.03
Cbei_3045	methyl-accepting chemotaxis sensory transducer	0.66	0.15
Acid345_0176	radical SAM protein	0.54	0.16
BFAG_02012	cobalamin biosynthesis protein CobD	0.82	0.01
SSQG_03772	uracil phosphoribosyltransferase	0.64	0.10
SSQG_02905	conserved hypothetical protein	0.49	0.00
SSQG_07592	secreted protein	0.43	0.08
SSQG_07014	secreted protein	0.34	0.04
SSQG_07014	secreted protein	0.46	0.15

Table 2. Cont.

Locus	function	fold change	p-value
SSQG_07014	secreted protein	0.73	0.00
MacnA			
SSQG_05040	transcription elongation factor GreA	1.37	0.06
SSQG_05128	translation-associated GTPase	1.24	0.06
SSQG_04311	anti-sigma factor	1.51	0.10
SSQG_04185	chaperone DnaK	1.38	0.11
SSQG_05430	methylmalonyl-CoA epimerase	1.90	0.08
SSQG_05406	ATP synthase F1, beta subunit	2.23	0.10
SSQG_01256	forkhead-associated protein	1.40	0.05
SSQG_02356	malonate decarboxylase, epsilon subunit	2.34	0.13
SSQG_03235	4-(cytidine 5′-diphospho)-2-C-methyl-D-erythritol kinase	1.59	0.06
pO86A1_p160	aminoglycoside-3′-O-phosphotransferase	1.45	0.02
SSQG_01691	secreted protein	1.41	0.05
SSQG_02341	conserved hypothetical protein	1.63	0.04
SSQG_02509	glycyl-tRNA synthetase	0.52	0.04
SSQG_05458	thioredoxin	0.53	0.07
SSQG_01736	3-oxoacyl-[acyl-carrier-protein] reductase	0.69	0.07
SSQG_01640	cell division protein SepF1	4.97	0.20
SSQG_02020	cell division protein SepF2	0.79	0.01
HMPREF0873_01794	ABC transporter, ATP-binding family protein	0.51	0.07
SSQG_06852	monomeric isocitrate dehydrogenase	0.44	0.16
SSQG_05319	dehydrogenase	0.75	0.03

doi:10.1371/journal.pone.0087905.t002

Aconitase controls EF-Tu expression upon oxidative stress

A set of differentially regulated, putative transcription and translation proteins, were identified in both strains. In the WT, the majority of translation-related proteins, such as 50S ribosomal protein L5 (HMPREF1013_05577, SP187300_0321), RNA binding S1 domain protein (FrEUN1fDRAFT_6253), tRNA uridine 5-carboxymethylaminomethyl modification enzyme MnmG (Niako_6338), translation elongation factor G (ThimaDRAFT_4816), as well as the alpha subunit of transcription enzyme DNA-directed RNA polymerase (SCO4729) were found to be upregulated after oxidative stress induction. Among the translation and transcription proteins upregulated in MacnA were the translation-associated GTPase (SSQG_05128), the transcription elongation factor GreA (SSQG_05040), the anti-sigma factor (SSQG_04311), and the translation elongation factor Tu (EF-Tu) (SSQG_04757). Interestingly, almost all isoforms of the putative EF-Tu protein (SSQG_04757) were significantly downregulated in the WT strain under the same stress conditions (Table S1). The downregulation of this protein in the WT and its upregulation in MacnA suggests that AcnA negatively influences the SSQG_04757 expression. This regulation may be governed directly by AcnA, since an IRE motif was identified at the 5′ end of the respective mRNA sequence (Table 1). This is another direct *in vivo* evidence for an AcnA-mediated regulation as observed vice versa for the expression of the tellurium resistance protein SSQG_02339.

EF-Tu is a highly abundant bacterial protein (5–10% of the total proteins) [40] that promotes the GTP-dependent binding of the aminoacyl-tRNA to the A-site of the ribosome during protein biosynthesis and contributes to translational accuracy. It was also one of the most abundant proteins in *S. viridochromogenes* WT and MacnA. Because of the central role of EF-Tu, its downregulation in the WT strain may lead to a significant reduction in protein synthesis. Perhaps such a downregulation has a function in reprograming cell metabolism to divert resources away from extensive protein production under stress conditions towards amino acid synthesis in order to promote survival, which could assist the process of stringent response (see below). Besides the well-established function of EF-Tu in protein synthesis, it is also involved in other cellular processes, including cell shape maintenance as shown for *B. subtilis* [41] or protection of proteins during heat stress in *E. coli* [42]. Contrary to our results, in proteome analysis of *E. coli*, EF-Tu reached its maximum expression as a result of the exposure of the strain to different environmental stress conditions [43]. Here it was suggested that this overexpression might be related with the chaperon function of EF-Tu [42,43]. In *E. coli* EF-Tu interacts with unfolded and denaturated proteins. For example, it promotes the correct folding of citrate synthase preventing its aggregation under heat shock conditions [42]. Even if it is hard to drive a firm conclusion, one can say that stress conditions have a significant influence on the cellular EF-Tu content.

AcnA-mediated regulation may contribute to carbon flux redistribution under oxidative stress

SSQG_00870 is a putative 6-phosphogluconate dehydrogenase that was significantly upregulated in the WT strain upon oxidative stress treatment. 6-phosphogluconate dehydrogenase is a key enzyme in the pentose phosphate pathway, where it catalyzes the

reaction from 6-phosphogluconate to ribulose-5-phosphate. This reaction is especially important for NADPH generation. NADPH provides reducing equivalents for the biosynthetic reactions and also for redox reactions involved in protection processes against ROS, such as the reduction of oxidized forms of glutathione and thioredoxin [44]. Thus, NADPH is a pivotal component of the oxidative stress defense. In yeast, a 6-phosphogluconate dehydrogenase mutant showed increased sensitivity to hydrogen peroxide, revealing the importance of this enzyme in protection against oxidative stress [45]. As it has been shown that redox cycling of MV leads to a destructive oxidation of NADPH [46], the upregulation of SSQG_00870 in *S. viridochromogenes* may meet the increased demand for reducing equivalents under oxidative stress conditions. However, this regulation might be only indirectly mediated by AcnA as no IRE motif was identified on the respective 6-phosphogluconate dehydrogenase gene sequence.

Also enzymes involved in glycolysis were identified in the WT to be differentially expressed during the period of oxidative stress. The phosphopyruvate hydratase (SCO3096) was downregulated, whereas phosphoglycerate kinase (SSQG_01870) was upregulated. On the corresponding gene sequence of SSQG_01870, an IRE motif was identified, which suggests an AcnA-mediated regulation of the respective mRNA (Table 1). For *Caenorhabditis elegans* it has been shown that the oxidative inhibitions of other glycolytic enzymes, such as glyceraldehyde 3-phosphate dehydrogenase (GADPH) or phosphate isomerase (TPI), leads to an increased resistance of the strain to oxidative stress [47]. This is because of the redirection of the carbohydrate flux from glycolysis to the pentose phosphate pathway, which results in the generation of NADPH and in this way supports the oxidative stress defense [47]. Perhaps a similar redirection of the carbohydrate flux as a contribution to oxidative stress defense exists in *S. viridochromogenes*. In our analysis the putative glyceraldehyde-3-phosphate dehydrogenase (GAPDH) (SSQG_01871, SSTG_00732) was also identified in the WT, however, since the protein was once up- and once downregulated, the meaning of its regulation is difficult to assess.

An IRE sequence was also identified upstream of the gene encoding the putative glycerol operon regulatory protein 302550310, which was found to be upregulated after MV treatment in MacnA. SSQG_01539 shows 94% identity on amino sequence level to the glycerol operon regulatory protein GylR of *S. coelicolor*, which is a repressor of the *gyl*CABX operon that is involved in glycerol catabolism [48]. The upregulation of SSQG_01539 in the aconitase mutant suggests that AcnA may negatively influence the SSQG_01539 expression. Glycerol is an important metabolite in cellular response to oxidative stress as for example it functions as an efficient free radicals scavenger and is crucial for the regulation of the redox processes [49]. Glycerol synthesis seems to be required for tolerance to MV in yeast [50]. Studies in *Entamoeba histolytica* and *Saccharomyces cerevisiae* suggest that the oxidative stress results in the inhibition of glycolysis leading to the redirection of the carbohydrate flux towards the regeneration of NADPH and glycerol production [49,51]. Consequently, in our analysis, the overexpression of the putative repressor SSQG_01539 of the glycerol catabolism pathway in MacnA can be regarded as an adaptation to the oxidative stress conditions, which probably leads to an accumulation of glycerol and regeneration of reducing equivalents.

A putative NADP-dependent isocitrate dehydrogenase (IDH-NADP) TBCG_03283 was found to be upregulated in response to oxidative stress in the WT strain. This protein was identified as homologue of *M. tuberculosis*. IDH-NADP is one of the key enzymes of the TCA cycle and catalyzes the reaction from isocitrate to α-ketoglutarate by generating one molecule of NADPH. The upregulation of TBCG_03283 is in agreement to what has been observed in *Pseudomonas fluorescens*, where the activity and expression of IDH-NADP were increased after exposure to an oxidative environment [52]. The overexpression of IDH-NADP leads to an increased NADPH level and in this way contributes to the metabolic adaptation to oxidative stress conditions [52]. In contrast, a downregulation of the putative IDH-NADP SSQG_06852 was observed in MacnA. Thus this downregulation may lead to a cellular $NADP^+$\NADPH imbalance, which could contribute to the oxidative stress sensitivity of MacnA. As the IDH-NADP was differentially expressed in the WT and in the aconitase mutant strain, the expression of this enzyme seems to be regulated by AcnA. However, as no IRE motif was identified on the respective IDH-NADP gene sequence, this regulation may be only indirect.

Altogether, our observations show that carbon metabolism pathways of *S. viridochromogenes*, such as pentose phosphate pathway, glycolysis and TCA cycle are significantly influenced by oxidative stress and that these changes may cause metabolic flux redistributions towards the generation of NADPH as protective response.

Aconitase regulates expression of proteins involved in cell growth and morphological differentiation

The cell division protein FtsZ (SSQG_02023) was significantly upregulated in the WT strain after MV application. By gel shifts assays it has been shown before that the *ftsZ* IRE motif is a target for AcnA binding, which strongly suggests an AcnA-mediated regulation of FtsZ expression [5]. The fact that SSQG_02023 was not identified in MacnA among the proteins with significant change in expression may be because of the missing AcnA-mediated regulation of this protein.

Two other putative cell division proteins associated with FtsZ, SepF1 (SSQG_01640) and SepF2 (SSQG_02020), were downregulated under oxidative stress conditions in MacnA. Moreover, a protein identified as secreted protein (SSQG_01691) was upregulated in MacnA, which is similar to the sporulation control protein Spo0M of *B. subtilis* [53].

Taking together, our proteomic results suggest that *S. viridochromogenes* undergoes some regulation of proteins involved in cell division and sporulation processes upon oxidative stress. The regulation of these proteins may be either mediated directly by AcnA as described for FtsZ or indirectly, such as in the case of the SepF1, SepF2 or Spo0M homologous proteins.

AcnA controls expression of proteins involved in phosphate uptake and phosphate metabolism

The putative PstS protein (SSQG_03670) was downregulated in the WT strain due to oxidative stress. Upstream of the *pstS* gene an IRE motif was identified, which suggests an AcnA-mediated regulation of the respective protein expression (Table 1). Pst proteins generally function as high-affinity-phosphate binding proteins [54,55]. For *Lactococcus lactis* it has been shown that inactivation of the *pst* genes, including *pstS*, results in higher resistance to oxidizing agents such as tellurite and H_2O_2 [56–58]. It was speculated that the inactivation of the major phosphate uptake pathway mimics phosphate starvation and induces a number of stress responses that cause cross-resistance to different stressors [56,57]. For example, in *Salmonella typhimurium* different proteins were overproduced upon phosphate starvation [59]. Induction of these proteins contributes to cell survival under various stress conditions [57,60]. The downregulation of PstS upon oxidative stress in the *S. viridochromogenes* wild-type most likely

also leads to phosphate starvation, which in turn may cause the elevated expression of stress response genes and thus a better cellular defense under this unfavorable condition.

A number of environmental stress conditions, including phosphate starvation can be signaled in cells by the alarmone guanosine pentaphosphate (p)ppGpp, which mediates the so-called stringent response [61,62]. Stringent response allows bacteria to quickly reprogram transcription in response to nutrient limitation or stress signals [63]. Via ppGpp several metabolic pathways are inhibited, such as RNA synthesis or protein synthesis, whereas others like those that are needed for the exploitation of nutrient sources, protein degradation or the synthesis of proteins for stress combat are activated. In *E. coli* the ppGpp production was observed to be induced as a response to the exposure to MV and H_2O_2 [64,65]. In our analysis a protein identified as guanosine pentaphosphate synthetase I/polyribonucleotide nucleotidyltransferase (FraEuI1c_1109), which is suggested to be responsible for (p)ppGpp biosynthesis, was upregulated in the WT strain upon MV treatment. This indicates that FraEuI1c_1109 is involved in adaptation of *S. viridochromogenes* to oxidative stress.

Proteins of fatty acids metabolism respond to oxidative stress conditions via indirect AcnA-mediated regulation

Three proteins were identified as putative enzymes involved in fatty acid metabolism: 3-oxoacyl-[acyl-carrier-protein] synthase (SSQG_02359), which was upregulated in the WT strain; methylmalonyl-CoA epimerase (SSQG_05430) upregulated in MacnA; and 3-oxoacyl-[acyl-carrier-protein] reductase (SSQG_01736) that was downregulated in MacnA due to oxidative stress treatment. Fatty acid metabolism influences the cellular membrane lipid composition. The saturation or unsaturation of membrane lipids is one of the factors determining the chance of survival of prokaryotic and eukaryotic cells under environmental stress conditions [66,67]. This has been shown for *S. coelicolor*, *S. cerevisiae*, *B. subtilis*, and *Bacillus megaterium*, which were more resistant to H_2O_2 or high temperature stress the higher the content of saturated fatty acid in their membrane lipids was [68–69]. For *S. viridochromogenes* it is known that fatty acids composition of their membrane lipids has a crucial effect on membrane rigidity and permeability [70]. Our data of the changed expression of proteins contributing to fatty acids metabolism also may reflect the importance of membrane lipid composition in oxidative stress response of *S. viridochromogenes*. As the corresponding mRNA sequences of the identified proteins were not found to possess any IRE element, their expression may only be indirectly mediated by AcnA.

The chaperones DnaK and GroL are a part of general oxidative stress response in *S. viridochromogenes*

In our analysis, DnaK (SSQG_04185) and GroL (SSQG_04836) were among the most abundant proteins identified in the WT strain after oxidative stress treatment. DnaK and GroL are stress- inducible chaperones that function in preventing protein misfolding and aggregation of potentially toxic proteins [71]. Our result correspond with the proteome data from *Deinococcus geothermalis*, where DnaK, GroEL and GroES were also detected as the predominant proteins in that strain, which itself is known for its capacity to overcome extremely harsh conditions including oxidative stress [72]. In our analysis DnaK and GroL were identified in both strains as multiple spots, which suggest post-transcriptional modifications of these proteins. All these spots, except one isoform of GroL, were upregulated in both, the WT and the MacnA strain, obviously as part of a general response of *S. viridochromogenes* to oxidative stress. Thus, as the upregulation was observed in both strains, this is suggested to happen independently from any regulation by AcnA.

Summing up, our proteome data together with the *in silico* analyses reveal evidences for a direct AcnA-mediated regulation upon oxidative stress and also give insight into the oxidative stress adaptation of *S. viridochromogenes*. In prospective experiments the regulatory binding capability of AcnA to the newly identified target mRNAs will be analyzed by *in vitro* shift studies and mutational analyses.

Supporting Information

Figure S1 Growth curve of *S. viridochromogenes* wild-type (A) and MacnA (B). Time point of methyl viologen (MV) supply is indicated as black arrow.
(TIF)

Figure S2 2D gel image of the methyl viologen-treated *S. viridochromogenes* wild-type (A) and untreated wild-type (B). 2D gel image of the methyl viologen-treated *S. viridochromogenes* MacnA (**C**) and untreated MacnA (**D**). Significantly changed spots are outlined in green. They showed a statistically significant variation of spot volume and minimal fold variation of 1.1. These spots (73 for WT and 36 for MacnA) were excised for subsequent protein identification by mass spectrometry. White arrows indicate the spots that were identified in both, WT and MacnA strain (see Table 1 for code assignment).
(TIF)

Table S1 Proteins differentially expressed in *S. viridochromogenes* WT and MacnA due to oxidative stress treatment identified by MALDI TOF/TOF
(DOCX)

Acknowledgments

We thank Thilo Mast for statistical evaluations.

Author Contributions

Conceived and designed the experiments: YM EM WW. Performed the experiments: EM. Analyzed the data: EM YM. Contributed reagents/materials/analysis tools: WD SZ KB HR RW. Wrote the paper: YM EM.

References

1. Flärdh K, Buttner MJ (2009) Streptomyces morphogenetics: dissecting differentiation in a filamentous bacterium. Nat Rev Microbiol 7: 36–49.
2. Schinko E, Schad K, Eys S, Keller U, Wohlleben W (2009) Phosphinothricin-tripeptide biosynthesis: an original version of bacterial secondary metabolism? Phytochemistry 70: 1787–1800.
3. Schwartz D, Kaspar S, Kienzlen G, Muschko K, Wohlleben W (1999) Inactivation of the tricarboxylic acid cycle aconitase gene from *Streptomyces viridochromogenes* Tü494 impairs morphological and physiological differentiation. J Bacteriol 181: 7131–7135.
4. Muschko K, Kienzlen G, Fiedler HP, Wohlleben W, Schwartz D (2002) Tricarboxylic acid cycle aconitase activity during the life cycle of *Streptomyces viridochromogenes* Tü494. Arch Microbiol 178: 499–505.
5. Michta E, Schad K, Blin K, Ort-Winklbauer R, Röttig M, et al. (2012) The bifunctional role of aconitase in *Streptomyces viridochromogenes* Tü494. Environ Microbiol. 14: 3203–3219.
6. Tang Y, Quail MA, Artymiuk PJ, Guest JR, Green J (2002) *Escherichia coli* aconitases and oxidative stress: post-transcriptional regulation of *sodA* expression. Microbiology 148: 1027–1037.
7. Muckenthaler MU, Galy B, Hentze MW (2008) Systemic iron homeostasis and the iron-responsive element/iron-regulatory protein (IRE/IRP) regulatory network. Annu Rev Nutr 28: 197–213.
8. Dupuy J, Volbeda A, Carpentier P, Darnault C, Moulis JM, et al. (2006) Crystal structure of human iron regulatory protein 1 as cytosolic aconitase. Structure 14: 129–139.

9. Tang Y, Guest JR (1999) Direct evidence for mRNA binding and post-transcriptional regulation by *Escherichia coli* aconitases. Microbiology 145: 3069–3079.
10. Banerjee S, Nandyala AK, Raviprasad P, Ahmed N, Hasnain SE (2007) Iron-dependent RNA-binding activity of *Mycobacterium tuberculosis* aconitase. J Bacteriol. 189: 4046–4052.
11. Alén C, Sonenshein AL (1999) *Bacillus subtilis* aconitase is an RNA-binding protein. Proc Natl Acad Sci U S A 96: 10412–10417.
12. Serio AW, Pechter KB, Sonenshein AL (2006) *Bacillus subtilis* aconitase is required for efficient late-sporulation gene expression. J Bacteriol 188: 6396–6405.
13. Núñez MT, Núñez-Millacura C, Tapia V, Muñoz P, Mazariegos D, et al. (2003) Iron-activated iron uptake: a positive feedback loop mediated by iron regulatory protein 1. Biometals 16: 83–90.
14. Herbert D, Phipps PJ, Strange RE (1971) Chemical analysis of microbial cells. *In*: Norris JR & Ribbons DW (eds.) Methods in Microbiology. 209–344. London, Academic Press.
15. Bradford MM (1976) A rapid and sensitive method for the quantitation of microgram quantities of protein utilizing the principle of protein-dye binding. Analytical Biochem 72: 248–254.
16. Yao Y, Sun H, Xu F, Zhang X, Liu S (2011). Comparative proteome analysis of metabolic changes by low phosphorus stress in two *Brassica napus* genotypes. Planta 233: 523–537.
17. Xiao M, Xu P, Zhao J, Wang Z, Zuo F, et al. (2011) Oxidative stress-related responses of *Bifidobacterium longum* subsp. *longum* BBMN68 at the proteomic level after exposure to oxygen. Microbiolgy 6: 1573–1588.
18. Perera IC, Grove A (2010) Molecular mechanisms of ligand-mediated attenuation of DNA binding by MarR family transcriptional regulators. J Mol Cell Biol 2: 2432–54.
19. Anantharaman V, Iyer LM, Aravind L (2012) Ter-dependent stress response systems: novel pathways related to metal sensing, production of a nucleoside-like metabolite, and DNA-processing. Mol Biosyst 8: 3142–3165.
20. Pérez JM, Calderón IL, Arenas FA, Fuentes DE, Pradenas GA, et al. (2007) Bacterial toxicity of potassium tellurite: unveiling an ancient enigma. PLoS One 2: 211.
21. De Mot R, Schoofs G, Nagy I (2007) Proteome analysis of *Streptomyces coelicolor* mutants affected in the proteasome system reveals changes in stress-responsive proteins. Arch Microbiol 188: 257–271.
22. Langlois P, Bourassa S, Poirier GG, Beaulieu C (2003) Identification of *Streptomyces coelicolor* proteins that are differentially expressed in the presence of plant material. Appl Environ Microbiol 69: 1884–1889.
23. Hammad Y, Maréchal J, Cournoyer B, Normand P, Domenach AM (2001) Modification of the protein expression pattern induced in the nitrogen-fixing actinomycete *Frankia* sp. strain ACN14a-tsr by root exudates of its symbiotic host *Alnus glutinosa* and cloning of the *sodF* gene. Can J Microbiol 47: 541–547.
24. Borsetti F, Tremaroli V, Michelacci F, Borghese R, Winterstein C, et al. (2005) Tellurite effects on *Rhodobacter capsulatus* cell viability and superoxide dismutase activity under oxidative stress conditions. Res Microbiol 156: 807–813.
25. Ballal A, Manna AC (2009) Regulation of superoxide dismutase (*sod*) genes by SarA in *Staphylococcus aureus*. J Bacteriol 191: 3301–3310.
26. Karavolos MH, Horsburgh MJ, Ingham E, Foster SJ (2009) Role and regulation of the superoxide dismutases of *Staphylococcus aureus*. Microbiology 149: 2749–2758.
27. Kvint K, Nachin L, Diez A, Nyström T (2003) The bacterial universal stress protein: function and regulation. Curr Opin Microbiol 6: 140–145.
28. Rosenkrands I, Slayden RA, Crawford J, Aagaard C, Barry CE 3rd, et al. (2002) Hypoxic response of *Mycobacterium tuberculosis* studied by metabolic labeling and proteome analysis of cellular and extracellular proteins. J Bacteriol 184: 3485–3491.
29. O'Toole R, Smeulders MJ, Blokpoel MC, Kay EJ, Lougheed K, et al. (2003) A two-component regulator of universal stress protein expression and adaptation to oxygen starvation in *Mycobacterium smegmatis*. J Bacteriol 185: 1543–1554.
30. Boes N, Schreiber K, Härtig E, Jaensch L, Schobert M (2006) The *Pseudomonas aeruginosa* universal stress protein PA4352 is essential for surviving anaerobic energy stress. J Bacteriol 188: 6529–6538.
31. Miyamoto Y, Koh YH, Park YS, Fujiwara N, Sakiyama H, et al. (2003) Oxidative stress caused by inactivation of glutathione peroxidase and adaptive responses. Biol Chem 384: 567–574.
32. Zeller T, Klug G (2006) Thioredoxins in bacteria: functions in oxidative stress response and regulation of thioredoxin genes. Naturwissenschaften 93: 259–266.
33. Ritz D, Patel H, Doan B, Zheng M, Aslund F, et al. (2000) Thioredoxin 2 is involved in the oxidative stress response in *Escherichia coli*. J Biol Chem 275: 2505–2512.
34. Wieles B, Ottenhoff TH, Steenwijk TM, Franken KL, de Vries RR, et al. (1997) Increased intracellular survival of *Mycobacterium smegmatis* containing the *Mycobacterium leprae* thioredoxin-thioredoxin reductase gene. Infect Immun 65: 2537–2541.
35. Comtois SL, Gidley MD, Kelly DJ (2003) Role of the thioredoxin system and the thiol-peroxidases Tpx and Bcp in mediating resistance to oxidative and nitrosative stress in *Helicobacter pylori*. Microbiology 149: 121–129.
36. Stefanková P, Perecko D, Barák I, Kollárová M (2006) The thioredoxin system from *Streptomyces coelicolor*. J Basic Microbiol 46: 47–55.
37. Clausen T, Southan C, Ehrmann M (2002) The HtrA family of proteases: implications for protein composition and cell fate. Mol Cell 10: 443–455.
38. Biswas T, Small J, Vandal O, Odaira T, Deng H, et al. (2010) Structural insight into serine protease Rv3671c that Protects *M. tuberculosis* from oxidative and acidic stress. Structure 18: 1353–1363.
39. Kim DY, Kim KK (2005) Structure and function of HtrA family proteins, the key players in protein quality control. J Biochem Mol Biol 38: 266–274.
40. Krab IM, Parmeggiani A (1998) EF-Tu, 1998. A GTPase odyssey. Biochim Biophys Acta 1443: 1–22.
41. Defeu Soufo HJ, Reimold C, Linne U, Knust T, Gescher J, et al. (2010) Bacterial translation elongation factor EF-Tu interacts and colocalizes with actin-like MreB protein. Proc Natl Acad Sci U S A 107: 3163–3168.
42. Caldas TD, El Yaagoubi A, Richarme G (1998) Chaperone properties of bacterial elongation factor EF-Tu. J Biol Chem 273: 11478–11482.
43. Muela A, Seco C, Camafeita E, Arana I, Orruño M, et al. (2008) Changes in *Escherichia coli* outer membrane subproteome under environmental conditions inducing the viable but nonculturable state. FEMS Microbiol Ecol 64: 28–36.
44. Buchanan BB, Balmer Y (2005) Redox regulation: a broadening horizon. Annu Rev Plant Biol 56: 187–220.
45. Juhnke H, Krems B, Kötter P, Entian KD (1996) Mutants that show increased sensitivity to hydrogen peroxide reveal an important role for the pentose phosphate pathway in protection of yeast against oxidative stress. Mol Gen Genet 252: 456–464.
46. Ilett KF, Stripp B, Menard RH, Reid WD, Gillette JR (1974) Studies on the mechanism of the lung toxicity of paraquat: comparison of tissue distribution and some biochemical parameters in rats and rabbits. Toxicol Appl Pharmacol 28: 216–226
47. Ralser M, Wamelink MM, Kowald A, Gerisch B, Heeren G, et al. (2007) Dynamic rerouting of the carbohydrate flux is key to counteracting oxidative stress. J Biol. 6: 10.
48. Hindle Z, Smith CP (1994) Substrate induction and catabolite repression of the *Streptomyces coelicolor* glycerol operon are mediated through the GylR protein. Mol Microbiol 12: 737–745.
49. Afzal H, Sato D, Jeelani G, Soga T, Nozaki T (2012) Dramatic Increase in Glycerol Biosynthesis upon Oxidative Stress in the Anaerobic Protozoan Parasite *Entamoeba histolytica*. PLoS Negl Trop Dis 6: 1831.
50. Pahlman AK, Granath K, Ansell R, Hohmann S, Adler L (2001) The yeast glycerol 3-phosphatases Gpp1p and Gpp2p are required for glycerol biosynthesis and differentially involved in the cellular responses to osmotic, anaerobic, and oxidative stress. J Biol Chem 276: 3555–3563.
51. Godon C, Lagniel G, Lee J, Buhler JM, Kieffer S, et al. (1998) The H_2O_2 stimulon in *Saccharomyces cerevisiae*. J Biol Chem 273: 22480–22489.
52. Singh R, Mailloux RJ, Puiseux-Dao S, Appanna VD (2007) Oxidative stress evokes a metabolic adaptation that favors increased NADPH synthesis and decreased NADH production in *Pseudomonas fluorescens*. J Bacteriol 189: 6665–6675.
53. Han WD, Kawamoto S, Hosoya Y, Fujita M, Sadaie Y, et al. (1998) A novel sporulation-control gene (*spo0M*) of *Bacillus subtilis* with a sigmaH-regulated promoter. Gene 217: 31–40.
54. Webb DC, Rosenberg H, Cox GB (1992) Mutational analysis of the *Escherichia coli* phosphate-specific transport system, a member of the traffic ATPase (or ABC) family of membrane transporters. A role for proline residues in transmembrane helices. J Biol Chem 267: 24661–24668.
55. Qi Y, Kobayashi Y, Hullet FM (1997) The *pst* operon of *Bacillus subtilis* has a phosphate-regulated promoter and is involved in phosphate transport but not in regulation of the *pho* regulon. J Bacteriol 179: 2534–2539.
56. Turner MS, Tan YP, Giffard PM (2007). Inactivation of an iron transporter in *Lactococcus lactis* results in resistance to tellurite and oxidative stress. Appl Environ Microbiol 73: 6144–6149.
57. Duwat P, Ehrlich SD, Gruss A (1999). Effects of metabolic flux on stress response pathways in *Lactococcus lactis*. Mol Microbiol 31: 845–858.
58. Rallu F, Gruss A, Ehrlich SD, Maguin E (2000). Acid- and multistress-resistant mutants of *Lactococcus lactis*: identification of intracellular stress signals. Mol Microbiol 35: 517–528.
59. Spector MP, Aliabani Z, Gonzalez T, Foster JW (1986). Global control in *Salmonella typhimurium*: two-dimensional electrophoretic analysis of starvation-, anaerobiosis-, and heat shock-inducible proteins. J Bacteriol 168: 420–424.
60. O'Neal CR, Gabriel WM, Turk AK, Libby SJ, Fang FC, et al. (1994) RpoS is necessary for both the positive and negative regulation of starvation survival genes during phosphate, carbon, and nitrogen starvation in *Salmonella typhimurium*. J Bacteriol 176: 4610–4616.
61. Potrykus K, Cashel M (2008) (p)ppGpp: still magical? Annu Rev Microbiol 62: 35–51.
62. Bougdour A, Gottesman S (2007) ppGpp regulation of RpoS degradation via anti-adaptor protein IraP. Proc Natl Acad Sci U S A 104: 12896–12901.
63. Boutte CC, Crosson S (2013) Bacterial lifestyle shapes stringent response activation. Trends Microbiol 21: 174–180.
64. Brown OR, Seither RL (1983) Oxygen and redox-active drugs: shared toxicity sites. Fundam Appl Toxicol 3: 209–214.
65. VanBogelen RA, Kelley PM, Neidhardt FC (1987) Differential induction of heat shock, SOS, and oxidation stress regulons and accumulation of nucleotides in *Escherichia coli*. J Bacteriol 169: 26–32.
66. Son MW, Ko JI, Doh HM, Kim WB, Park TS, et al. (1998) Protective effect of taurine on TNBS-induced inflammatory bowel disease in rats. Arch Pharm Res 21: 531–536.

67. Steels EL, Learmonth RP, Watson K (1994) Stress tolerance and membrane lipid unsaturation in *Saccharomyces cerevisiae* grown aerobically or anaerobically. Microbiology 140: 569–576.
68. Kim J, Shim A, Son S (1999) H_2O_2 resistance is linked to the degree of fatty acid unsaturation in *Streptomyces coelicolor* A3(2). Biotech Letters 21: 759–762.
69. Suutari M, Laakso S (1992) Unsaturated and branched chain-fatty acids in temperature adaptation of *Bacillus subtilis* and *Bacillus megaterium*. Biochim Biophys Acta 1126: 119–124.
70. Shim MS, Kim JH (1993) Fatty acid and lipid composition in mycelia from submerged or surface culture of *Streptomyces viridochromogenes*. FEMS Microbiol Lett 108: 11–14.
71. Hartl FU, Bracher A, Hayer-Hartl M (2011) Molecular chaperones in protein folding and proteostasis. Nature 475: 324–332.
72. Liedert C, Peltola M, Bernhardt J, Neubauer P, Salkinoja-Salonen M (2012) Physiology of resistant *Deinococcus geothermalis* bacterium aerobically cultivated in low-manganese medium. J Bacteriol 194: 1552–1561.

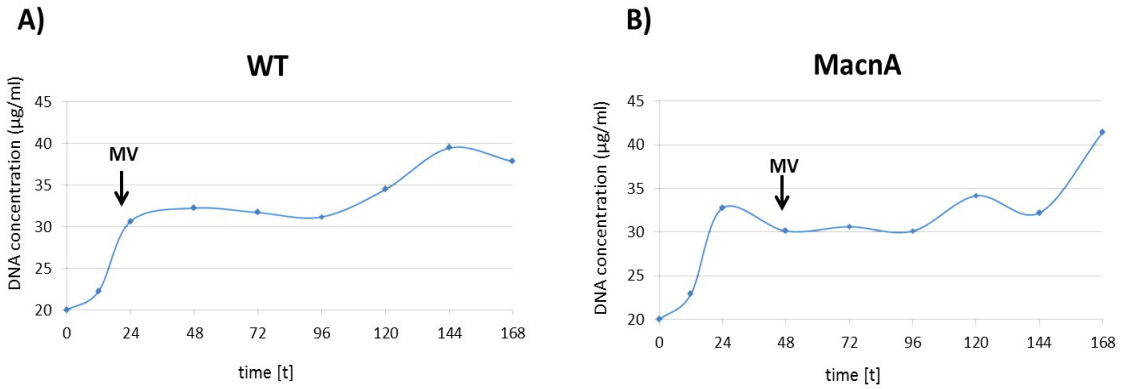

Supporting information, Fig. S1. Growth curve of *S. viridochromogenes* wild-type (A) and MacnA (B). Time point of methyl viologen (MV) supply is indicated as black arrow.

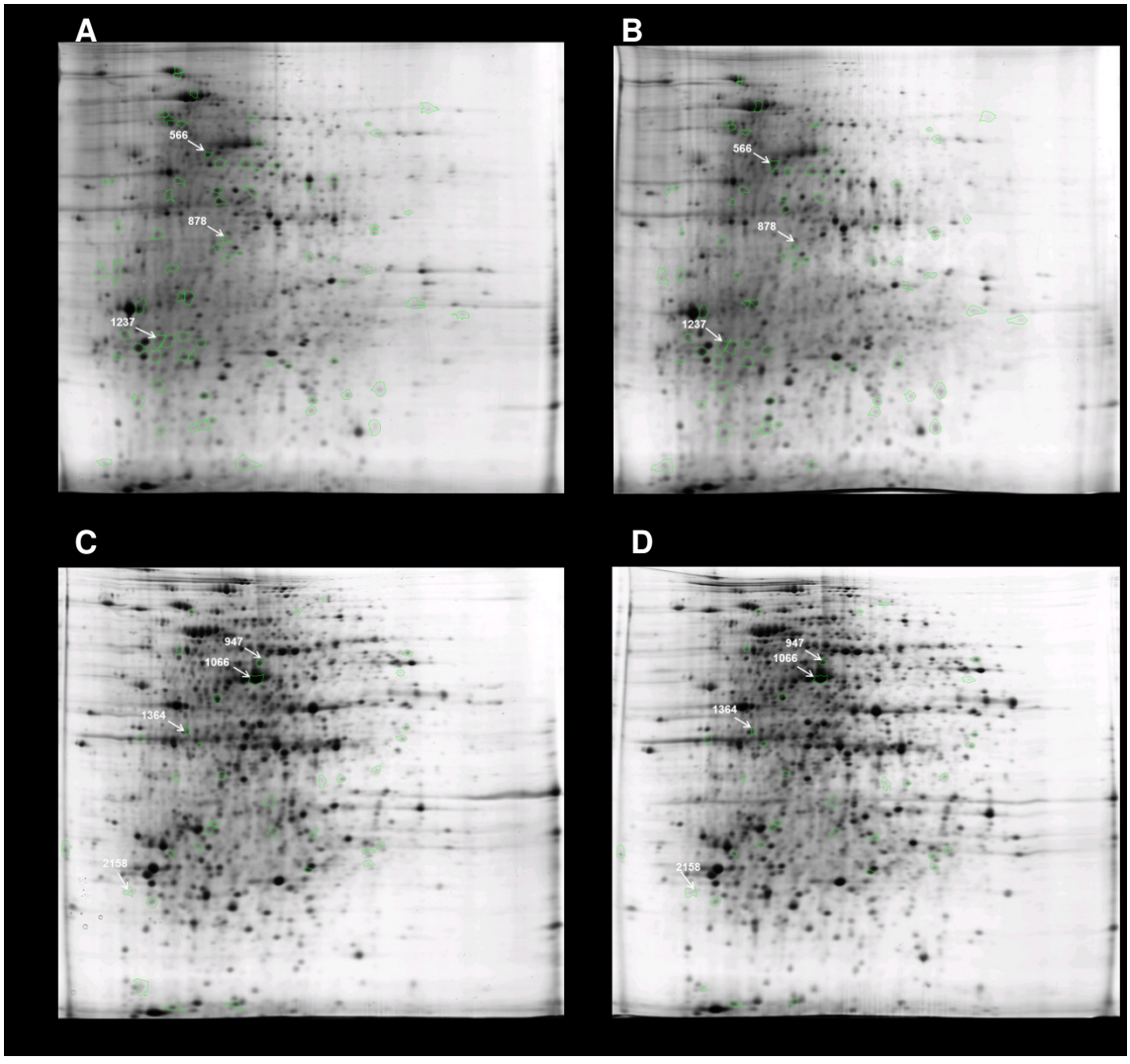

Supporting information, Fig. S2. 2D gel image of the methyl viologen-treated *S. viridochromogenes* wild-type (A) and untreated wild-type (B). 2D gel image of the methyl viologen-treated *S. viridochromogenes* MacnA (**C**) and untreated MacnA (**D**). Significantly changed spots are outlined in green. White arrows indicate the spots that were identified in both, WT and MacnA strain (see Table 1 in online published paper for code assignment).

9. Contribution

In publication 1 (Michta *et al*., 2012), I overexpressed and purified all recombinant proteins, performed RT-PCR analysis and the majority of the electrophoretic mobility shift experiments. Also the phenotypic comparison of *S. viridochromogenes* WT grown with different concentrations of various organic acids, as well as the analysis of the susceptibility of the *S. viridochromogenes* strains to stress conditions was performed by me. I contributed to the analysis and interpretation of the data and to some scientific ideas about how to perform the experiments. I also took part in editing the manuscript. K. Schad wrote the manuscript, performed cloning of the point-mutated AcnA derivatives, the Western-blot analysis, part of the electrophoretic shift experiments and susceptibility experiments of the *S. viridochromogenes* strains to stress conditions. R. Ort-Winklbauer performed cloning experiments. The bioinformatic part of the work has been done by K. Blin, M. Röttig and O. Kohlbacher. E. Schinko and Y. Mast designed the experiments, wrote and edited the manuscript. Y. Mast, E. Schinko and W. Wohlleben supervised the project.

In publication 2 (Michta *et al*., 2014), all the experiments were performed by me, with the help of the people from the Shanghai Applied Protein Technology. I analyzed and interpreted the data and wrote the manuscript. People from Prof. W. Jiang group reviewed the manuscript and provided helpful suggestions. The bioinformatic search for IRE elements in *S. viridochromogenes* genome has been done by K. Blin. Y. Mast took part in designing the experiments and edited the manuscript. Y. Mast and W. Wohlleben supervised the project.

Curriculum Vitae

PERSONAL INFORMATION

Name:	Ewelina
Surname:	Atasayar
Maiden surname:	Michta
Date of birth:	30.10.1986
Place of birth:	Gdańsk/Poland
Nationality:	Polish

EDUCATION

09/2002 – 06/2005 **High school in Kościerzyna, Poland.**
Graduation with Abitur certificate.

10/2005 – 06/2008 **Bachelor's Degree, Intercollegiate Faculty of Biotechnology, Medical University of Gdansk and University of Gdansk, Poland.**
Faculty of Biotechnology

Thesis title: "The role of Toll-like receptors in pathogens recognition"

10/2008 – 06/2010 **M.Sc., Intercollegiate Faculty of Biotechnology, Medical University of Gdansk and University of Gdansk, Poland.**
Faculty of Biotechnology

Thesis title: "The role of superoxide dismutases in response of *Staphylococcus aureus* to photodynamic inactivation"

10/2010 – 04/2014 **PhD, Eberhard-Karls University of Tübingen, Germany.**
Inter-Faculty Institute of Microbiology and Infection Medicine

Thesis title: "Analysis of the post-transcriptional regulatory role of aconitase from *Streptomyces viridochromogenes* Tü494"

SCHOLARSHIPS

09/2012 – 01/2013	Scholarship from the state of Baden-Württemberg (Aufenthalt für anwendungsorientierte Biowissenschaftler(innen) und Biotechnolog(inn)en in Shanghai und Jiangsu/China).
07/2009 – 09/2009	Scholarship from the Leonardo da Vinci Programme for industrial internship abroad.
09/2008 – 02/2009	Scholarship from Erasmus Lifelong Learning Programme to study abroad.